Stony Brook University

Diversity of Skates (Batoidea: Rajoidei) and the Spatial Structure of NW Atlantic Communities

A Dissertation Presented

by

Christopher Michael Martinez

to

The Graduate School

in Partial Fulfillment of the

Requirements

for the Degree of

Doctor of Philosophy

in

Marine and Atmospheric Sciences

Stony Brook University

August 2014

Stony Brook University

The Graduate School

Christopher Michael Martinez

We, the dissertation committee for the above candidate for the

Doctor of Philosophy degree, hereby recommend

acceptance of this dissertation.

Michael G. Frisk – Dissertation Advisor
Associate Professor
School of Marine and Atmospheric Sciences

Jeffrey S. Levinton - Chairperson of Defense
Distinguished Professor
School of Marine and Atmospheric Sciences *(Joint Faculty)*

Demian D. Chapman
Assistant Professor
School of Marine and Atmospheric Sciences

F. James Rohlf
Distinguished Professor, Emeritus
Ecology and Evolution

Daniel E. Duplisea
Research Scientist
Fisheries and Oceans, Canada

This dissertation is accepted by the Graduate School

Charles Taber
Dean of the Graduate School

Abstract of the Dissertation

Diversity of Skates (Batoidea: Rajoidei) and the Spatial Structure of NW Atlantic Communities

by

Christopher Michael Martinez

Doctor of Philosophy

in

Marine and Atmospheric Sciences

Stony Brook University

2014

Trait diversity often underlies complexity observed in biological systems. Whether it is behavior, life history, form or function, variation imparts differential performance on the organism, which may influence processes at higher levels of organization. Using two approaches, my dissertation research concerns the appraisal of diversity in fishes and its consequences for their ecology and evolution.

The first two chapters focus on variety of spatial behaviors in northwest Atlantic marine communities. Temporal changes in community habitat utilization, as quantified by the interspecific abundance-occupancy (A-O) relationship, were the focus of chapter one. Trends in the A-O relationship indicated large-scale reorganization in some communities, with assemblage structure shifting towards organisms with shorter life histories and rapid colonization potential. For chapter two, I developed a Monte Carlo simulation to investigate the role of spatial distribution in the realization of temporal A-O trends. This work showed that the empirical results obtained in chapter one may be recreated from a collection of negative binomial-distributed catches derived from natural communities. Changes in spatial behaviors of species were implicated in a notable example of rapid community change in the Gulf of Maine.

The second half of my dissertation examines the morphological diversity of Batoid fishes (skates, rays and allies) and its relation to factors associated with ecology and life history. In chapter three, I used geometric morphometrics to provide an initial assessment of pectoral fin diversity among many of the existing Batoid families. A majority of shape variation corresponded with taxa having rounded versus triangular fins. This was highly correlated with aspect ratio, a characteristic related to swimming mode and lifestyle. In my final chapter, I examined developmental shape trajectories in three species of northwest Atlantic skate. Divergence of body shapes in these fishes appears to be related to the development of sexual organs at maturity. Patterns of variation between the species are discussed relative to the evolution of disparate reproductive strategies and life histories.

Dedication Page

This dissertation is dedicated to my family, who worked hard with little recognition so that I may follow my passions and dreams.

Table of Contents

List of Tables vii
List of Figures ix
List of Abbreviations xiv
Acknowledgements xv

Introduction 1

Chapter 1: Patterns and trends of community habitat occupation in the northwest Atlantic coastal shelf ecosystem 3

- Introduction 3
- Methods 6
- Results 12
- Discussion 18
- Tables 26
- Figures 31

Chapter 2: Exploration of Interspecific Abundance-Occupancy Relationships using Empirically Derived Pseudo-Communities 37

- Introduction 37
- Methods 41
- Results 44
- Discussion 48
- Tables 53
- Figures 58

Chapter 3: Reassessment of morphological diversity of the batoid pectoral fin, with an emphasis on skates (Suborder Rajoidei) 64

- Introduction 64
- Methods 66
- Results 72
- Discussion 75
- Tables 82
- Figures 89

Chapter 4: Pectoral fin dimorphism in sister species of skate, *Leucoraja erinacea* and *Leucoraja ocellata*, and its potential relationship to reproductive strategies 101

Introduction 101
Methods 104
Results 108
Discussion 110
Tables 114
Figures 118

Summary 131

References Cited 133

List of Tables

Chapter 1: Patterns and trends of community habitat occupation in the northwest Atlantic coastal shelf ecosystem

Table 1.1. List of common and scientific names of species composing regional communities. Bold letters represent inclusion of species into one of thtree groups (P = predators & competitors, S = schoolers & colonizers and O = others) 26

Table 1.2. Kendall's τ from Mann-Kendall trend tests on A-O indices. Time periods over which trends were calculated were determined using breakpoint analysis. P-values on trends are shown in parentheses 28

Table 1.3. Summary of autocorrelation tests and regressions of A-O indices on external factors. Durbin-Watson (D-W) test statistics shown with p-values in parentheses. The slopes of GLS regressions with and without autocorrelation are also provided with p-values in parentheses. Significant relationships are bold and asterisks denote regressions where normal and autocorrelation models were both significant 29

Chapter 2: Exploration of Interspecific Abundance-Occupancy Relationships using Empirically Derived Pseudo-Communities

Table 2.1. Trends (Kendall's **τ**) of mean NB parameter estimates with p-values provided in pararentheses 53

Table 2.2. Summary of autocorrelation tests and regressions of mean NB parameters on external factors. Durbin-Watson (D-W) test statistics shown with p-values in parentheses. The slopes of GLS regressions with and without autocorrelation are also provided with p-values in parentheses. Significant relationships are bold and asterisks denote regressions where normal and autocorrelation models were both significant 54

Table 2.3. Empirical and mean simulated trends (Kendall's **τ**) for A-O relationships estimated with GMA and LMA. Empirical trends are shown with p-values and simulated trends with 95% confidence intervals (based on percentile). Significant trends and those excluding zero from 95% confidence intervals appear in bold. The percent of significant trends (out of 500 simulations) is also provided 56

Table 2.4. Mean simulated trends for A-O relationships, estimated with constant NB parameters across all years. Trends are shown with 95% confidence intervals. The percent of significant trends (out of 500 simulations) is also provided 57

Chapter 3: Reassessment of morphological diversity of the batoid pectoral fin, with an emphasis on skates (Suborder Rajoidei)

Table 3.1. List of species analyzed. Wherever available, information was also provided for sex, preservation method and image contributor. For specimens that are part of an institutional collection, the catalog number was listed. Abbreviations are as follows: AMNH = American Musuem of Natural History; ANSP = Academy of Natural Sciences of Philadelphia; MCZ = Harvard Museum of Comparative Zoology; ME = Mar-Eco; MNHN = Muséum National D'Histoire Naturelle; NMNH = National Museum of Natural History (Smithsonian); SIO = Scripps Institute of Oceanography, VIMS = Virginia Institute of Marine Science; ZMUB = Museum für Naturkunde, Humboldt Universität 82

Table 3.2. Morphological disparity for all families invesigated here. The number of observations/species included (n) is also given 88

Chapter 4: Pectoral fin dimorphism in sister species of skate, *Leucoraja erinacea* and *Leucoraja ocellata*, and its potential relationship to reproductive strategies

Table 4.1. von Bertalanffy growth parameters from Frisk and Miller (2006). Estimates are shown for asymptotic length (L_∞), growth rate (k) and the theoretical age at size zero (t_0) 114

Table 4.2. Interspecific and intraspecific tests of allometric slopes (MANCOVA) 115

Table 4.3. Regressions of Procrustes-aligned shapes on clasper lengths and cloaca depths 116

Table 4.4. Regressions of Procrustes-aligned shapes on log-centroid size (CS) 117

List of Figures

Chapter 1: Patterns and trends of community habitat occupation in the northwest Atlantic coastal shelf ecosystem

Figure 1.1. Sum of commercial landings in the GOM (A), GB (B), SNE (C) and MAB (D). For reference, the year 1976 is marked to denote the Magnuson-Stevens Fishery Conservation and Management Act (dashed gray lines) 31

Figure 1.2. Climate-related variables used in this study. Panels display mean regional bottom temperature (A), mean regional surface temperature (B), the Gulf Stream index (C) and the Atlantic Multidecadal Oscillation index (D)..... 32

Figure 1.3. Local abundance trends in the GOM (A), GB (B), SNE (C) and MAB (D). Values are divided among species groups, representing predators & competitors (dark gray), schoolers & colonizers (light gray) and others (black) 33

Figure 1.4. Forms of variation for interspecific A-O regression indices. Differences in slope (A) result in individuals occupying fewer regions (gray horizontal lines) at a given abundance. Changes in the A-O intercept (B, regression lines) reflect a uniform shift in the total proportion of sites occupied. The r^2 (B, dark gray shaded area) describes the diversity of spatial of occupancy strategies (light gray bars) utilized by species in a region. Often the slope and intercept both vary (C), and the degree to which each does, speaks to the nature of variation..34

Figure 1.5. Regional time series of the interspecific A-O slope (A-D), intercept (E-H) and r^2 (I-L), with 95% confidence bands (gray area). Dashed linear regressions indicate segments chosen by breakpoint analyses, with asterisks denoting a significant trend with the Mann-Kendall trend test. Map after Lucy and Nye (2010) 35

Figure 1.6. Selected yearly A-O relationships in the GOM (A-C), GB (D-F), SNE (G-I) and MAB (J-L). Dashed regression lines are yearly OLS fits. Species are divided among predators & competitors (open circles, dark gray convex hull), schoolers & colonizers (open circles, light gray convex hull) and others (filled circles) 36

Chapter 2: Exploration of Interspecific Abundance-Occupancy Relationships using Empirically Derived Pseudo-Communities

Figure 2.1. Flow diagram showing methods for generating pseudo-communities and assessing A-O trends within a region..... 58

Figure 2.2. Time series of the natural log of mean negative binomial parameters (rows) for communities in each of four NWACS communities (columns). Standard error is shown as the shaded gray region 59

Figure 2.3. Mean of simulated A-O regression statistics (solid black lines) for relationships calculated with GMA. 95% confidence intervals on yearly values are shown in grey. For comparison, empirical estimates of the A-O relationship are provided (dashed red lines) 60

Figure 2.4. Mean of simulated A-O regression statistics (solid black lines) for relationships calculated with LMA. 95% confidence intervals on yearly values are shown in grey. For comparison, empirical estimates of the A-O relationship are provided (dashed blue lines) 61

Figure 2.5. Mean A-O regression statistics for simulations with NB parameters held constant. Results are given for relationships estimated with GMA (A-C) and LMA (D-F). In each plot, 95% confidence intervals are color-coded by region..... 62

Figure 2.6. Mean A-O regression statistics for simulations in the GOM from 1973 to 1982. Results are given for relationships estimated with GMA (A-C) and LMA (D-F). Simulations including all species are shown in gray and those with schooling and colonizing species removed are in red (GMA) and blue (LMA). 95% confidence intervals are shown as shaded regions around yearly means 63

Chapter 3: Reassessment of morphological diversity of the batoid pectoral fin, with an emphasis on skates (Suborder Rajoidei)

Figure 3.1. Diagrams showing the definition of pectoral fin outlines used in this study (blue lines) versus that of Franklin *et al*. (2014) (red lines) for typical Rajoidei (A), Myliobatoidei (B), Torpedinoidei (C), Pristidae (D) and guitarfish (E)..... 89

Figure 3.2. Radiograph of *Raja eglanteria*, displaying the two components used in aspect ratio calculations; maximum chord width of the pectoral fin (red bar originating at the scapulocoracoid and extending 90° relative to the axis of symmetry) and fin area (light blue shaded region). Boundaries of the pectoral fin were demarcated by the extent of pectoral radials. The anterior point of the fin area is the intersection of the propterygium and disc outline..... 90

Figure 3.3. Scree plots from PCAs of shape data for all batiods (A), Rajoidei (B), and Dasyatidae (C). Results are shown for the original outline configuration (solid line) and the configuration with an additional anterior landmark (dashed line). For ease of visualization, only data for the first 10 PCs are provided..... 91

Figure 3.4. Principal components (PCs) 1 and 2 for all batoid specimens (A), with points colored by family. Shapes represent higher-level taxonomic groupings for Myliobatoidei (circles), Rajoidei (triangles) and Torpedinoidei (squares), with Platyrhinodei, Pristidae and guitarfishes all represented by diamonds. The percent of total shape variance explained by PCs is listed on

respective axes. Shapes of PC endpoints (B), estimated with the thin-plate spline transformation, are also included (black outlines) and shown relative to consensus shape (gray outlines) 92

Figure 3.5. Principal components (PCs) 1 and 2 for Rajoidei specimens, with points colored and labeled by genus. The percent of total shape variance explained by PCs is listed on respective axes. Shapes of PC endpoints (B), estimated with the thin-plate spline transformation, are also included (black outlines) and shown relative to consensus shape (gray outlines)..... 93

Figure 3.6. Principal components (PCs) 1 and 2 for Dasyatidae specimens, with points colored and labeled by genus. The percent of total shape variance explained by PCs is listed on respective axes. Shapes of PC endpoints (B), estimated with the thin-plate spline transformation, are also included (black outlines) and shown relative to consensus shape (gray outlines) 94

Figure 3.7. Principal component 1 versus aspect ratio. All aesthetics are as in figure 4..... 95

Figure 3.8. Maximum likelihood phylogenetic tree used for comparative analysis of PC 1 shape variation versus aspect ratio. For reference, aspect ratios are superimposed on the tree. Molecular sequences were collected from Aschliman *et al*. (2012) 96

Figure 3.9. Pectoral wave numbers from Rosenberger (2001) plotted against aspect ratios (A) and PC 1 scores (B)..... 97

Figure 3.10. Principal components 1 and 2 for batoid specimens with an additional anterior landmark. All aesthetics are as in figure 4..... 98

Figure 3.11. Thin-plate spline transformed outlines for all batoids (A), Rajoidei (B) and Myliobatoidei (C) with an additional anterior landmark (red dots). Shapes are shown for positive and negative PC extremes (black outlines) relative to consensus shape (gray outlines). Only the PC that best displayed the influence of the added landmark is shown 99

Figure 3.12. Principal components 1 and 3 for batoid specimens with an additional anterior landmark. All aesthetics are as in figure 4..... 100

Chapter 4: Pectoral fin dimorphism in sister species of skate, *Leucoraja erinacea* and *Leucoraja ocellata*, and its potential relationship to reproductive strategies

Figure 4.1. Comparison of sexual dimorphism in pectoral fin shapes for a selection of skate species; male (A) and female (B) *Raja eglanteria*; male (C) and female (D) *Rajella Fyllae*; male (E) and female (F) *Bathyraja minispinosa*; and male (G) and female (H) *Bathyraja pallida*. Images A and B came from personal collection, C from Claude Nozeres (DFO, Canada), D from Roberta Miller (DFO, Canada), E & F from Duane Stevenson (NMFS AFSC), and G & H from Alexei Orlov (VNIRO, Russia)..... 118

Figure 4.2. Pectoral shape variation in male *L. erinacea* (A), female *L. erinacea* (B), male *L. ocellata* (C) and female *L. ocellata* (D). On the left half of images are juveniles (with 1cm bar below) and the right side of images are adults (with 5cm bar below) 119

Figure 4.3. Skate endoskeleton diagram (right) with features of interest labeled; rostrum length used in this study (*ros*), rostral appendix (*rap*), propterygium (*pt*), mesopterygium (*msp*), metapterygium (*mtp*) and scapulocoracoid (*sc*). In addition, the outlines used for morphological analyses are shown (right), with the number of landmarks on each provided in parentheses. The pectoral fin margin was evaluated as a single outline (blue dashed line) and the endoskeleton configuration included five (red dashed lines). Sliding landmarks were evenly spaced along the outlines shown, with a true landmark on each end (colored circles). Note that for the endoskeleton, the anteriormost landmark is shared among two outlines (making 94 total endoskeleton landmarks) 120

Figure 4.4. From Sulikowski *et al*. (2004); monthly means of gonadosomatic indices for male (dark blue) and female (light blue) *L. ocellata* in the Gulf of Maine. Vertical bars are standard errors 121

Figure 4.5. PC 1 and PC 2 for shape analyses of pectoral margins. Also included are shapes representing PC extremes (black outlines), relative to consensus shape (gray outlines). Shape visualizations were made with the thin-plate spline transformation..... 122

Figure 4.6. PC 1 and PC 2 for endoskeleton shape analyses. Also included are shapes representing PC extremes (black outlines), relative to consensus shape (gray outlines). Shape visualizations were made with the thin-plate spline transformation..... 123

Figure 4.7. 3D plots of log-centroid size versus PC1 and PC2 in separate PCAs for *L. erinacea* fin margins (A), *L. erinacea* endoskeletons (B), *L. ocellata* fin margins (C) and *L. ocellata* endoskeletons (D). Shaded regions are 95% equal frequency ellipses. Color schemes are as in figures 6 and 7..... 124

Figure 4.8. 3D plots of log-centroid size versus PC1 and PC2 in separate PCAs for male skate fin margins (A), male endoskeletons (B), female fin margins (C) and female endoskeletons (D). Shaded regions are 95% equal frequency ellipses. Color schemes are as in figures 6 and 7 125

Figure 4.9. Clasper length (A) and cloaca depth (B) versus log-centroid size. Color schemes are as in figures 6 and 7. For reference, data are included on additional specimens collected by the National Marine Fisheries Service, Northeast Fishery Science Center (light points in background) 126

Figure 4.10. Rostrum length versus total length. Color schemes are as in figures 6 and 7 127

Figure 4.11. Gonadosomatic index (GSI) versus log-total length. Color schemes are as in figures 6 and 7. Local regression lines are added to display overall directions of variation 128

Figure 4.12. Total length versus centroid size. Color schemes are as in figures 6 and 7 129

Figure 4.13. Radiographs of male (A) and female (B) *L. erinacea*, displaying pectoral "cramming" in the former. Red circles indicate areas where the effect is most noticeable. For reference, black bars are 2cm in length 130

List of Abbreviations

A-O – abundance-occupancy

AMO – Atlantic Multidecadal Oscillation

AR – aspect ratio

CS – centroid size

GSI – gonadosomatic index

GB – Georges Bank

GMA – global mean abundance

GOM – Gulf of Maine

LMA – local mean abundance

MAB – Mid-Atlantic Bight

NEFSC – Northeast Fishery Science Center

NWACS – northwest Atlantic coastal shelf

NMFS – National Marine Fisheries Service

SNE – Southern New England

TL – total length

Acknowledgments

A number of people contributed, in varying capacities, to the completion of this dissertation. Work for the first two chapters was funded by a joint grant with the National Science Foundation and NOAA-National Marine Fisheries Service (funding code NMFS-FHQ-2008-2001345) for the Comparative Analysis of Marine Ecosystem Organization (CAMEO). In addition, research for chapters three and four was completed with the help of several lab assistants, namely Wesley Robinson, Danielle Francois and Emily Nocito. Finally, the Frisk Lab and staff of the RV Seawolf were instrumental in the collection of skate specimens.

Introduction

"…is variety the spice of life, or is it a necessity for the long life of the total ecosystem comprising man and nature?"

(Eugene P. Odum, 1969)

In many ways, the work presented in this dissertation concerns the appraisal of biological diversity and consequences thereof. There are myriad ways in which one may assess diversity. Behavioral diversity, for example, may define the response of organisms to external threats, like predators (Stone *et al*. 1994). Likewise, both the range of species' responses to perturbations (Elmqvist *et al*. 2004) and the diversity of functional species types (Petchey and Gaston 2002) may impact community dynamics and resilience. However measured, investigations of variety and diversity provide valuable insight for biological systems.

My dissertation research is centered on two primary focal themes. The first involves temporal analyses of community spatial utilization. The goal of this work is to summarize the variety of organismal spatial patterns within four northwest Atlantic communities in order to understand overriding trends and processes in each. These regions have a long history of fishing and human activity (Lear 1998), which have led to well-documented assemblage disturbances (Fogarty and Murawski 1998). Therefore, a detailed understanding of the nature of changes is vital to management and conservation. I used the interspecific abundance-occupancy relationship to describe regional patterns of habitat utilization and assess how they have changed over time. I also studied the extent to which natural community variation may be recreated by simple modeling of species' distributions. This work provided a platform to test hypotheses concerning biological response to external drivers.

The next section of my dissertation focuses on the morphological variety of batoid fishes (i.e. skates, rays and allies) and the implications for lifestyle diversity. All batoids have modified, expanded pectoral fins that create the main feature of their bodies, a lozenge-shaped disc (Aschliman *et al*. 2012). Disc shapes vary among batoid taxa and are often associated with differences in swimming mode and lifestyle (Rosenberger 2001). However, much is still unknown about these fishes and the true lifestyle diversity of groups, like skates, has likely been underestimated. For this work, I used geometric morphometrics to evaluate pectoral fin shape diversity in a wide range of batoids. Shapes were compared to fin aspect ratios and also with available kinematic data in a subset of species.

The final section of my research scaled down from a survey of batoid morphological diversity to sexual dimorphism in skates. Particularly, I investigated allometry of pectoral fin development in the closely related little skate (*L. erinacea*) and winter skate (*L. ocellata*). These species are sympatric over much of their respective ranges and have evolved divergent life histories. *L. erinacea* displays rapid growth, precocious maturation and small body size relative to *L. ocellata* (Frisk and Miller 2006). In addition, *L. erinacea* has a more intense dimorphism, which occurs at sexual maturation. These patterns suggest a potential relationship between fin shape, growth and reproductive biology. I compared allometric shape trajectories between sexes and species. In addition, I tested for relationships between shape change and development of sex organs.

Chapter 1

Patterns and trends of community habitat occupation in the northwest Atlantic coastal shelf ecosystem

Introduction

Demersal communities on the US northwest Atlantic coastal shelf (NWACS) have traditionally supported some of the most productive fisheries in the world (Lear 1998). Intensive harvests from these waters, especially by non-domestic fleets in the 1960's and 1970's, drastically reduced population sizes of commercially valuable species such as cod (*Gadus morhua*, Gadidae), haddock (*Melanogrammus aeglefinus*, Gadidae) and herring (*Clupea harengus*, Clupeidae) (Bourne 1987). Given the importance of these once-dominant species to overall community dynamics, the aforementioned disturbance is believed to have fundamentally altered the composition, structure and competitive environment of NWACS ecosystems (Fogarty & Murawski 1998). Ecological theory suggests that once disturbed, communities may subsequently undergo successional change (Odum 1969, Connell and Slatyer 1977), with assemblages often being quite different from their initial condition (Collie *et al*. 2004). For example, projection models indicate a two-thirds decline in higher trophic species in the north Atlantic over the second half of the 19th century (Christensen *et al*. 2003), creating ecosystems that favor lower trophic species with rapid turnover. The Magnuson-Stevens Fishery Conservation and Management Act of 1976 prohibited foreign fishing fleets from harvesting within 200 miles of US coastlines (Lear 1998), but by this time it is widely believed that fishing had already caused substantial changes to community structure in many areas (fig. 1.1). In addition, continued fishing by domestic sources would further deplete demersal communities (Fogarty and Murawski 1998).

Simultaneous with the effects of harvest, organisms on the NWACS have also experienced environmental changes (fig. 1.2). Because fishery reductions often lead to a narrowing of age structure (Berkeley *et al.* 2004), it has been suggested that exploited populations may be more susceptible to the effects of environmental variability (Chih-hao *et al.* 2006). Therefore interactions between fishery removals and environmental change may be expected. Currently, climate-related change is among the most relevant of factors affecting biological processes at multiple levels of organization (Walther *et al.* 2002, Parmesan and Yohe 2003). Both large-scale climatic processes and local warming in the north Atlantic have been connected to geographic shifts in marine populations (Perry *et al.* 2005, Dulvy *et al.* 2008, Lucy and Nye 2010). It has also been proposed that the velocity of climate (i.e. local rates and direction of isotherm migration) may explain variability in observed shifts (Pinsky *et al*. 2013). The reality is, however, that our understanding of climate impacts on species remains fairly tenuous and studies on the effects of climate on distributions have focused on a limited number species that show strong and clear responses. However, when large numbers of species are assessed, it becomes evident that reactions are varied and are sometimes opposite in direction (Nye *et al.* 2009).

A community-level approach is often useful to reduce the complexity of numerous interacting populations to a manageable set of descriptors that may be used to identify overriding trends of diversity and distribution (Storch and Gaston 2004). In this way, it offers a different means of assessing the impacts of climate and other disturbances than traditional approaches in fisheries. Given the complex nature of communities, it is unclear how factors such as climate and fishing would impact their structure. This research attempts to identify community changes within NWACS regions and to recover potential relationships with climate and harvest.

Patterns of habitat or area occupancy have been used to assess the state of communities (Webb *et al.* 2007, Zuckerberg *et al.* 2009). These may reflect density-dependent processes, the distribution and suitability of resources and/or the diversity of life histories contained within an assemblage of species. A positive association between interspecific abundance and occupancy (A-O) is among the most widely encountered patterns in macroecology (Hartley 1998, Holt *et al.* 2002, Borregaard and Rahbek 2010). In addition, A-O relationships can be quite dynamic over time and responsive to disturbances (Fisher and Frank 2004, Frisk *et al.* 2011). For example, Webb *et al.* (2007) linked a decline in the strength of A-O relationships in British birds to habitat fragmentation.

I examined interspecific A-O relationships to investigate trends in habitat occupation on the NWACS, providing information at a scale that is relevant to distinct biological communities (Lucy and Nye 2010) as well as the management of economically vital marine resources. Utilizing a well-documented biological disturbance from commercial fishing, I tracked community responses as local organismal abundance increased with time across much of the NWACS (fig. 1.3). Both Fogarty and Murawski (1998) and later Lucy and Nye (2010) have suggested that the intense harvest of competitively dominant groundfish in this system during the 1960's and 70's, created the initial conditions for large-scale reorganization of communities, a process in which rising temperature played an important role. In this context, my primary objective was to identify and characterize significant temporal changes in the spatial utilization of communities. Regression statistics were interpreted as indices of spatial structure and were subsequently assessed with respect to yearly fishery landings and four external variables related to climate.

Methods

Survey Data

I examined A-O relationships in adjacent offshore regions ranging from Cape Hatteras, NC to the U.S.-Canadian border. These were the Gulf of Maine (GOM), Georges Bank (GB), Southern New England (SNE) and the Mid-Atlantic Bight (MAB). I utilized fishery-independent trawl data from the Northeast Fisheries Science Center's (NEFSC) autumn survey during the period 1963-2008. It should be noted that surveying did not begin in the MAB until 1967. The survey employs a depth-stratified, random sampling design such that effort per area is uniform across surveyed regions (Sosebee and Cadrin 2006). In order to avoid potential bias due to changes in the survey fleet (Miller *et al.* 2010), I did not to use data after 2008.

Interspecific A-O Relationships

For each regional assemblage, I defined the yearly abundance of a species as the number of individuals caught divided by the number of sites in which they occurred (i.e. not including empty sites). This definition is equivalent to local mean abundance (LMA) in the A-O literature and is generally the preferred measure in A-O studies (Borregaard and Rahbek 2010). Occupancy was defined as the percentage of all sites sampled within each region that had at least one individual of the target species present. I created yearly A-O relationships by plotting the abundance and occupancy of each species in their respective regional communities.

Yearly A-O relationships included 30 species that represented the biological assemblages of each region (table 1.1). I also evaluated relationships with 45 species (not shown here), which did not drastically change results, but did include some seldom-caught species. The number of species is an important consideration in A-O research as it determines the number of

observations in yearly regressions of occupancy on abundance (i.e. each observation in the interspecific A-O relationship represents the abundance and occupancy of a single species). As a result, including too many species increases the prospect of sampling artifacts that result from artificially low catch probabilities in rare species (Brown 1984). However, using too few species may not reliably capture overall patterns of spatial use within a community. Species inclusion was determined using a ranked index (S) that takes into account relative numerical dominance as well as prevalence across survey years. In other words, species that were most abundant and most commonly caught were preferentially chosen. For each region, the top 30 species were chosen based on the following:

$$S = \frac{H_i}{H_{max}} + \frac{y_i}{y_{tot}} \quad (1)$$

The first term is the ratio of the total catch of species i (H_i) over all survey years relative to that of the most caught species in the region (H_{max}). The second term is the percent of total surveyed years (y_{tot}) that species i was caught.

Yearly variation in the A-O relationship provided information on the manner by which communities collectively used available habitat. Ordinary least-squares regression (OLS) was used to describe annual relationships (e.g. Webb *et al.* 2007, Frisk *et al.* 2011). The arcsine transformation was employed to normalize the inherently non-normal proportion data that made up community occupancy values. Abundance, which is often right-skewed, was transformed by its natural logarithm. Accordingly, the regression relationship was given by:

$$sin^{-1}\left(\sqrt{o}\right) = s \times ln(A) + C \quad (2)$$

where s and C are the fitted slope and intercept, respectively. These statistical calculations provided A-O relationships for each region that were homoscedastic across years (Bartlett test of homogeneity of variances; K^2=35.62, p=0.84 in the GOM; K^2=35.31, p=0.85 in GB; K^2=35.64,

p=0.84 in SNE; K^2=37.94, p=0.61 in the MAB). For comparison, I also evaluated A-O relationships for non-transformed occupancy counts, estimated using a generalized linear model (GLM) with binomial errors and found that patterns of temporal variation were similar to those computed with OLS (results not shown here). In addition, Duplisea and colleagues (2009) showed no major differences in residual structure for the A-O relationship in GB using GLM, reduced major axis regression and cubic spline regression. Given these results, I found no reason to stray from my use of the transformed, linearized form as a relative indicator of community variation.

As an additional measure to take into account the sensitivity of A-O relationships to the removal of species, I performed a cross-validation routine where I randomly selected and removed 3 out of 30 species in each region (~10%, depending on absence of some species in particular years) and then re-evaluated yearly relationships. This was repeated 5,000 times to insure that a majority of the 4,060 possible $_{30}C_3$ combinations of species groups were included. The yearly means from the cross-validation were then used as my measure of temporal variation in the A-O relationship. 95% confidence intervals based on percentile were also calculated as a measure of variance attributed to species removal.

Temporal Evaluation of A-O Relationships

I used estimates of mean yearly slopes, intercepts and coefficients of determination (r^2) after cross-validation as temporal indices of the spatial characteristics underlying community structure. Again, the linear model itself was not intended to infer a mechanism governing the relationship between A and O; rather it was used to summarize the diversity of spatial behaviors exhibited by a community. Together, the A-O slope and intercept determine the relative nature of

habitat occupation. Other indices being constant, the A-O slope measures variation in the rate of habitat filling with increasing abundance. Decreasing slopes, therefore mean that a given abundance overall average density or species packing increases (fig. 1.4a). Changes in the A-O intercept reflect upward or downward shifts in the total amount of available space occupied. Like slope, a decrease in the intercept denotes higher species packing for a given abundance level (fig. 1.4b). Trends must be evaluated with caution as slope and intercept are often negatively correlated. At the same time, the way in which they interact provides evidence about the nature of community change. For example, in figure 1.4A change is disproportionally concentrated at high abundance levels, such that the intersection of the two regressions occurs near the origin. In contrast, regressions intersecting at intermediate abundances (fig. 1.4C) result from species' changes at both low and high abundance. For these reasons, it is also essential to assess community trends within the context of the internal dynamics of the species that compose them (i.e. individual points in A-O relationships). Lastly, the A-O r^2 may be thought of as an index of the spatial heterogeneity expressed by species within each community. Communities with high r^2 will have small variation with respect to spatial habitat occupation (fig. 1.4b, dashed line). Conversely, low r^2 values (fig. 1.4b, solid line) indicate relatively large variance around predicted values, corresponding to a wider range of occupancy strategies at a given abundance. The use of A-O indices here assumes consistency in sampling across years and that species catchability due to gear selectivity does not change markedly.

In order to identify potential shifts in the overall direction of trends, I performed a breakpoint analysis on all time series with the R package "strucchange" (Zeileis *et al*. 2013). This method uses the Bayesian information criterion (BIC) to parsimoniously break up indices into a number of linear regressions that maximizes the fit over the entire set. This does not

suggest that the linear model is always the best choice to describe temporal changes in AO indices, as some sections are clearly not linear (e.g. A-O intercept in SNE, fig. 1.5). Rather, the analysis is meant to aide in the identification of marked changes in the times series, potentially signifying important biological shifts within communities. I used the Mann-Kendall trend test in the Kendall package in R (R Core Team 2013) to determine the direction and strength of trends for each segment chosen by breakpoint analyses (McLeod 2011). This calculates rank correlations with time, making it an appropriate test for monotonic data, regardless of linearity.

Internal Community Dynamics (Intraspecific Variation)

Understanding the relative variations of a community's constituent species is important to inform discussions of potential mechanisms underlying observed interspecific A-O trends (Buckley and Freckleton 2010). To assess interspecific interactions, I attempted to identify subsets of communities that were believed to respond differently to disturbances. I divided species into two main groups based on lifestyle, which were each characterized by a suite of ecological and life history characteristics (see table 1.1 for full species listing). Whenever possible, I referred to available species documentation from fishbase.org, fishery status information from the Northeast Fishery Science Center (NEFSC) as well as NOAA's fish watch webpage (fishwatch.gov).

The first species group, which I referred to as "schoolers and colonizers" were organisms that had had rapid life-histories, were likely to respond quickly to variable environment, tended to school and were at low trophic levels. Examples include the Atlantic herring (*Clupea harengus*, Clupeidae), longfin squid (*Doryteuthis pealeii*, Loliginidae) and northern sand lance (*Ammodytes dubius*, Ammodytidae). Species in the second group, called "predators and

competitors", had delayed life history characteristics and were either higher-level predators or demersal space competitors. These included organisms like the winter skate (*Leucoraja ocellata*, Rajidae) and haddock (*Melanogrammus aeglefinus*, Gadidae).

Most species clearly fit into one group or another, with relatively little subjectivity involved in assignment. However some had lifestyles that may be seen as mix of the two groups, like the spiny dogfish (*Squalus acanthias*, Squalidae), which is a higher trophic species but is also known to school at times. In such cases they were placed in the group in which they exhibited most characteristics (clearly dogfish are more similar to species in the second group than the first). Still, there were a small number of species that I could not place with confidence and were put in a group that I called "others".

External Influences on Community Trends

I tested the effects of regional fishery landings and four climate-related variables on A-O relationships. Landings data were collected for each region from National Marine Fisheries Service (NMFS) records. I summed landings over all species to get a measure of overall harvest intensity. The first two climate-related variables, surface temperature and bottom temperature, consisted of yearly averages of on-board measurements from NEFSC surveys. Because these data came from the same source as catches, they represented the thermal conditions experienced by each community at the instant that they were sampled. I also considered the Gulf Stream Index (Joyce *et al.* 2000), which tracks latitudinal oscillations of the northern wall of the warm water current. Because of the Gulf Stream's interaction with the Deep Western Boundary Current, its location affects slope water circulation, thus impacts sea surface temperatures in the northwest Atlantic (Peña-Molino and Joyce 2008). Northerly migrations of the Gulf Stream (i.e.

larger index values) are associated with warm sea surface temperature anomalies landward of it, with the opposite for southern positions. Lastly, I used an index of the Atlantic Multidecadal Oscillation (AMO), a large-scale cycle of climate variability with periods occurring on the order of several decades (Knight *et al*. 2006). The index is based on sea surface temperature (SST) anomalies that have been detrended for recent anthropogenic rises in temperature (Nye *et al*. 2009). Positive AMO indices are associated with higher SST. Both the Gulf Stream and AMO indices were obtained from a database managed under a joint NSF-NOAA project that funded this work (NMFS-FHQ-2008-2001345, OCE-1041716) and were originally provided to the project by Janet Nye (of Nye *et al*. 2009, above). To assess the relationship between each external factor and reported community trends, I first used the Durbin-Watson test (D-W) to look for evidence of first-order autocorrelation between variables. I evaluated relationships using generalized least-squares (GLS) regression for models with and without specified error structures accounting for first-order autocorrelation.

Results

Temporal Evaluation of A-O Relationships

Trends in the A-O relationship varied regionally and for specific A-O indices (table 1.2). In the GOM, time series breakpoints were identified in 1972 and 1982 for the A-O slope, in 1973 and 1981 for the intercept and in 1985 for the r^2 (fig. 1.5). Significant negative A-O slope trends occurred in the GOM during the period from 1973-1982 (Mann-Kendall τ=-0.87, p=0.00068) and 1983-2008 (Mann-Kendall τ=-0.32, p=0.025). Intercepts in the GOM increased from 1974-1981 (Mann-Kendall τ=1, p=0.00084), but decreased for r^2 from 1963-1985 (Mann-Kendall τ=-0.605, p=0.000060). Breakpoints in GB did not occur in the slope time series, but were found in

1981 for both the intercept and r^2. The GB slope trend decreased over the entire time series from 1963-2008 (Mann-Kendall τ=-0.30, p=0.0040). There was no evidence for a trend in the intercept or r^2 in GB from 1963-1981, however both indices changed markedly from 1982-2008 in opposite directions from each other (intercept: Mann-Kendall τ=0.60, p=0.000015; r^2: Mann-Kendall τ=-0.52, p=0.00018). No valid breakpoints were designated for any of the A-O indices in SNE, so trends were evaluated over the entire time series. However, there did appear to be a slight shift in the rate of trends in the early to mid-1980's, as there was in GB. The slope in SNE increased, although not significantly (Mann-Kendall τ=0.19, p=0.058), while the intercept significantly decreased (Mann-Kendall τ=-0.22, p=0.032) and the r^2 increased (Mann-Kendall τ=0.23, p=0.027). Finally, 1994 was a breakpoint year for the slope and intercept in the MAB, with no breaks found for r^2. Slopes increased in MAB from 1967-1994, but the p-value on the trend was over the p=0.05 significance threshold (Mann-Kendall τ=0.25, p=0.061). During this time period, the intercept did change significantly, however (Mann-Kendall τ=-0.30, p=0.026). There was no trend in r^2 in the MAB.

Internal Community Dynamics (Intraspecific Variation)

As noted above, the GOM community showed signs of rapid change during early years of the time series and most notably between 1973 and 1982 (fig. 1.5). As the A-O trends indicate, changes occurring during this period largely corresponded with a weakening of the interspecific relationship (decreasing r^2). This was caused by the rapid increase in species with high abundance but limited spatial occurrence, which also drove down the slope, thereby increasing the average density of organisms within the community. When yearly relationships are partitioned between schoolers and colonizers versus predators and competitors (fig. 1.6A & B),

an interesting pattern emerges. It becomes apparent that much of the community change may be, in fact, attributed to a change in the species within the former group, namely Atlantic argentine (*Argentina silus*, Argentinidae), longfin squid and Atlantic sea scallop (*Placopecten magellanicus*, Pectinidae). There is little evidence of changes among demersal fishes during this time. Along with trends in relative local abundance (fig. 1.3), these results indicate that lower trophic species with faster life histories became a larger component of the GOM community. Given their tendency to occur in dense aggregations over relatively small spatial scales, their rise in abundance represented a growing negative faction in the community with respect to the A-O relationship. Such a changes is noteworthy because of its relationship to successional dynamics and also because a negative interspecific A-O relationship (as exhibited among the schoolers and colonizers in the early 1980's) is exceedingly rare in natural communities. In fact, one of the few circumstances in which they are thought to arise is in assemblages containing highly aggregative species (Webb *et al*. 2012).

Following 1982, the GOM community underwent a second, less drastic period of change. Unlike the years preceding it, species in the predator and competitor group played a more important role in observed trends, with several increasing in local abundance (fig. 1.3) and thereby also occupying a larger range of occupancy strategies (fig. 1.6B & C). These species began to occupy areas of the A-O space that schoolers and colonizers had recently moved into (i.e. high local abundance with limited spatial coverage). The most prominent of these include spiny dogfish, winter flounder (*Pseudopleuronectes americanus*, Pleuronectidae) and longhorn sculpin (*Myoxocephalus octodecemspinosus*, Cottidae). At the same time the groundfish, silver hake (*Merluccius bilinearis*, Gadidae) and pelagic fish, Atlantic herring contributed to the high abundance and high occupancy region of the GOM A-O space. Collectively, species' changes

resulted in significantly greater organismal density (i.e. smaller A-O slope) over the latter period, with relatively little change in other A-O indices (fig. 1.5).

In the GB region, signs of A-O change were most pronounced between 1982 and 2008, with values before this showing relatively large variance and little temporal directionality (fig. 1.5). However, despite the lack of trends from 1963 to 1981, increasing habitat occupancy in species like butterfish (*Peprilus triacanthus*, Stromateidae) and northern shortfin squid (*Illex illecebrosus*, Ommastrephidae) caused the schoolers and colonizers to fill in a wider range of spatial behaviors relative to the other early years (fig. 1.6D & E). After 1982, the strength of the A-O relationship decreased considerably, owing to community-wide (i.e. both groups) spreading out in multiple directions of the A-O space (fig. 1.6E & F). By the end of the time series, several species with lower/intermediate abundances, including the American lobster (*Homarus americanus*, Nephropidae), northern shortfin squid, little skate (*Leucoraja erinacea*, Rajidae) and winter skate actually increased in spatial occupation. At the same time, some of the more abundant species like the longfin squid, Atlantic herring and pollock (*Pollachius virens*, Gadidae) occurred at lower occupancy levels.

Although no breakpoints were identified for A-O indices in SNE, significant community changes did occur (fig. 1.5). During the first few years, local abundance was roughly equivalent for the schoolers and colonizers relative to the predators and competitors. However, the former quickly outnumbered the latter (fig. 1.3) as round herring (*Etrumeus teres*, Dussumieriidae), butterfish and Atlantic sea scallop increased in abundance, joining the longfin squid as the species with highest local abundances (information from survey data not shown here). The largest consequence of these changes was an increase of the A-O slope. However, a number of subtle changes in low and moderately abundant species also appeared to contribute to the decline

of intercept (fig. 1.6H). During the second half of the time series, the longfin squid continued to increase in local and global (i.e. absolute) abundance. As this occurred, the Atlantic sea scallop and butterfish (which had increased in local abundance in recent years) declined and Atlantic herring replaced scup (*Stenotomus chrysops*, Sparidae) as the abundant schooler/colonizer with low spatial occupancy.

Finally in the MAB, significant community change was identified from 1967 to 1994. This period was characterized by changes in the both species groups compared here, with each showing marked abundance declines in several sepecies (fig. 1.6J & K). Notably among these are the silver hake, spiny dogfish and butterfish. In addition, the longfin squid increased in spatial occupancy. These caused the A-O intercept to decline significantly until 1994. After this, the trend appears to reverse (fig. 1.5) and community structure began to resemble the early years once again (fig. 1.6J & L).

External Influences on Community Trends

The D-W test suggested significant autocorrelation in all regressions of A-O indices on external factors in the GOM (table 1.3). For GLS models not taking into account autocorrelation, there were numerous significant relationships identified (table 1.3). Variations in surface temperature were negatively associated with A-O slopes (slope=-0.016, $p< 0.001$) and positively with intercepts (slope=0.015, $p< 0.016$). The same relationships were observed for the Gulf Stream Index and the AMO, although associations were strongest with the AMO (table 1.3). In addition, the Gulf Stream Index was significantly related to the A-O r^2 (slope=-0.046 p=0.020). Finally, landings had a positive relationship with slope (slope=0.023 p=0.023), which is opposite from those with climate-related variables. After accounting for autocorrelation in GOM

regressions, all aforementioned relationships were rendered non-significant. In addition, the relationship between bottom temperature and the A-O r^2 became significant (slope=0.053 p=0.047), where it had not been in the non-autocorrelation model.

In GB, autocorrelation was identified for all associations between the A-O intercepts and external factors but the AMO. Surface temperature had a fairly weak but significant relationship with the A-O slope (slope=-0.0042, p=0.022). However, it was the AMO that displayed the strongest relationships with indices in GB. In the non-autocorrelation model, the A-O slope (slope=-0.042, $p<0.01$), intercept (slope=0.12, $p<0.01$), and r^2 (slope=-0.18, $p<0.034$) were all related to AMO. Regressions with autocorrelation were similar, with slope (slope=-0.045, $p<0.01$) and intercept (slope=0.12, $p<0.01$) remaining significant and r^2 (slope=0.17, p=0.065) falling slightly below the p=0.05 threshold.

Among the four regions considered here, SNE had the highest number of significant associations between community relationships and external factors (although several factors are not independent). In addition, there was no indication of first order autocorrelation among any of the relationships. For the non-autocorrelation model, increasing bottom temperature was related to larger A-O slopes (slope=0.0089, p=0.026), smaller intercepts (slope=-0.027, $p<0.01$) and larger r^2 (slope=0.048, p=0.012). Surface temperature was not related to the A-O slope but did have significant associations with intercepts (slope=-0.010, p=0.014) and r^2 (slope=0.023, $p<0.01$). As expected from its impact on coastal circulation, the location of the Gulf Stream's north wall often had similar relationships on communities as did water temperatures. Northernmost positions of the Gulf Stream were significantly related to reductions in the A-O intercept (slope=-0.027, $p<0.01$) and increases in r^2 (slope=0.049). Notably, the AMO did not have any significant relationships with A-O indices in SNE as it had in the northern two regions.

Yearly commercial landings in SNE had weak yet antagonistic relationships relative to those of climate-related factors, with higher fishery yields relating to smaller slopes (slope=-0.0015, p=0.026) and larger intercepts (slope=0.0039, p=0.014). Results for all above relationships in SNE were similar for models taking into accounts autocorrelation and are therefore not listed here (but see table 1.3). This makes sense, as D-W tests were all non-significant in this region. The autocorrelation model did, however, recover a significant relationship between the Gulf Stream Index and the A-O slope (slope=0.0072, p=0.031), which was not the case with the non-autocorrelation model (slope=0.0071, p=0.058). Finally, the MAB did not have any significant relationships between A-O indices and external factors tested herein.

Discussion

Research Overview

My results point to marked temporal trends in spatial structuring within NWACS communities. Overall, I believe that the methods used here provided an appropriate test for the identification of significant community variation. A-O regression statistics appeared to capture the underlying diversity of community-level processes. During each time period over which a significant trend was identified (fig. 1.5), examinations of yearly relationships clearly showed tangible features of internal community structure relating to the set of quantitative A-O indices used (fig. 1.6). The strength and manner of community change, was variable among regions. The strongest trends occurred in northern areas (i.e. GOM and GB), but there was some evidence of significant change in at least one of the three A-O regression indices in both SNE and the MAB (fig. 1.5). The results suggest that community variation within regions was often non-uniform with time. In several instances, A-O indices displayed periods significant increase or decrease,

only to be followed by a change in the rate (GOM) or even direction of the trend (GB, SNE, MAB).

The cross-validation exercise did suggest a level of sensitivity of the interspecific A-O relationship, as treated here, to the removal small subsets of observations (fig. 1.5). Although this result is not completely surprising, it implies that most of the observed trends did not likely reflect a concerted and directed shift in all (or even most) members of communities. However, depending on their role in overall community processes, a change in even a small number of species may exert disproportionate influences of community structure (e.g. Estes and Duggins 1995). Therefore, the species that do change create situations of potential ecological release that have ramifications on community reorganization.

Taking into account instances of autocorrelation, relationships between A-O trends and external variables differed by region, especially between high and low latitude sites (table 1.3). This could speak to latitudinal variation in species assemblages and/or environmental factors (fig. 1.1 & 1.2). In addition, several relationships had relatively low effect sizes, even when significant. This could simply be because species do not always respond similarly to the same factor. In fact, in a community of interacting species, opposing responses may even be expected (a negative impact on a predator can have a net positive impact on its prey, e.g. Konishi *et al*. 2001). My results demonstrate the difficulties in quantitatively linking external factors to community-level processes containing complex interaction networks, a detail that is certainly involved in the lack of consensus on overriding processes governing A-O relationships (Borregaard and Rahbek 2010). Despite apparent complications however, much may still be learned through detailed discussion of the potential impacts of external factors and by noting the correspondence of observed community trends to them.

Impacts of Harvest and Community Consequences

Significant relationships between yearly commercial landings and A-O indices were few in number and relatively weak when they did occur (table 1.3). In SNE, larger landings were associated with increased density (smaller slope) and an increase in the number of occupied sites (larger intercepts). In contrast, increased GOM landings were related to increased density for the non-autocorrelation model only. These results are not expected and highlight difficulties in comparing yearly harvest intensity with long-term community processes. At the same time, it is important to reiterate that it is not the purpose of this research to implicate commercial fishing as a source of substantial disturbance to NWACS communities. Rather, the case has been well documented (see introduction) and the work at hand tracks community variation given an established disturbed state as the starting condition. Therefore, the general lack of relationships with yearly landings becomes less concerning.

In reality, the most relevant harvest effects to the community traits evaluated here are those that are long lasting and cumulative in nature. Prolonged size-selective harvest, for instance, may lead to a progressive shift toward smaller sized individuals (Bianchi *et al.* 2000). In a study similar to this, Fisher and Frank (2004) suggested that temporal increases in the density of fishes on the Scotian Shelf were consistent with decreases in body size, where lower resource utilization allowed smaller individuals to be more spatially aggregated. This may explain why several predator/competitor species in the GOM and GB increased in abundance in later years, but were still spatially restricted (fig. 1.6 C & F). For longer-lived species, recovery from exploitation will take time and sustained harvest may continue to have effects even if landings decrease. Another known impact of fishing is the gradual degradation of habitats from

destructive harvest methods, like benthic trawling, which often decreases benthic habitat complexity (Norse and Watling 1999). Sustained trawl fisheries therefore have the potential to reduce the total amount of habitable area within a region. Similar fragmentation of habitat has been implicated in the breakdown or weakening of A-O relationships (Freckleton *et al.* 2006, Webb *et al.* 2007, Frisk *et al.* 2011).

Drinkwater (2006) hypothesized that a supposed regime shift in the north Atlantic, beginning in the 1920's, may have resulted from a combination of top-down, bottom-up and even mid-level or "wasp-waisted" control. I believe that disturbances from intense fishing through the 1960's and 1970's created conditions in NWACS communities where similar cascading effects were possible, and maybe even likely. Several of the species that were most impacted during this time were historically important harvest fishes falling within the predator and competitor group defined above (Fogarty and Murawski 1998). Due to their generally slower life histories, these organisms are inherently less resilient than other fished species like the Atlantic herring. In addition, the consequences of the removal of higher trophic species from communities have been examined in many marine systems and at numerous scales, from the tropical Pacific (Dulvy *et al.* 2004), to the North Atlantic (Christensen *et al.* 2003, Frank *et al.* 2005) and the Black Sea (Daskalov *et al.* 2007). A common theme among these examples is the subsequent rise of lower-trophic species with the ability to respond rapidly to changes in resources and environment (i.e. the schooler and colonizer group). Therefore, commercial fishing in the NWACS created, and continues to create, opportunities for the expression of top-down effects (*sensu* Carpenter *et al.* 1985) through the reduction of predators and competitors and the subsequent competition among species that these species had once consumed and excluded, respectively.

Community changes in the GOM and GB arguably provided the strongest support for cascading effects. In both regions, schooling and colonizing species progressively increased in local abundance, and importantly, in their ranges of spatial behaviors utilized (light gray polygons in fig. 1.6A-G & D-F). The patterns were especially striking in the GOM, where a rapid change in the schooling and colonizing species dominated an early shift in the interspecific A-O relationship. Additionally, it is even possible that increases in schoolers and colonizers in the GOM and GB could have been more pronounced if not for the rise of other predators and competitors like spiny dogfish and skates that are not traditionally targeted by fisheries. Overall, the patterns displayed here are typical for a system exhibiting successional response to disturbance, with a rise in species with rapid life histories and increases in spatial heterogeneity (declining r^2) among all species (Odum 1969, Connell and Slatyer 1977).

In contrast to the northern regions, increases in pelagic and schooling species in SNE occurred abruptly near the beginning of the time series (fig. 1.3). Consequently, A-O trends appeared to reflect less the relative assemblage structure between high and low trophic species (as in the GOM and GB), and more the competitive dynamics within the schooling and colonizing species. In early years, when schoolers and colonizers were still at relatively low abundance, two species with potentially overlapping diets were dominant, scup and longfin squid (Jacobson 2005, Sagarese *et al*. 2011). Scup would quickly decline and other species would temporarily rise in abundance (fig. 1.6H). Eventually however, longfin squid became the dominant species, with only the planktivorous Atlantic herring also remaining at high local abundance. Based on diet, Atlantic herring may overlap briefly with younger stages of longfin squid (Jacobson 2005), but not with most post-juvenile individuals (Reid *et al*. 1999). An argument can be made that because higher predators and competitively dominant species did not

increase in SNE to the extent they did in the GOM and GB (fig. 1.3), the longfin squid was able to exclude most similar species though numerical dominance and resource exploitation (e.g. Hardin 1960).

Impacts of Climate and Community Consequences

Unlike commercial landings, climate-related factors were more commonly associated with community A-O indices. I found that local water temperatures were significantly related to aspects of A-O variation in three of four regions assessed, regardless of the regression model used (table 1.3). Increasing bottom temperature was associated with stronger A-O relationships (larger r^2) in the SNE and in the GOM when autocorrelation was taken into account. It was also related to overall decreases in organismal density (larger slope) and the proportion of occupied habitat (smaller intercepts) in SNE. Surface temperature exhibited significant relationships with organismal density and occupied space in the GOM (for non-autocorrelation models) and SNE. In GB it was related to overall increases in density observed in that region.

When present, associations between community trends and large-scale oceanic and atmospheric patterns were generally consistent with those observed for local thermal conditions. In the GOM, the Gulf Stream index had similar relationships with A-O indices that surface temperature did for non-autocorrelation models. In addition, regression results in SNE were consistent among surface temperature, bottom temperature and Gulf Stream index for both types of models used. Here poleward movements of the Gulf Stream's northern wall were related to decreases in occupied sites and a strengthening of the A-O relationship as they were with local water temperature. In the GB region, increasing AMO index values (which is calculated from surface temperature) was related to increasing organismal density in addition to increases in sites

occupied and a weakening of the A-O relationship. Links between community spatial trends and both local thermal variation and basin-wide thermohaline processes suggest that temperature-related community impacts are not a spatially insular matter and predictions of future biological change should take such considerations into account.

Previous research also confirms relationships between species' geographic distributions and climate factors in the eastern (Perry *et al.* 2005, Dulvy *et al.* 2008) and western (Nye *et al*. 2009) Atlantic. Whether moving latitudinally or to greater depth, climate-driven distribution shifts may translate into community spatial trends through multiple mechanisms. Community change can occur through the simple alteration of assemblage structure, bringing about new combinations and proportions of interacting life histories. Lucy and Nye (2010) found that climatic variations were related to NWACS assemblages becoming more similar over time to those historically at lower (and warmer) latitudes. Even within a single species, geographic displacement may cause the gain or loss of functional spatial behaviors within a defined region. If one accepts that some species exhibit spatial heterogeneity relative to their population centroid (Brown 1984, Gaston *et al*. 1998) or ecological niches (e.g. Martínez-Meyer *et al.* 2013), substantial distribution shifts may eventually cause changes in spatial utilization within a given locale as species move relative to regional boundaries. A study on 36 fish stocks (comprising 30 species) on the NEFSC showed that 17 displayed significant poleward movements (Nye *et al.* 2009). It is possible that such movements were reflected in A-O relationships observed in this study, which were evaluated over the same area and included many of the same species. Although I analyzed communities in discrete geographic units, connectivity across adjacent regions is likely an important element in observed trends and should be investigated further.

Conclusions

Whether observed transformations in NWACS communities represent ephemeral responses to disturbance or new and long-term regimes remains to be seen, but the continued fishing of higher trophic level species suggests that a return to past states is a goal that may be increasingly unattainable (Christensen *et al.* 2003). Furthermore, the prospect of prolonged climate change represents an additional source of uncertainty regarding the future of coastal communities. The macro-scale approach presented here addresses questions that are relevant to ecological and density-dependent processes that regulate demographic rates within communities. Through the identification of community trends and of potential drivers, we are better equipped to address questions concerning variability of individual populations. This information is critical for management and conservation efforts that attempt to understand the nature of past change and predict future conditions of natural marine resources.

Table 1.1. List of common and scientific names of species composing regional communities. Bold letters represent inclusion of species into one of thtree groups (**P** = predators & competitors, **S** = schoolers & colonizers and **O** = others).

Gulf of Maine (GOM)	**Georges Bank (GB)**
Acadian Redfish (*Sebastes fasciatus*, Sebastidae), **P**	Acadian Redfish (*Sebastes fasciatus*, Sebastidae), **P**
Alewife (*Alosa pseudoharengus*, Clupeidae), **S**	American Lobster (*Homarus americanus*, Nephropidae), **O**
Alligatorfish (*Aspidophoroides monopterygius*, Agonidae), **P**	American Plaice (*Hippoglossoides platessoides*, Pleuronectidae), **P**
American Lobster (*Homarus americanus*, Nephropidae), **O**	Atlantic Cod (*Gadus morhua*, Gadidae), **P**
American Plaice (*Hippoglossoides platessoides*, Pleuronectidae), **P**	Atlantic Herring (*Clupea harengus*, Clupeidae), **S**
American Shad (*Alosa sapidissima*, Clupeidae), **S**	Atlantic Mackerel (*Scomber scombrus*, Scombridae), **S**
Atlantic Argentine (*Argentina silus*, Argentinidae), **S**	Butterfish (*Peprilus triacanthus*, Stromateidae), **S**
Atlantic Cod (*Gadus morhua*, Gadidae), **P**	Fourspot Flounder (*Paralichthys oblongus*, Paralichthyidae), **P**
Atlantic Hagfish (*Myxine glutinosa*, Myxinidae), **O**	Goosefish (*Lophius americanus*, Lophiidae), **P**
Atlantic Herring (*Clupea harengus*, Clupeidae), **S**	Gulf Stream Flounder (*Citharichthys arctifrons*, Paralichthyidae), **P**
Atlantic Wolffish (*Anarhichas lupus*, Anarhichadidae), **P**	Haddock (*Melanogrammus aeglefinus*, Gadidae), **P**
Cusk (*Brosme brosme*, Lotidae), **P**	Little Skate (*Leucoraja erinacea*, Rajidae), **P**
Fourbeard Rockling (*Enchelyopus cimbrius*, Lotidae), **P**	Longfin Squid (*Doryteuthis pealeii*, Loliginidae), **S**
Goosefish (*Lophius americanus*, Lophiidae), **P**	Longhorn Sculpin (*Myoxocephalus octodecemspinosus*, Cottidae), **P**
Haddock (*Melanogrammus aeglefinus*, Gadidae), **P**	Northern Sand Lance (*Ammodytes dubius*, Ammodytidae), **S**
Longfin Squid (*Doryteuthis pealeii*, Loliginidae), **S**	Northern Shortfin Squid (*Illex illecebrosus*, Ommastrephidae), **S**
Longhorn Sculpin (*Myoxocephalus octodecemspinosus*, Cottidae), **P**	Ocean Pout (*Macrozoarces americanus*, Zoarcidae), **P**
Northern Shortfin Squid (*Illex illecebrosus*, Ommastrephidae), **S**	Pollock (*Pollachius virens*, Gadidae), **P**
Ocean Pout (*Macrozoarces americanus*, Zoarcidae), **P**	Red Hake (*Urophycis chuss*, Phycidae), **P**
Pollock (*Pollachius virens*, Gadidae), **P**	Sea Raven (*Hemitripterus americanus*, Hemitripteridae), **P**
Red Hake (*Urophycis chuss*, Phycidae), **P**	Sea Scallop (*Placopecten magellanicus*, Pectinidae), **S**
Sea Raven (*Hemitripterus americanus*, Hemitripteridae), **P**	Silver Hake (*Merluccius bilinearis*, Merlucciidae), **P**
Sea Scallop (*Placopecten magellanicus*, Pectinidae), **S**	Spiny Dogfish (*Squalus acanthias*, Squalidae), **P**
Silver Hake (*Merluccius bilinearis*, Merlucciidae), **P**	Thorny Skate (*Amblyraja radiata*, Rajidae), **P**
Smooth Skate (*Malacoraja senta*, Rajidae), **P**	White Hake (*Urophycis tenuis*, Phycidae), **P**
Spiny Dogfish (*Squalus acanthias*, Squalidae), **P**	Windowpane (*Scophthalmus aquosus*, Scophthalmidae), **P**
Thorny Skate (*Amblyraja radiata*, Rajidae), **P**	Winter Flounder (*Pseudopleuronectes americanus*, Pleuronectidae), **P**
White Hake (*Urophycis tenuis*, Phycidae), **P**	Winter Skate (*Leucoraja ocellata*, Rajidae), **P**
Winter Flounder (*Pseudopleuronectes americanus*, Pleuronectidae), **P**	Witch Flounder (*Glyptocephalus cynoglossus*, Pleuronectidae), **P**
Witch Flounder (*Glyptocephalus cynoglossus*, Pleuronectidae), **P**	Yellowtail Flounder (*Limanda ferruginea*, Pleuronectidae), **P**

Table 1.1. *(continued)*

Southern New England (SNE)	Mid-Atlantic Bight (MAB)
American Lobster (*Homarus americanus*, Nephropidae), **O**	American Lobster (*Homarus americanus*, Nephropidae), **O**
American Shad (*Alosa sapidissima*, Clupeidae), **S**	Atlantic Croaker (*Micropogonias undulatus*, Sciaenidae), **P**
Atlantic Cod (*Gadus morhua*, Gadidae), **P**	Atlantic Rock Crab (*Cancer irroratus*, Cancridae), **O**
Blackbelly Rosefish (*Helicolenus dactylopterus*, Sebastidae), **P**	Black Sea Bass (*Centropristis striata*, Serranidae), **P**
Butterfish (*Peprilus triacanthus*, Stromateidae), **S**	Blackbelly Rosefish (*Helicolenus dactylopterus*, Sebastidae), **P**
Fawn Cusk-Eel (*Lepophidium profundorum*, Ophidiidae), **P**	Buckler Dory (*Zenopsis conchifera*, Zeidae), **O**
Fourspot Flounder (*Paralichthys oblongus*, Paralichthyidae), **P**	Butterfish (*Peprilus triacanthus*, Stromateidae), **S**
Goosefish (*Lophius americanus*, Lophiidae), **P**	Chain Dogfish (*Scyliorhinus retifer*, Scyliorhinidae), **P**
Gulf Stream Flounder (*Citharichthys arctifrons*, Paralichthyidae), **P**	Clearnose Skate (*Raja eglanteria*, Rajidae), **P**
Haddock (*Melanogrammus aeglefinus*, Gadidae), **P**	Fawn Cusk-Eel (*Lepophidium profundorum*, Ophidiidae), **P**
Little Skate (*Leucoraja erinacea*, Rajidae), **P**	Fourspot Flounder (*Paralichthys oblongus*, Paralichthyidae), **P**
Longfin Squid (*Doryteuthis pealeii*, Loliginidae), **S**	Goosefish (*Lophius americanus*, Lophiidae), **P**
Longhorn Sculpin (*Myoxocephalus octodecemspinosus*, Cottidae), **P**	Gulf Stream Flounder (*Citharichthys arctifrons*, Paralichthyidae), **P**
Northern Searobin (*Prionotus carolinus*, Triglidae), **P**	Unclassified Lanternfish (Myctophidae), **S**
Northern Shortfin Squid (*Illex illecebrosus*, Ommastrephidae), **S**	Little Skate (*Leucoraja erinacea*, Rajidae), **P**
Ocean Pout (*Macrozoarces americanus*, Zoarcidae), **P**	Longfin Squid (*Doryteuthis pealeii*, Loliginidae), **S**
Red Hake (*Urophycis chuss*, Phycidae), **P**	Northern Searobin (*Prionotus carolinus*, Triglidae), **P**
Round Herring (*Etrumeus teres*, Dussumieriidae), **S**	Northern Shortfin Squid (*Illex illecebrosus*, Ommastrephidae), **S**
Scup (*Stenotomus chrysops*, Sparidae), **S**	Red Hake (*Urophycis chuss*, Phycidae), **P**
Sea Raven (*Hemitripterus americanus*, Hemitripteridae), **P**	Rosette Skate (*Leucoraja garmani*, Rajidae), **P**
Sea Scallop (*Placopecten magellanicus*, Pectinidae), **S**	Round Herring (*Etrumeus teres*, Dussumieriidae), **S**
Silver Hake (*Merluccius bilinearis*, Merlucciidae), **P**	Scup (*Stenotomus chrysops*, Sparidae), **S**
Spiny Dogfish (*Squalus acanthias*, Squalidae), **P**	Sea Scallop (*Placopecten magellanicus*, Pectinidae), **S**
Spotted Hake (*Urophycis regia*, Phycidae), **P**	Silver Hake (*Merluccius bilinearis*, Merlucciidae), **P**
Summer Flounder (*Paralichthys dentatus*, Paralichthyidae), **P**	Smooth Dogfish (*Mustelus canis*, Triakidae), **P**
White Hake (*Urophycis tenuis*, Phycidae), **P**	Spiny Dogfish (*Squalus acanthias*, Squalidae), **P**
Windowpane (*Scophthalmus aquosus*, Scophthalmidae), **P**	Spotted Hake (*Urophycis regia*, Phycidae), **P**
Winter Flounder (*Pseudopleuronectes americanus*, Pleuronectidae), **P**	Summer Flounder (*Paralichthys dentatus*, Paralichthyidae), **P**
Winter Skate (*Leucoraja ocellata*, Rajidae), **P**	Weitzmans Pearlsides (*Maurolicus weitzmani*, Sternoptychidae), **S**
Yellowtail Flounder (*Limanda ferruginea*, Pleuronectidae), **P**	Windowpane (*Scophthalmus aquosus*, Scophthalmidae), **P**

Table 1.2. Kendall's τ from Mann-Kendall trend tests on A-O indices. Time periods over which trends were calculated were determined using breakpoint analysis. P-values on trends are shown in parentheses.

	GOM	GB	SNE	MAB
slope	**1963-1972**: 0.067 (0.858)	**1963-2008**: -0.295 (0.004)	**1963-2008**: 0.194 (0.058)	**1967-1994**: 0.254 (0.061)
	1973-1982: -0.867 (< 0.001)			**1995-2008**: -0.187 (0.381)
	1983-2008: -0.317 (0.025)			
intercept	**1963-1973**: -0.127 (0.640)	**1963-1981**: -0.029 (0.889)	**1963-2008**: -0.219 (0.032)	**1967-1994**: -0.302 (0.026)
	1974-1981: 1.000 (< 0.001)	**1982-2008**: 0.595 (< 0.001)		**1995-2008**: 0.165 (0.443)
	1982-2008: 0.100 (0.478)			
r^2	**1963-1985**: -0.605 (< 0.001)	**1963-1981**: 0.099 (0.576)	**1963-2008**: 0.227 (0.027)	**1967-2008**: -0.134 (0.217)
	1986-2008: -0.107 (0.492)	**1982-2008**: -0.516 (< 0.001)		

Table 1.3. Summary of autocorrelation tests and regressions of A-O indices on external factors Durbin-Watson (D-W) test statistics shown with p-values in parentheses. The slopes of GLS regressions with and without autocorrelation are also provided with p-values in parentheses. Significant relationships are bold and asterisks denote regressions where normal and autocorrelation models were both significant.

region	index	extrernal factor	D-W	$slope_{non\text{-}auto.}$	$slope_{auto.}$
GOM	**slope**	surface temperature	**1.03 (< 0.001)**	**-0.016 (< 0.001)**	-0.0078 (0.13)
		bottom temperature	**0.70 (< 0.001)**	0.0032 (0.71)	0.0088 (0.27)
		Gulf Stream index	**0.87 (< 0.001)**	**-0.014 (0.031)**	-0.00015 (0.99)
		AMO index	**1.05 (< 0.001)**	**-0.084 (< 0.01)**	0.016 (0.65)
		commercial landings	**1.02 (< 0.001)**	**0.023 (0.022)**	-0.0040 (0.67)
	intercept	surface temperature	**1.02 (< 0.001)**	**0.015 (0.016)**	0.0045 (0.50)
		bottom temperature	**0.80 (< 0.001)**	-0.0017 (0.87)	-0.012 (0.27)
		Gulf Stream index	**0.97 (< 0.001)**	**0.020 (0.014)**	0.012 (0.29)
		AMO index	**0.95 (< 0.001)**	**0.11 (< 0.01)**	0.070 (0.12)
		commercial landings	**1.10 (< 0.01)**	-0.024 (0.070)	0.019 (0.13)
	r^2	surface temperature	**1.00 (< 0.001)**	-0.029 (0.064)	-0.013 (0.44)
		bottom temperature	**0.86 (< 0.001)**	0.0042 (0.87)	**0.053 (0.047)**
		Gulf Stream index	**1.06 (< 0.01)**	**-0.046 (0.020)**	-0.022 (0.44)
		AMO index	**0.90 (< 0.001)**	-0.067 (0.51)	0.018 (0.88)
		commercial landings	**1.00 (< 0.001)**	0.047 (0.15)	-0.0010 (0.97)
GB	**slope**	surface temperature	2.08 (0.85)	**-0.0042 (0.022) ***	**-0.0042 (0.019) ***
		bottom temperature	1.94 (0.77)	-0.0029 (0.27)	-0.0027 (0.32)
		Gulf Stream index	1.87 (0.58)	-0.0058 (0.077)	-0.0058 (0.097)
		AMO index	2.29 (0.36)	**-0.042 (< 0.01) ***	**-0.045 (<0.01) ***
		commercial landings	2.00 (0.92)	0.0024 (0.25)	0.0023 (0.28)
	intercept	surface temperature	**1.39 (0.02)**	-0.0025 (0.61)	-0.0054 (0.34)
		bottom temperature	**1.40 (0.03)**	-0.0073 (0.27)	-0.0092 (0.22)
		Gulf Stream index	**1.33 (0.01)**	-0.0049 (0.56)	-0.0034 (0.76)
		AMO index	1.75 (0.34)	**0.12 (< 0.01) ***	**0.12 (< 0.01) ***
		commercial landings	**1.45 (0.04)**	0.00032 (0.95)	0.0025 (0.70)
	r^2	surface temperature	1.58 (0.12)	0.0017 (0.87)	0.00025 (0.98)
		bottom temperature	1.62 (0.16)	0.012 (0.39)	0.0091 (0.55)
		Gulf Stream index	1.61 (0.14)	0.014 (0.44)	0.013 (0.54)
		AMO index	1.87 (0.58)	**-0.18 (0.034)**	-0.17 (0.065)
		commercial landings	1.61 (0.15)	-0.0031 (0.78)	-0.0052 (0.69)

Table 1.3. *(continued)*

region	index	extrernal factor	D-W	slope (norm.)	slope (auto.)
SNE	**slope**	surface temperature	2.10 (0.80)	0.0022 (0.20)	0.0028 (0.069)
		bottom temperature	2.11 (0.70)	**0.0089 (0.026) ***	**0.0091 (0.019) ***
		Gulf Stream index	2.05 (0.95)	0.0071 (0.058)	**0.0072 (0.031)**
		AMO index	2.04 (0.97)	0.013 (0.51)	0.014 (0.46)
		commercial landings	2.12 (0.78)	**-0.0015 (0.026) ***	**-0.0014 (0.020) ***
	intercept	surface temperature	2.24 (0.45)	**-0.010 (0.014) ***	**-0.012 (< 0.01) ***
		bottom temperature	2.22 (0.44)	**-0.027 (< 0.01) ***	**-0.029 (< 0.01) ***
		Gulf Stream index	2.31 (0.34)	**-0.027 (< 0.01) ***	**-0.028 (< 0.001) ***
		AMO index	1.94 (0.77)	-0.0090 (0.85)	-0.0055 (0.91)
		commercial landings	2.16 (0.67)	**0.0039 (0.014) ***	**0.0039 (0.011) ***
	r^2	surface temperature	2.47 (0.12)	**0.023 (< 0.01) ***	**0.026 (< 0.001) ***
		bottom temperature	2.27 (0.36)	**0.048 (0.012) ***	**0.050 (< 0.01) ***
		Gulf Stream index	2.34 (0.30)	**0.049 (< 0.01) ***	**0.050 (< 0.001) ***
		AMO index	2.07 (0.88)	0.028 (0.76)	0.028 (0.76)
		commercial landings	2.11 (0.79)	-0.0054 (0.089)	-0.0054 (0.086)
MAB	**slope**	surface temperature	1.73 (0.34)	0.000018 (0.99)	0.000024 (0.99)
		bottom temperature	1.71 (0.32)	-0.0021 (0.52)	-0.0022 (0.50)
		Gulf Stream index	1.91 (0.69)	0.0050 (0.30)	0.0051 (0.31)
		AMO index	1.92 (0.70)	-0.036 (0.061)	-0.035 (0.069)
		commercial landings	1.70 (0.28)	0.0039 (0.52)	0.0055 (0.39)
	intercept	surface temperature	1.54 (0.11)	-0.00069 (0.91)	-0.00064 (0.92)
		bottom temperature	1.51 (0.10)	0.0059 (0.49)	0.0067 (0.43)
		Gulf Stream index	1.68 (0.25)	-0.011 (0.40)	-0.0090 (0.52)
		AMO index	1.72 (0.30)	0.085 (0.081)	0.076 (0.16)
		commercial landings	1.51 (0.09)	-0.0091 (0.56)	-0.016 (0.35)
	r^2	surface temperature	1.84 (0.56)	-0.0040 (0.75)	-0.0040 (0.75)
		bottom temperature	1.86 (0.63)	0.0036 (0.83)	0.0031 (0.86)
		Gulf Stream index	1.99 (0.87)	0.013 (0.60)	0.014 (0.59)
		AMO index	1.98 (0.85)	-0.14 (0.15)	-0.14 (0.15)
		commercial landings	1.83 (0.52)	0.033 (0.29)	0.036 (0.27)

Figure 1.1. Sum of commercial landings in the GOM (A), GB (B), SNE (C) and MAB (D). For reference, the year 1976 is marked to denote the Magnuson-Stevens Fishery Conservation and Management Act (dashed gray lines).

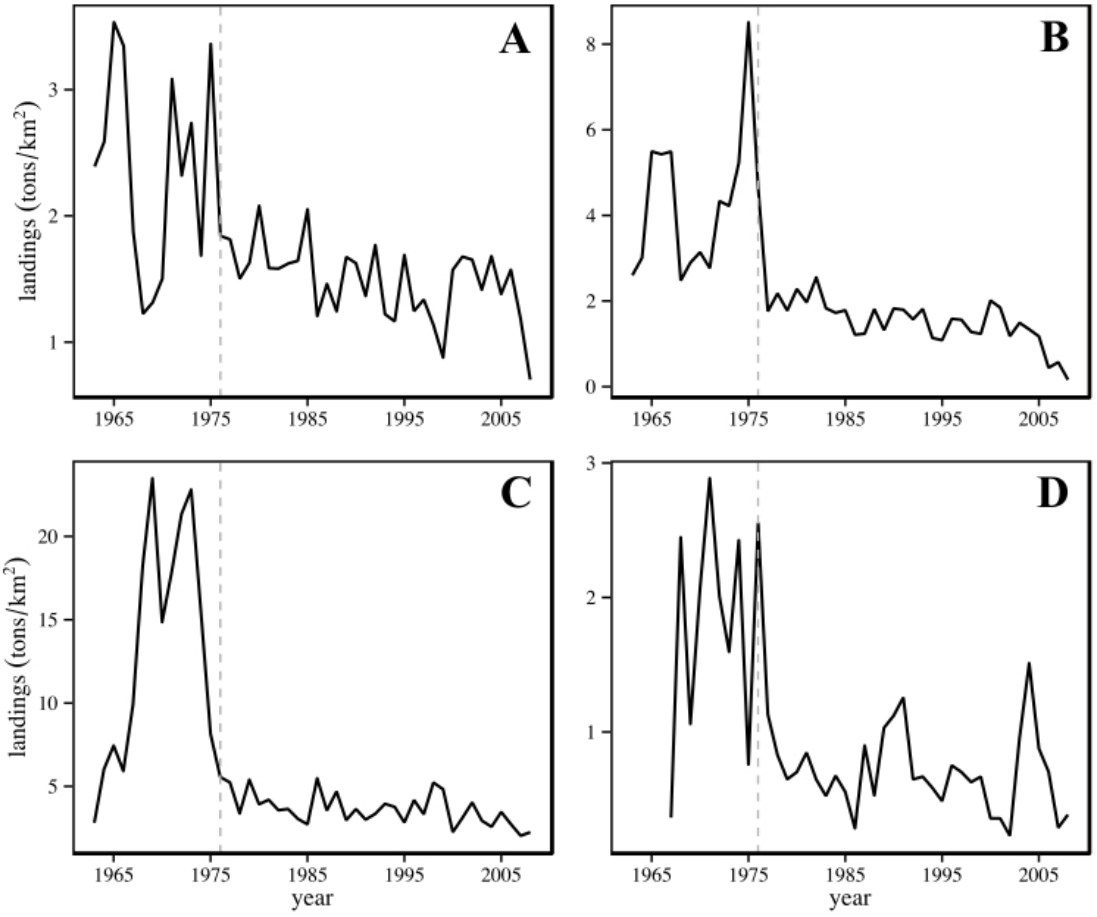

Figure 1.2. Climate-related variables used in this study. Panels display mean regional bottom temperature (A), mean regional surface temperature (B), the Gulf Stream index (C) and the Atlantic Multidecadal Oscillation index (D).

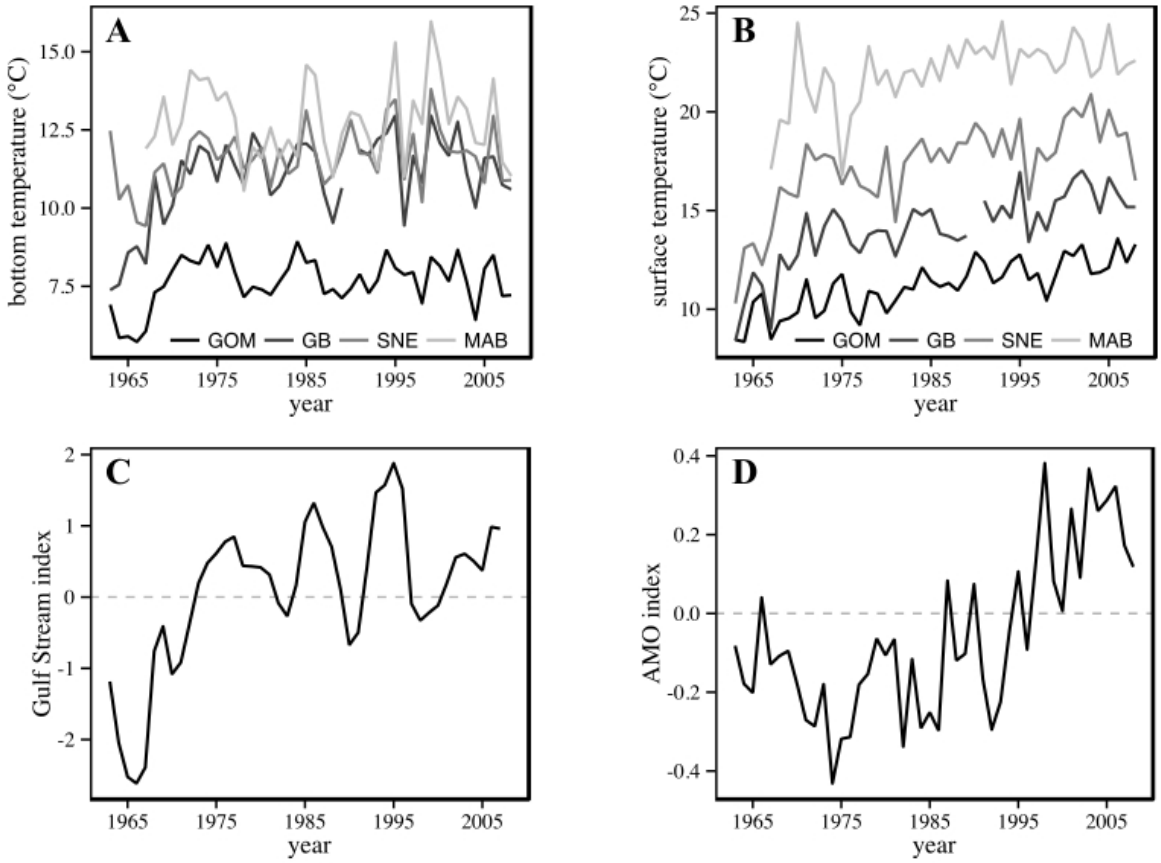

Figure 1.3. Local abundance trends in the GOM (A), GB (B), SNE (C) and MAB (D). Values are divided among species groups, representing predators & competitors (dark gray), schoolers & colonizers (light gray) and others (black).

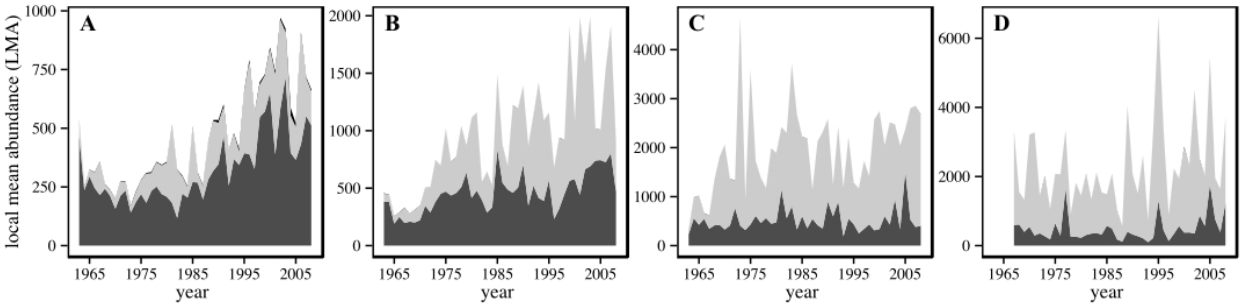

Figure 1.4. Forms of variation for interspecific A-O regression indices. Differences in slope (A) result in individuals occupying fewer regions (gray horizontal lines) at a given abundance. Changes in the A-O intercept (B, regression lines) reflect a uniform shift in the total proportion of sites occupied. The r^2 (B, dark gray shaded area) describes the diversity of spatial of occupancy strategies (light gray bars) utilized by species in a region. Often the slope and intercept both vary (C), and the degree to which each does, speaks to the nature of variation.

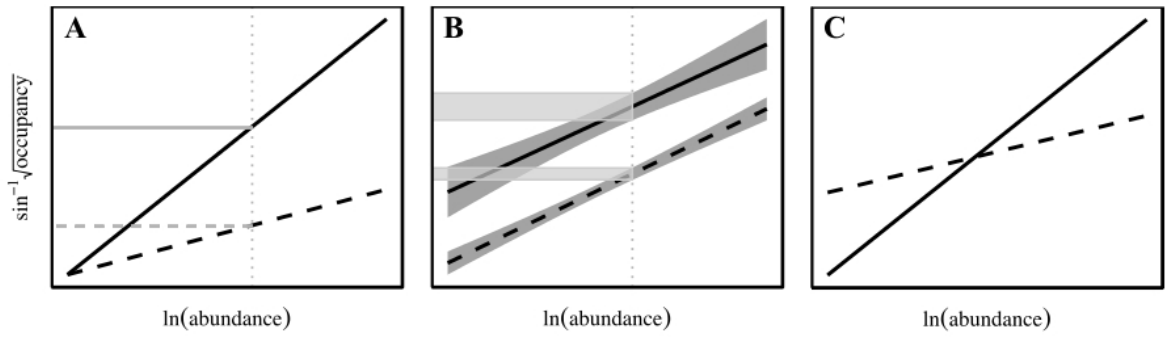

Figure 1.5. Regional time series of the interspecific A-O slope (A-D), intercept (E-H) and r^2 (I-L), with 95% confidence bands (gray area). Dashed linear regressions indicate segments chosen by breakpoint analyses, with asterisks denoting a significant trend with the Mann-Kendall trend test. Map after Lucy and Nye (2010).

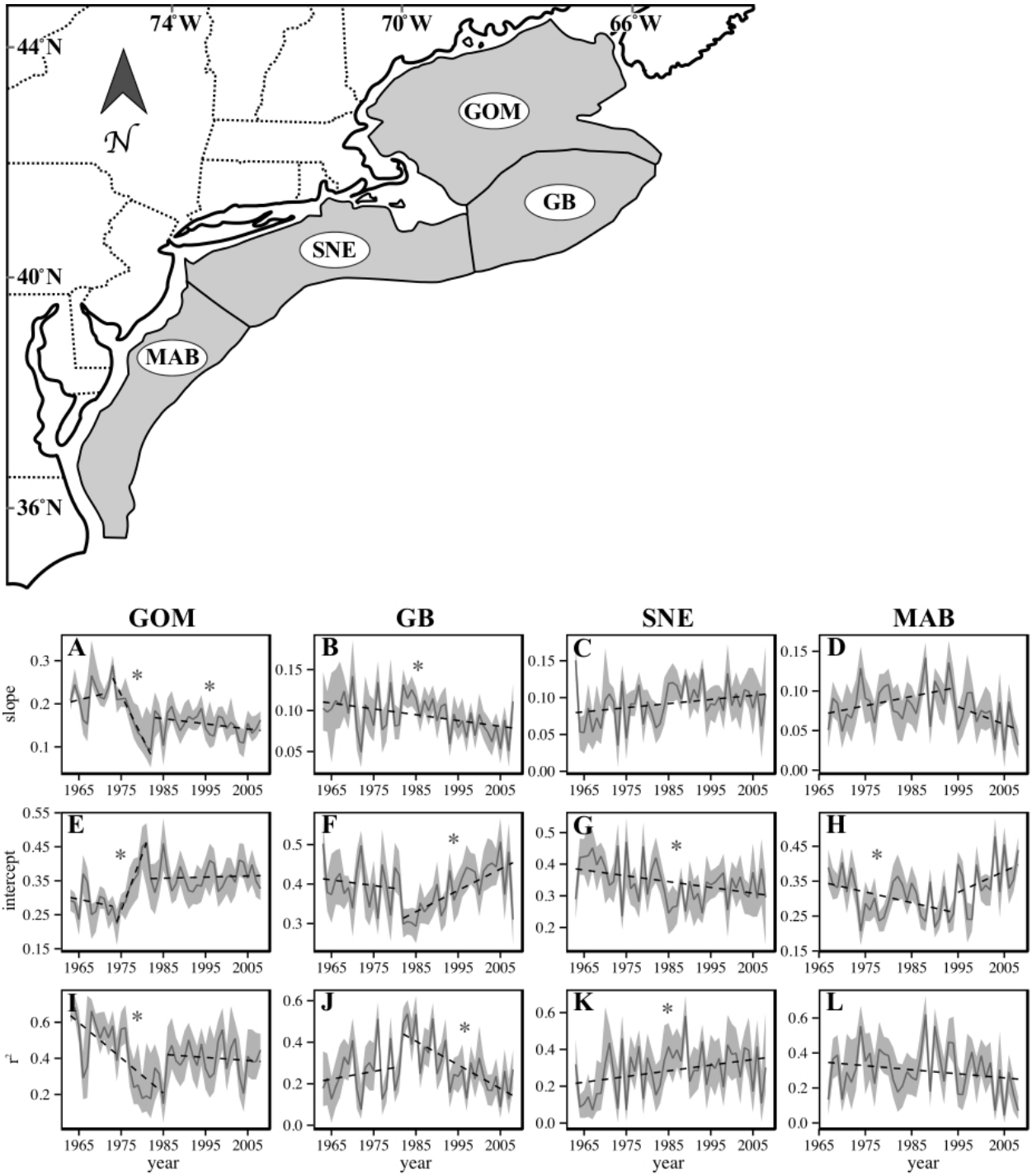

Figure 1.6. Selected yearly A-O relationships in the GOM (A-C), GB (D-F), SNE (G-I) and MAB (J-L). Dashed regression lines are yearly OLS fits. Species are divided among predators & competitors (open circles, dark gray convex hull), schoolers & colonizers (open circles, light gray convex hull) and others (filled circles).

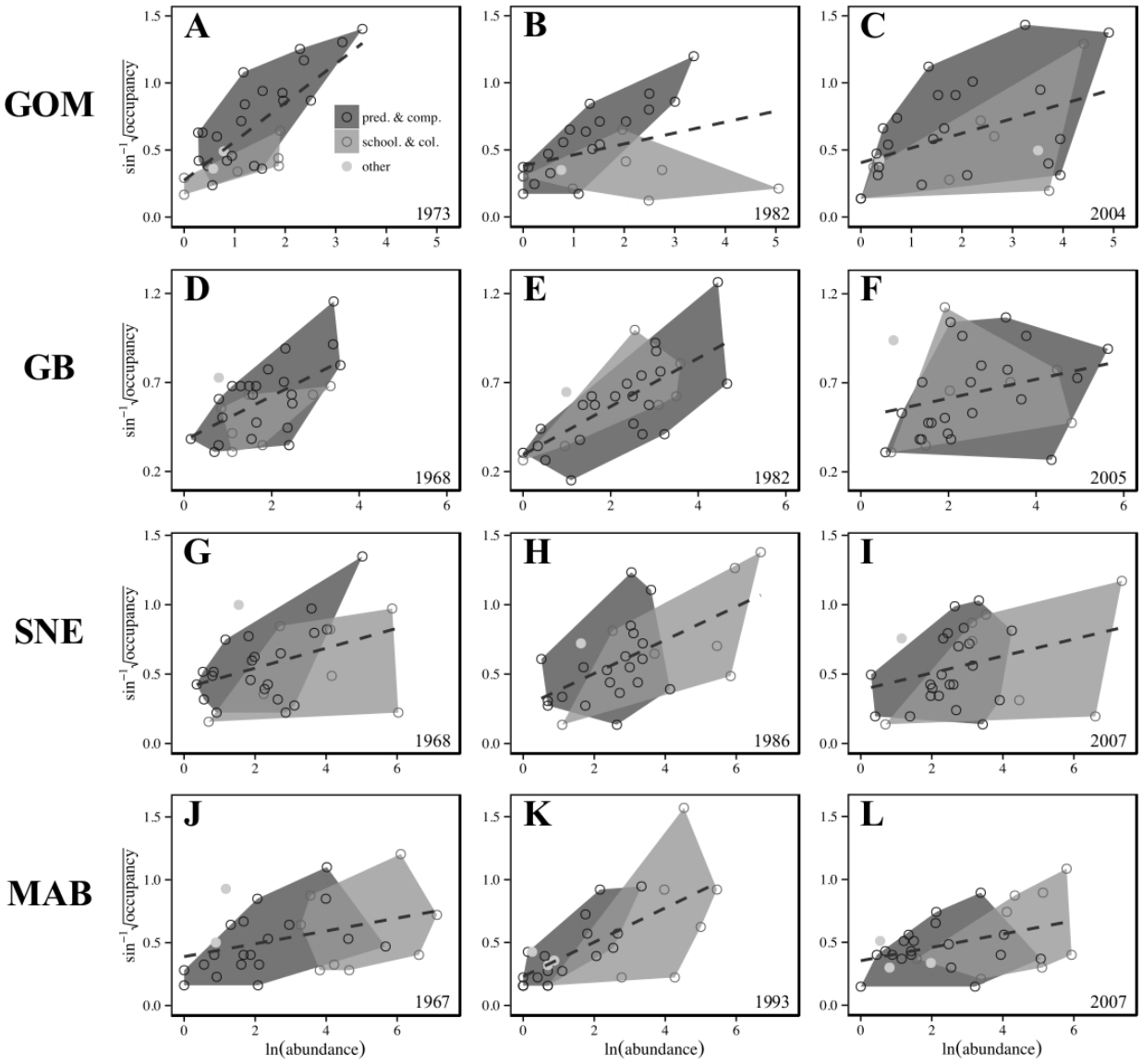

Chapter 2

Exploration of Interspecific Abundance-Occupancy Relationships using Empirically Derived Pseudo-Communities

Introduction

The relationship between organism and habitat is among the most fundamental concerns in ecology. A commonly used method to assess this association is to measure changes in site occupancy over a range of abundances. The abundance-occupancy (A-O) relationship, as it is often called, has been used to describe spatial organization in a wide variety of systems from terrestrial (Gaston and Blackburn 2003, Buckley and Freckleton 2010), to marine (Fisher and Frank 2004, Martinez *et al*. 2014), freshwater (Heino 2005) and even experimentally controlled protist communities (Gaston and Warren 1997). In its interspecific form, the A-O relationship has been used to investigate overriding patterns of spatial organization within communities, with its structure being attributed to factors such as species interactions (Holt *et al*. 2004), environmental/habitat change (Webb *et al*. 2007) and direct anthropogenic impacts (Frisk *et al*. 2011). This area of research provides a potentially powerful tool to assess macro-scale patterns and drivers of community structure.

A positive interspecific A-O relationship has been cited as one of the most ubiquitous of ecological phenomena (e.g. Cowley *et al*. 2001, Holt *et al*. 2002, Buckley and Freckleton 2010). However, the frequency of positive relationships may not be as compelling as sometimes portrayed. In fact, depending on the definition of abundance used (i.e. local or global abundance), the A-O relationship may be constrained to be positive (Wilson 2011). If so, a null relationship does not exist, even when individuals are uniformly dispersed, following a Poisson distribution (Hartley 1998). Therefore trying to pin down mechanisms can be a particularly

dubious exercise, as the removal of factors cannot completely eliminate the positive relationship. For example, Gaston and Warren (1997) were unable to coerce significant changes in A-O relationships for experimental microcosms exposed to a range of disturbance regimes. Understandably, this has led to varying opinions on the utility of A-O relationships and on the presence of potential artifacts (Gaston *et al*. 1998, Hartley 1998, Wilson 2008, Rindorf and Lewy 2012, Webb *et al*. 2012) as well as a general lack of consensus regarding mechanisms (Gaston *et al*. 1997, Borregaard and Rahbek 2010).

Despite concerns, investigations of A-O relationships have proved useful in a great variety of studies in spatial ecology (Borregaard and Rahbek 2010). A fairly unexplored application is the utility of the relationship as a relative indicator of community state. In this sense, there is less emphasis on the generation or existence of the positive relationship itself, but on trends in its structure and their relation to macroecological processes (although the two are certainly not independent). The key is the power of comparison that the approach inherently engenders, whereby relationships may be observed over a range of conditions and states. It is therefore possible to identify characteristics of communities that are particularly influential to observed changes. The products of temporal analyses are also tractable to comparisons with external factors that vary with time. For these reasons, a temporal evaluation of A-O relationships may also provide insights into A-O mechanisms.

Storch and Gaston (2004) suggested that macroecological studies are useful for untangling complexity at lower levels of organization, as they extract the emergent properties of large systems with extensive interaction networks. It follows then that the reverse should be true; to understand the inner workings of the A-O relationship, one must start with models or properties of the individual species that compose it. It can be asserted without much controversy

that distribution characteristics of individual species may be influenced by any number of factors, from extrinsic variation (e.g. climate, habitat quality, harvest…*et cetera*) to biological interactions (e.g. competition and predation). Therefore, forces that influence the abundance of any species, its overall distribution or use of available habitat are also expected to determine its relative location in the interspecific A-O space, and will be linked to the collective structure of the community relationship.

The above framework focuses on the distributional properties of species. Likewise, some researchers have suggested that generally positive interspecific A-O relationships are the expected result of an assemblage of species with variable dispersion characteristics (Wright 1991, Hartley 1998, Holt *et al*. 2002). Others have tested this idea through simulation methods. Wilson (2011) investigated the use of abundance measures in A-O relationships with species generated under multiple statistical distributions and with varying parameter values. A-O relationships that were calculated with the global abundance measure were constrained to be above zero, whereas those calculated from local abundance may be positive, negative or zero. Wilson's approach provides potentially useful information on theoretical and methodological possibilities, but details of his methods often lack relevance to natural systems (for detailed discussion, see Webb *et al*. 2012). Other A-O work has relied on simulated communities (e.g. Gaston *et al*. 1998), but for specific application. Reducing a community of organisms to its basic statistical components places the investigator in a position to approach questions regarding mechanistic forces underlying interspecific A-O relationships. Further, simulations that are rooted in distribution parameters derived from the actual spatial occurrence of organisms allow for direct hypothesis testing hypotheses that are relevant to natural communities.

In chapter 1, I investigated spatial trends in demersal communities on the northwest Atlantic coastal shelf (NWACS). I found that changes to community structure varied both temporally and spatially and were variably associated with local temperature/climate trends and commercial fishing activity. This work suggested that fundamental transformations had occurred in organism-habitat associations within some NWACS regions, sometimes owing to assemblage variation, but also to intraspecific changes in habitat use. The implications of these changes for ecological interactions within regional communities are great indeed (see also Fisher and Frank 2004, Frisk *et al*. 2011). In addition, NWACS regions are home to a number of historically important fisheries (Lear 1998) and determining the patterns and drivers of spatial and assemblage dynamics is key to the management of their marine resources.

Here I apply a simulation method to explore the use of A-O relationships in interspecific spatial analyses with empirical data analyzed in Chapter 1. To do this, I fit species-specific yearly survey catch data (i.e. fishery-independent) to negative binomial (NB) distributions, which were then used to generate simulated communities (pseudo-communities, hereafter) for Monte Carlo simulations of the A-O relationship. With this procedure, I aimed to capture temporal changes in abundance and spatial aggregation over biologically realistic ranges, something that has not been done previously in the A-O literature. My primary interest was to observe whether pseudo-communities displayed temporal trends comparable to those observed empirically. In other words, does realistic A-O variation result from a collection of NB-distributed species? In addition, I investigated preliminary manipulations of NB parameters to begin to understand processes underlying observed changes. The first concerned the role of intraspecific variation in distribution characteristics and the formation of community trends. Second, I focused on a period of particularly intense community change observed in the Gulf of

Maine from 1973-1982 as a case study to explore temporal changes in the A-O relationship. Particularly, I was interested in how ecological processes, here top-down effects, may be expressed as a trend in the relationship. Lastly, I provided recommendations for other studies of similar scope and objective.

Methods

Empirical data

I used bottom trawl survey data from the Northeast Fisheries Science Center (NEFSC) for all years available between 1963 and 2008. The survey uses a depth-stratified, random sampling design where effort is proportional to strata area (Sosebee and Cadrin 2006). Data were divided among four contiguous regions that comprise much of the Northwest Atlantic Coastal Shelf (NWACS) ecosystem, and are largely accepted divisions based on physical topography and biological communities (Lucey & Nye, 2010). Regions (from north to south) were the Gulf of Maine (GOM), Georges Bank (GB), Southern New England (SNE) and the Mid-Atlantic Bight (MAB). For simplicity, I limited regional communities to unique combinations of 30 species, whose inclusion was based on a ranked index that reflected both catch values and the proportion of years encountered. Details on selection criteria and lists of species can be found in Chapter 1. Within a region, the same 30 species were used for all years present to insure a level of consistency in the assemblage over the time series.

Statistical distributions and relation to external factors

I used the MASS package (Venables and Ripley 2002) in R (R core team 2013) to estimate yearly NB parameters for each species' catches among sampled sites. The NB distribution was used because of its incorporation of aggregation, an essential element in density-

dependent ecological interactions, and also due to its prevalence in wide-ranging investigations of distribution and spatial structure (Holt *et al*. 2002). For the NB distribution, the parameter μ describes species' mean catches across sampled sites and the size parameter k is a measure of spatial aggregation. As k deceases, aggregation or spatial clumping increases, and vice versa. Additionally, I used the estimated parameters to calculate a composite parameter p (equation 1), which is the probability of success in a NB trial and is analogous to site occupancy (Holt *et al*. 2002). For fitting purposes, I only included species in years where they were caught more than twice. In addition, I removed NB fits that were anomalous and unrealistic (e.g. k = 100).

$$p = \frac{k}{k+\mu} \qquad \text{Equation 1}$$

Finally, I regressed yearly mean parameter values on several external factors of interest. This analysis provided direct comparisons to regressions performed in Martinez (chapter 1) for empirical A-O relationships. The first four factors were related to temperature and climate variation (i.e. local surface temperature, local bottom temperature, the Gulf Stream Index and the Atlantic Multidecadal Oscillation Index) and the last was commercial landings. For full details of each external factor, see Martinez (Chapter 1). The Durbin-Watson test was used to determine whether there was temporal autocorrelation between NB parameters and external factors. This was followed by generalized least-squares (GLS) regression. All relationships were estimated with and without autocorrelated errors.

Monte Carlo Simulations

Figure 2.1 presents a flow chart for the overall steps included in the simulation methods used here. Using randomly generated variates (i.e. catches) from fitted NB distributions, I created pseudo-communities for 30 species, distributed among 10,000 sites. This assumes that

species' catches are representative of their true abundance, which is explicitly assumed whenever catches are used to infer relative abundance. Based on previous unpublished work, I chose 10,000 sites in order to create a sufficiently large pool of values to sample from as to avoid potential biases due to unrealistically low variation in catches. Pseudo-community data were generated for all survey years, creating a full time series that reflected the temporally variable mix of distributions within natural communities. This routine was replicated for each of 500 Monte Carlo simulation runs.

I imitated a yearly trawl survey by randomly selecting 55 sites per region, out of the 10,000 available. This level of sampling effort was well within the range of yearly trawls attempted within a region for NEFSC fall surveys. I calculated interspecific occupancy values and two measures of abundance from the resulting catch data. The regional or global mean abundance (GMA) was the total number of individuals caught divided by the total number of sites sampled. In comparison, the local mean abundance (LMA) of a species was the number of individuals caught divided by the number of occupied sites. Occupancy was the number of sites where at least one individual was caught divided by the total number of sampled sites. I evaluated A-O relationships in each year using ordinary least-squares regression of arcsine transformed O on the natural logarithm of A (equation 2), where s is the slope and C is the intercept. Yearly regression statistics (slopes, intercepts and coefficients of determination r^2) were used as indices of community state (for further details, see Martinez, chapter 1).

$$O = sA + C \qquad \text{Equation 2}$$

For each simulation run I tested for evidence of overall temporal change in A-O indices using the Mann-Kendall trend test, which uses rank correlations to assess trends in monotonic variables (McLeod 2011).

NB parameter manipulations

Two additional sets of simulations were attempted in order to investigate different scenarios relating to the variety of distributions within communities. First, I examined the role of intraspecific variation in spatial behavior on overall trends. To do this, I determined each species' median NB parameters over all years and ran simulations with these values held constant for the entire time series. With this procedure, the relative interspecific variation among communities was still preserved. A second set of simulations was also run to look at a more specific ecological question. I concentrated on the period between 1973 and 1982 in the GOM, where especially strong A-O trends were identified. During this time, Martinez (chapter 1) suggested that a relatively small subset of species with highly aggregative tendencies appeared to be the primary, direct participants in observed community changes as they responded to top-down (indirect) effects of fishery removals. In order to assess the relative impacts of these species on trends, I ran simulations with and without seven species identified as "schoolers and colonizers" (chapter 1, table 1.1).

Results

Statistical distributions and relation to external factors

Parameter estimates were variable with time and also among regions (fig. 2.2). The two northern areas (GB and the GOM) displayed the strongest evidence for trends in mean parameter values (table 2.1), although changes in two of three parameters in SNE were also significant. In

general, regressions of mean NB parameters on external factors (table 2.2) displayed stronger relationships than those with A-O indices (compare with table 1.3 in chapter 1). Among variables tested, surface temperature was most often significantly associated with NB parameters, followed by the Gulf Stream Index (table 2.2). In the GOM, GB and SNE, the Atlantic Multidecadal Oscillation (AMO) had consistently positive relationships with the parameter mu μ. Finally, bottom temperature and commercial landings each had only a single significant association with NB parameters.

Temporal trends in A-O indices

Positive A-O relationships were identified in all simulations evaluated with GMA. In other words, a negative slope was never encountered in 90,000 possible instances, across all years, regions and simulation iterations. When LMA was used, only 11 (0.012%) negative A-O relationships were found. Of these, 1 occurred in the GOM, 6 in GB, 1 in SNE and 3 were in the MAB.

Overall, mean yearly values of simulated A-O indices estimated with GMA showed strong coherence to empirical relationships (fig. 2.3). This means that both empirical and simulated trends occurred in the same direction and were generally of comparable magnitude (table 2.3). Time series trends were strongest and most prevalent in northern regions. In the GOM, mean values of Kendall's τ ($\bar{\tau}$) pointed to significant trends in 100% of iterations for slope ($\bar{\tau}$ = -0.42, 95% CI [-0.52, -0.33]), intercept ($\bar{\tau}$ = -0.37, 95% CI [-0.48, -0.25]) and r^2 ($\bar{\tau}$ = -0.41, 95% CI [-0.51, -0.30]). Similar results were found for GB slopes ($\bar{\tau}$ = -0.46, 95% CI [-0.56, -0.37]) intercepts ($\bar{\tau}$ = -0.26, 95% CI [-0.37, -0.14]) and r^2 values ($\bar{\tau}$ = -0.31, 95% CI [-0.42, -0.19]), although tests for the latter two were not statistically significant over all iterations. In

SNE, simulations supported weak evidence of intercept trends in 12% of iterations ($\bar{\tau}$ = -0.13, 95% CI [-0.24, -0.02]) and in r^2 for 23.4% ($\bar{\tau}$ = 0.15, 95% CI [0.01, 0.29]). These results mean that r^2 had an opposite trend in SNE than in the GOM and GB, resulting in an A-O relationship that increased in strength over time. There were no signs of overall trends for any A-O index in the MAB.

Simulated A-O relationships with LMA were similar to empirical results (fig. 2.4), but not to the extent that GMA relationships were. Despite a few evident deviations, their overall patterns of variation were again comparable with respect to directions and magnitudes of change (table 2.3). Compared to GMA simulations, there were generally lower proportions of significant trends encountered. In addition, within regions, slope and r^2 trends from LMA relationships shared directionality (i.e. both positive or both negative) and intercept trends were always opposite of them (table 2.3). This pattern was not observed for simulations with GMA. In the GOM, there was evidence for trends in slope ($\bar{\tau}$ = -0.35, 95% CI [-0.46, -0.25]), intercept ($\bar{\tau}$ = 0.21, 95% CI [0.08, 0.32]) and r^2 ($\bar{\tau}$ = -0.18, 95% CI [-0.30, -0.07]). Here, significant slope trends were present in 99.8% of simulation iterations, compared to 56.8% for the intercept and 36.6% for the r^2. For the GB region, only slope had consistent trends ($\bar{\tau}$ = -0.29, 95% CI [-0.42, -0.17]). Trends were present in fairly lower number for SNE intercepts ($\bar{\tau}$ = -0.15, 95% CI [-0.28, -0.02]) and r^2 values ($\bar{\tau}$ = 0.15, 95% CI [0.03, 0.28]). Finally, indices in the MAB once again had little or no evidence of trends.

Constant spatial behaviors

Simulations run with constant median parameters resulted in relationships that were generally stable with time (fig. 2.5), with variation around yearly means that was comparable to

simulations with variable parameters (figs. 2.3 and 2.4). Still, relative regional differences in interspecific composition were preserved, as indicated by different levels of mean index values maintained in each. Results for GMA (fig. 2.5 A-C) and LMA (fig. 2.5 D-F) were similar, but as expected the latter did often have larger variance around mean values. The mean trends of simulations were all very small with relatively large 95% confidence intervals (table 2.4), compared to simulations with variable NB parameters (table 2.3). Although centered on zero, large variance in yearly relationships did result in a small number of significant trends. Averaging over regions, GMA relationships resulted in 5% (± 0.34 SE) of simulations having a trend, with 4.8% (± 0.20 SE) for LMA.

Impact of schoolers and colonizers

Removals of seven highly aggregative species in the GOM from 1973 to 1982 caused numerous changes in A-O index trends (fig. 2.6). In general the impacts of species removals were greater for simulations calculated with LMA than GMA. For GMA, the mean slope trend ($\bar{\tau}$) changed from -0.55 (95% CI -0.78, -0.29) to -0.42 (95% CI -0.78, -0.29) when species were removed. This corresponded with a decline from 72% of simulated trends being significant at the p = 0.05 level, down to 32%. Much of the variation among sets of simulations appears to be concentrated in the last few years (fig. 2.6A). In contrast, for LMA relationships, divergence in slopes occurs much earlier on (fig. 2.6D). In this case, mean slope trends declined from -0.63 (95% CI -0.91, -0.33) to -0.37 (95% CI -0.69, -0.02), with percentages of significant trends dropping from 80% to 26%.

For GMA relationships, removals of species caused the A-O intercepts to increase uniformly in absolute value but very little with respect to their trends ($\bar{\tau}$ = -0.33, 95% CI [-0.60,

-0.02] to $\bar{\tau}$ = -0.26, 95% CI [-0.56, -0.02]) (fig. 2.6B). In addition, already low occurrences of significant trends decreased further when species were removed (16% to 6%). Larger changes were observed for LMA relationships, where intercepts dropped from 0.50 (95% CI 0.16, 0.80) to 0.25 (95% CI -0.07, 0.56) following removals. Here, 57% of simulation trials were significant when all species were present compared to 8% with removals.

Among A-O indices, removals had the largest impacts on r^2 trends (fig. 2.6C and F). GMA relationships saw a decline in trends from -0.56 (95% CI -0.82, -0.20) to -0.26 (95% CI -0.51, 0.02), with significant trends dropping from 68% of simulation trials to 5%. Again, the decrease drove trends down such that a trend of zero was included in the 95% confidence interval. A similar decrease in trend was seen for LMA relationships ($\bar{\tau}$ = -0.49, 95% CI [-0.78, -0.11] to $\bar{\tau}$ = -0.07, 95% CI [-0.38, 0.20]), where 55% of simulation trends were significant before removals and 0% after.

Discussion

My work shows that A-O relationships of NWACS communities can be approximated by a collection of NB distributions that vary in a manner largely consistent with those observed empirically. Even with randomly selected catch values from species' estimated distributions, simulated communities shared major patterns and features of variation with natural communities. Given that NB distributions tended to preserve the relative spatial relationships among species from year to year, I interpret the existence of trends in A-O indices to reflect genuine changes in the relative spatial diversity contained within pseudo-communities. This work lends credence to the idea that the structure of interspecific A-O relationships may be thought of as a collection of spatial behaviors (Wright 1991, Holt *et al*. 2002, Webb *et al*. 2012). Consequently, I suggest that

the A-O relationship is a suitable indicator of change at the community level, encompassing processes relating to assemblage structure, ecological interactions and any other factor affecting species' distributions. However, this work does imply that community structure may alternatively be assessed with NB parameters alone. Mean NB parameters displayed similar temporal trends (table 2.1) as A-O indices and had generally stronger relationships to external factors (table 2.2). Further investigation of the collective structure of community distributional parameters as indicators of community state is therefore warranted.

For this research, I ran Monte Carlo simulations for A-O relationships estimated with GMA as well as LMA. Which method a researcher should use is dependent on the goals of their work (Webb *et al*. 2012). It did appear that the NB fits resulted in slightly better agreement with empirical results for GMA (fig. 2.3) than LMA (fig. 2.4). This is not completely surprising as relationships using GMA often have larger slopes and are less variable (higher r^2), as indicated by their limitation to positive A-O relationships. However, LMA is often regarded as a more ecologically relevant measure to use in A-O relationships (Borregaard and Rahbek 2010). In fact, its larger variance and ability to achieve negative relationships make it desirable; for species that follow a NB distribution, distances in A-O space between different spatial strategies are exaggerated for LMA relative to GMA (see fig. 2.2B in Webb *et al*. 2012). Assuming an ecological basis underlying species' differences, LMA provides a better opportunity to identify species with disparate strategies for habitat occupation.

Despite LMA relationships displaying obvious deviations between empirical and simulated results, their resulting trends were consistent. Any time that an empirical result was significant, zero was excluded from the 95% confidence intervals of simulated trends (table 2.3), meaning that both methods were in agreement on the existence of trends. For GMA this was also

true for all relationships except the A-O intercept in SNE, where the empirical trend was not significant ($p = 0.14$) but the 95% confidence interval for simulations just barely excluded a zero trend (CI -0.12, -0.02). In addition, there were two instances for GMA relationships (GOM intercept and MAB r^2) and three for LMA (GOM intercept, MAB intercept and MAB r^2) where the empirical trend fell outside of the 95% confidence interval of simulation trends. When these instances did occur, however, the differences were not so marked as to affect interpretations regarding community change. It is possible that the aforementioned discrepancies may not fully be a failure of NB distributions to adhere to empirical variation, but can also due to concessions that were necessary for parameter fitting (i.e. removal of species from certain years where catches were too low or fitted NB parameters were anomalous). Even so, the overall similarities of yearly variation suggest that simulations offer an adequate stand-in for natural communities for further exploration of the role of distribution diversity in A-O relationships.

Holt *et al*. (2002) questioned whether, "…spatial distribution strictly provides an explanation of interspecific occupancy-abundance relationships, rather than simply a rephrasing of one macroecological pattern in terms of another". While the concern is valid, I argue that the link is not trivial as it provides researchers a path with which to explore the fundamental underpinnings of A-O relationships, primarily though manipulations of distribution diversity. My preliminary efforts to alter the structure of A-O relationships through the modification of NB parameters are by no means elegant, but give further evidence of the role of spatial behaviors in A-O relationships and provide a glimpse into the types of questions that one my approach within this framework. The ability to largely eliminate trends in regional pseudo-communities by holding NB parameters constant over time confirmed that while a collection of spatial behaviors will recreate an A-O relationship, yearly variation is only achieved through changes in species'

spatial diversity. The variability in yearly A-O indices was enough that a small percent of simulation runs did display significant temporal variation (table 2.4). However, a review of these results reveals that the yearly variation in A-O indices for this exercise (fig. 2.5) does not resemble that of simulations with naturally variable distributions (figs. 2.3 and 2.4). It is also clear from the range of simulated trends (table 2.4), that there is no real or compelling evidence for temporal change.

Factors influencing the distribution characteristics of species, and therefore the form of the A-O relationship, are numerous and vary both temporally and regionally. In harvested systems, for example, species are often confronted by both habitat degradation and direct removals of organisms (Frisk *et al*. 2011). Notably, the depletion of generally higher trophic species has led to top-down affects in the north Atlantic (Christensen *et al*. 2003). These conditions favor species with short life histories and the ability to rapidly colonize space. With this in mind, I looked at the role that seven schooling and colonizing species (defined in Martinez, chapter 1) played in trends observed during a particularly rapid period of change in the GOM between 1973 and 1982. The apparent impact of species removals on the A-O slope was clearer for relationships with LMA versus GMA (fig. 2.6A and D). This likely reflects the nature of change, where a rise in highly aggregative species with patchy distributions will be more evident at local scales than regional. Furthermore, the existence of intercept trends in GMA simulations with and without species removals (fig. 2.6B) points to an additional source of decline in habitat occupation than the one tested here. Finally, trends in the strengths of A-O relationships were similar for both measures of abundance (fig. 2.6C & F). The large decline in r^2 trends suggest that the increase in colonizing species over this time period added a new source of variation to communities that was different from that of the demersal species.

Overall, the work presented here suggests that A-O relationships are useful for assessing changes in the state of communities as it relates to the distribution characteristics of its inhabitants. Additionally, these methods evaluate aspects of communities that may not be explicitly apparent with other metrics like diversity or assemblage structure alone (Solow 1993, Rochet and Trenkel 2003). In fact, an advantage of the A-O relationship is that it is the net result of numerous community processes and may reasonably detected changes in any one of them. This makes it desirable as an initial indicator of community state that does not have extensive data requirements (e.g. Hughes *et al*. 1998, Link *et al*. 2002). The ability of A-O relationships to identify change, however, may vary by system. For example, the effect size of the interspecific A-O relationship is often stronger in marine environments than terrestrial and freshwater (Blackburn *et al*. 2006).

In addition to the utility of the A-O relationship as an indicator of community structure, I believe that the approach used here offers a framework from which researchers may test numerous ecological hypotheses. I provided two simple examples, but more elegant designs can certainly be tested with these methods. For example, one may imagine a simulation where NB parameters are allowed to vary based on expected species' response to changing levels of climate change or harvest. In this way, I believe that much may be learned about specific communities as well as the nature of the A-O relationship and mechanisms driving it.

Table 2.1. Trends (Kendall's τ) of mean NB parameter estimates with p-values provided in pararentheses.

region	A-O index	τ (p-val.)
GOM	size	**-0.22 (0.036)**
	mu	**0.52 (< 0.001)**
	probability	**-0.55 (< 0.001)**
GB	size	**-0.38 (< 0.001)**
	mu	**0.50 (< 0.001)**
	probability	**-0.53 (< 0.001)**
SNE	size	-0.040 (0.70)
	mu	**0.33 (< 0.01)**
	probability	**-0.32 (< 0.01)**
MAB	size	-0.064 (0.56)
	mu	-0.17 (0.12)
	probability	0.12 (0.28)

Table 2.2. Summary of autocorrelation tests and regressions of mean NB parameters on external factors. Durbin-Watson (D-W) test statistics shown with p-values in parentheses. The slopes of GLS regressions with and without autocorrelation are also provided with p-values in parentheses. Significant relationships are bold and asterisks denote regressions where normal and autocorrelation models were both significant.

region	index	extrernal factor	D-W	$slope_{non\text{-}auto.}$	$slope_{auto.}$
GOM	**size**	surface temperature	1.93 (0.73)	**-0.052 (0.0023)**	**-0.052 (< 0.01) ***
		bottom temperature	1.70 (0.26)	-0.033 (0.26)	-0.029 (0.37)
		Gulf Stream index	1.88 (0.60)	**-0.050 (0.024)**	**-0.049 (0.037) ***
		AMO index	1.64 (0.17)	-0.017 (0.88)	0.036 (0.78)
		commercial landings	1.73 (0.31)	0.067 (0.066)	0.065 (0.093)
	mu	surface temperature	**1.40 (0.028)**	**0.16 (< 0.001)**	**0.12 (< 0.01) ***
		bottom temperature	**0.9 (< 0.001)**	0.048 (0.48)	0.055 (0.44)
		Gulf Stream index	**0.98 (< 0.001)**	0.092 (0.072)	0.075 (0.31)
		AMO index	1.53 (0.080)	**1.08 (< 0.001)**	**0.90 (< 0.01) ***
		commercial landings	**1.12 (< 0.01)**	-0.14 (0.11)	0.075 (0.37)
	probability	surface temperature	1.55 (0.095)	**-0.18 (< 0.001)**	**-0.16 (< 0.001) ***
		bottom temperature	**0.92 (< 0.001)**	-0.059 (0.39)	-0.056 (0.43)
		Gulf Stream index	**1.06 (< 0.001)**	**-0.11 (0.027)**	-0.085 (0.24)
		AMO index	1.62 (0.16)	**-0.99 (< 0.001)**	**-0.72 (< 0.01) ***
		commercial landings	**1.18 (< 0.01)**	0.16 (0.056)	-0.028 (0.74)
GB	**size**	surface temperature	1.71 (0.26)	**-0.064 (< 0.001)**	**-0.065 (< 0.001) ***
		bottom temperature	1.69 (0.25)	**-0.078 (< 0.001)**	**-0.075 (< 0.001) ***
		Gulf Stream index	1.98 (0.84)	**-0.10 (< 0.001)**	**-0.10 (< 0.001) ***
		AMO index	**1.05 (< 0.001)**	-0.067 (0.59)	0.12 (0.46)
		commercial landings	**1.26 (< 0.01)**	**0.040 (< 0.01)**	0.030 (0.11)
	mu	surface temperature	**1.35 (0.017)**	**0.12 (< 0.001)**	0.040 (0.24)
		bottom temperature	**1.09 (< 0.001)**	**0.14 (< 0.01)**	0.037 (0.38)
		Gulf Stream index	**1.09 (< 0.001)**	**0.21 (< 0.001)**	**0.14 (0.051) ***
		AMO index	**0.82 (< 0.001)**	**0.88 (< 0.01)**	**0.67 (0.024) ***
		commercial landings	**1.12 (< 0.01)**	**-0.12 (< 0.01)**	-0.014 (0.73)
	probability	surface temperature	**1.29 (< 0.01)**	**-0.17 (< 0.001)**	**-0.085 (0.017) ***
		bottom temperature	**1.04 (< 0.001)**	**-0.20 (< 0.001)**	-0.063 (0.16)
		Gulf Stream index	**1.10 (< 0.001)**	**-0.30 (< 0.001)**	**-0.18 (0.030) ***
		AMO index	**0.64 (< 0.001)**	**-0.89 (< 0.01)**	-0.43 (0.18)
		commercial landings	**0.95 (< 0.001)**	**0.15 (< 0.001)**	0.0023 (0.96)

Table 2.2. *(continued)*

region	index	extrernal factor	D-W	slope (norm.)	slope (auto.)
SNE	**size**	surface temperature	**1.45 (0.040)**	**-0.027 (0.013)**	**-0.028 (0.026) ***
		bottom temperature	**1.37 (0.025)**	-0.025 (0.32)	0.0030 (0.92)
		Gulf Stream index	1.55 (0.091)	**-0.055 (0.016)**	-0.051 (0.059)
		AMO index	**1.28 (< 0.01)**	0.17 (0.16)	0.16 (0.27)
		commercial landings	**1.27 (< 0.01)**	0.0010 (0.78)	-0.0030 (0.59)
	mu	surface temperature	1.97 (0.82)	**0.048 (0.010)**	**0.046 (0.019) ***
		bottom temperature	1.58 (0.14)	0.061 (0.17)	0.045 (0.30)
		Gulf Stream index	1.64 (0.17)	0.060 (0.14)	0.051 (0.30)
		AMO index	1.59 (0.13)	**0.51 (0.013)**	**0.53 (0.021) ***
		commercial landings	1.79 (0.39)	**-0.017 (0.015)**	**-0.016 (0.043) ***
	probability	surface temperature	1.91 (0.67)	**-0.074 (< 0.001)**	**-0.071 (< 0.01) ***
		bottom temperature	**1.40 (0.034)**	-0.081 (0.11)	-0.036 (0.46)
		Gulf Stream index	1.55 (0.095)	**-0.11 (0.016)**	-0.096 (0.089)
		AMO index	**1.26 (< 0.01)**	-0.33 (0.17)	-0.38 (0.19)
		commercial landings	**1.47 (0.049)**	**0.017 (0.040)**	0.011 (0.29)
MAB	**size**	surface temperature	1.63 (0.20)	0.032 (0.095)	0.034 (0.082)
		bottom temperature	1.66 (0.25)	-0.0040 (0.87)	0.0070 (0.79)
		Gulf Stream index	1.62 (0.18)	0.027 (0.52)	0.046 (0.33)
		AMO index	1.62 (0.17)	-0.21 (0.17)	-0.26 (0.15)
		commercial landings	1.65 (0.21)	-0.0040 (0.93)	0.0089 (0.87)
	mu	surface temperature	1.69 (0.28)	**-0.064 (0.028)**	-0.054 (0.069)
		bottom temperature	**1.40 (0.043)**	0.048 (0.24)	0.053 (0.19)
		Gulf Stream index	1.80 (0.44)	**-0.14 (0.022)**	-0.13 (0.064)
		AMO index	**1.45 (0.049)**	-0.11 (0.67)	-0.11 (0.72)
		commercial landings	1.6 (0.16)	0.10 (0.18)	0.053 (0.51)
	probability	surface temperature	1.93 (0.76)	**0.079 (< 0.01)**	**0.078 (< 0.01) ***
		bottom temperature	1.64 (0.23)	-0.050 (0.22)	-0.046 (0.26)
		Gulf Stream index	1.96 (0.79)	**0.15 (0.014)**	**0.15 (0.019) ***
		AMO index	1.62 (0.17)	-0.11 (0.64)	-0.15 (0.59)
		commercial landings	1.76 (0.39)	-0.090 (0.24)	-0.067 (0.39)

Table 2.3. Empirical and mean simulated trends (Kendall's τ) for A-O relationships estimated with GMA and LMA. Empirical trends are shown with p-values and simulated trends with 95% confidence intervals (based on percentile). Significant trends and those excluding zero from 95% confidence intervals appear in bold. The percent of significant trends (out of 500 simulations) is also provided.

method	region	A-O index	$\tau_{empirical}$ (p-val.)	mean $\tau_{simulated}$ (95% CI)	% sig.
GMA	**GOM**	slope	**-0.39 (< 0.001)**	**-0.42 (-0.52, -0.33)**	100
		intercept	**-0.49 (< 0.001)**	**-0.37 (-0.48, -0.25)**	100
		r^2	**-0.44 (< 0.001)**	**-0.41 (-0.51, -0.30)**	100
	GB	slope	**-0.53 (< 0.001)**	**-0.46 (-0.56, -0.37)**	100
		intercept	**-0.29 (< 0.01)**	**-0.26 (-0.37, -0.14)**	86.8
		r^2	**-0.30 (< 0.01)**	**-0.31 (-0.42, -0.19)**	96.6
	SNE	slope	0.15 (0.16)	0.07 (-0.08, 0.20)	2.6
		intercept	-0.15 (0.14)	**-0.13 (-0.24, -0.02)**	12
		r^2	**0.23 (0.02)**	**0.15 (0.01, 0.29)**	23.4
	MAB	slope	-0.01 (0.93)	-0.01 (-0.15, 0.13)	0.2
		intercept	-0.10 (0.36)	-0.08 (-0.18, 0.02)	0.6
		r^2	-0.19 (0.09)	-0.002 (-0.13, 0.12)	0.0
LMA	**GOM**	slope	**-0.43 (< 0.001)**	**-0.35 (-0.46, -0.25)**	99.8
		intercept	**0.35 (< 0.001)**	**0.21 (0.08, 0.32)**	56.8
		r^2	**-0.21 (0.04)**	**-0.18 (-0.30, -0.07)**	36.6
	GB	slope	**-0.29 (< 0.01)**	**-0.29 (-0.42, -0.17)**	91
		intercept	0.13 (0.22)	0.10 (-0.03, 0.22)	5.6
		r^2	-0.06 (0.56)	-0.10 (-0.23, 0.02)	8.2
	SNE	slope	0.20 (0.051)	0.11 (-0.03, 0.25)	10.8
		intercept	**-0.21 (0.04)**	**-0.15 (-0.28, -0.02)**	23.4
		r^2	**0.22 (0.03)**	**0.15 (0.03, 0.28)**	23.8
	MAB	slope	-0.11 (0.31)	0.01 (-0.11, 0.14)	0.0
		intercept	0.08 (0.45)	-0.08 (-0.18, 0.03)	0.8
		r^2	-0.13 (0.23)	0.03 (-0.09, 0.15)	0.0

Table 2.4. Mean simulated trends for A-O relationships, estimated with constant NB parameters across all years. Trends are shown with 95% confidence intervals. The percent of significant trends (out of 500 simulations) is also provided.

method	region	A-O index	mean $\tau_{simulated}$ (95% CI)	% sig.
GMA	**GOM**	slope	-0.0047 (-0.215, 0.190)	6.2
		intercept	-0.0014 (-0.196, 0.194)	4.0
		r^2	0.0097 (-0.169, 0.203)	3.8
	GB	slope	0.00042 (-0.200, 0.197)	4.4
		intercept	-0.0052 (-0.198, 0.202)	4.8
		r^2	0.0025 (-0.194, 0.194)	4.4
	SNE	slope	-0.00012 (-0.219, 0.206)	6.4
		intercept	0.0038 (-0.190, 0.209)	4.6
		r^2	-0.0012 (-0.192, 0.196)	4.4
	MAB	slope	0.0017 (-0.231, 0.216)	7.2
		intercept	0.0032 (-0.199, 0.210)	3.8
		r^2	0.0018 (-0.217, 0.209)	5.0
LMA	**GOM**	slope	-0.0048 (-0.213, 0.187)	5.8
		intercept	-0.0038 (-0.206, 0.183)	4.4
		r^2	-0.00041 (-0.211, 0.206)	5.8
	GB	slope	0.010 (-0.194, 0.189)	4.2
		intercept	0.0097 (-0.191, 0.195)	4.0
		r^2	0.010 (-0.195, 0.199)	4.8
	SNE	slope	0.00032 (-0.188, 0.204)	4.6
		intercept	-0.0011 (-0.197, 0.207)	4.4
		r^2	-0.00020 (-0.179, 0.206)	3.6
	MAB	slope	-0.0014 (-0.200, 0.215)	5.4
		intercept	-0.00062 (-0.215, 0.202)	5.2
		r^2	-0.00071 (-0.207, 0.210)	4.8

Figure 2.1. Flow diagram showing methods for generating pseudo-communities and assessing A-O trends within a region.

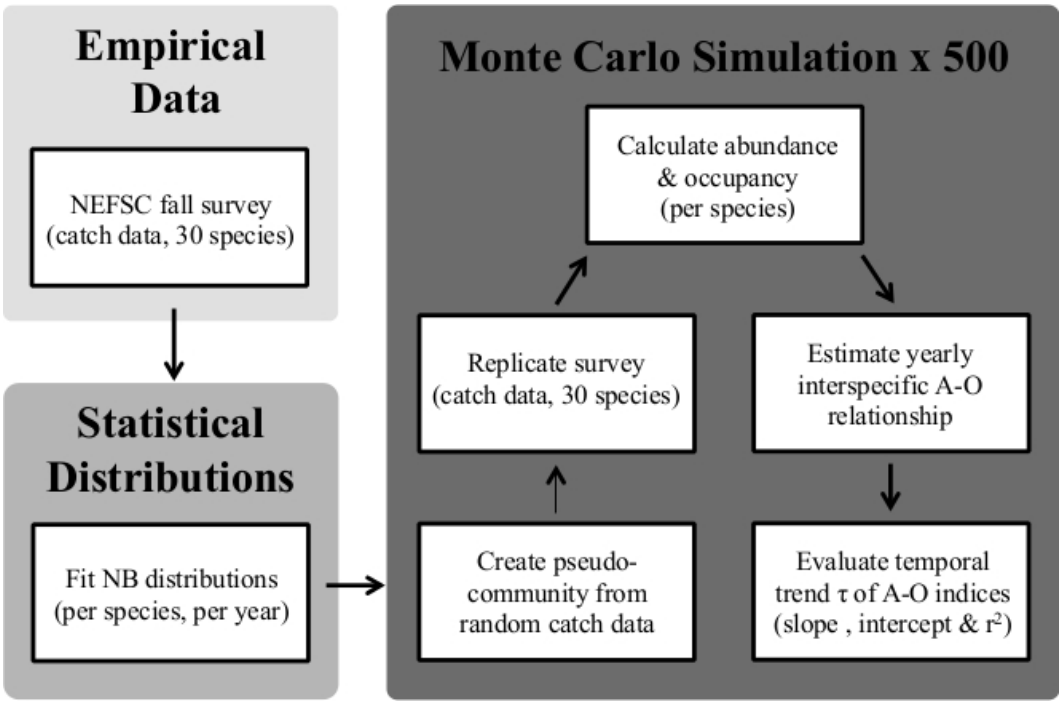

Figure 2.2. Time series of the natural log of mean negative binomial parameters (rows) for communities in each of four NWACS communities (columns). Standard error is shown as the shaded gray region.

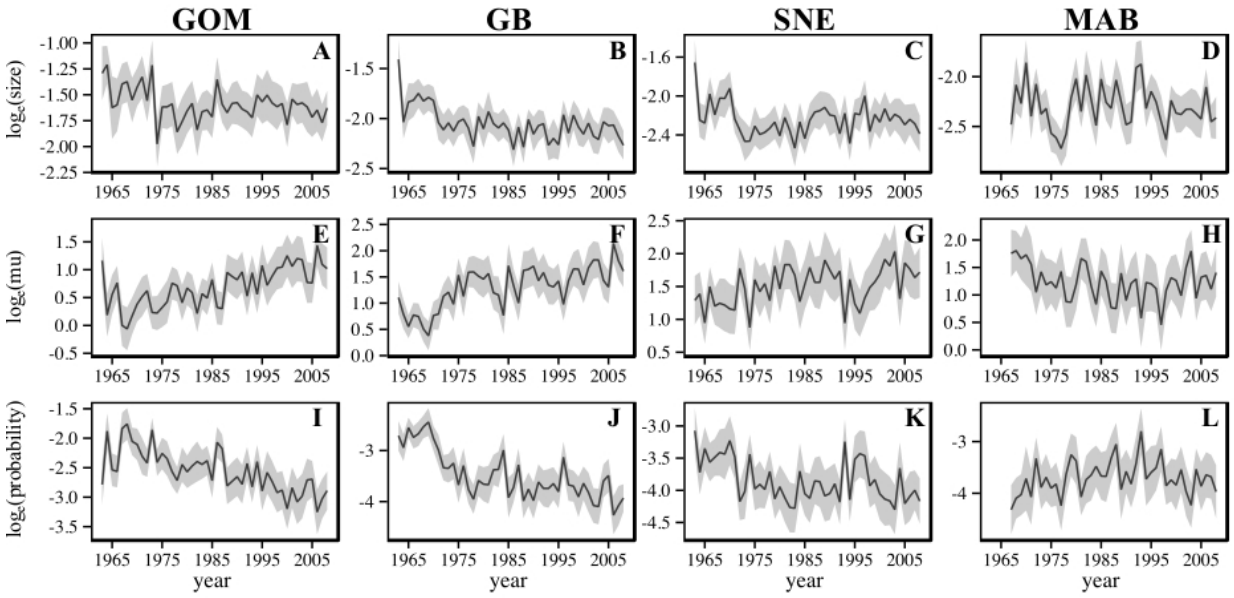

Figure 2.3. Mean of simulated A-O regression statistics (solid black lines) for relationships calculated with GMA. 95% confidence intervals on yearly values are shown in grey. For comparison, empirical estimates of the A-O relationship are provided (dashed red lines).

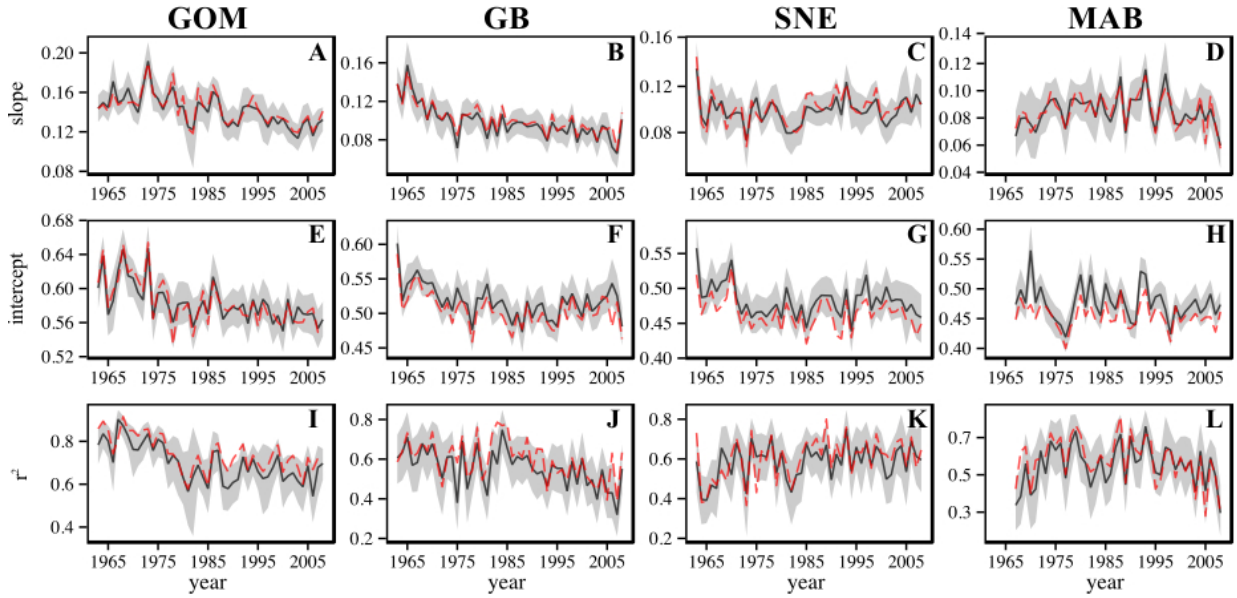

Figure 2.4. Mean of simulated A-O regression statistics (solid black lines) for relationships calculated with LMA. 95% confidence intervals on yearly values are shown in grey. For comparison, empirical estimates of the A-O relationship are provided (dashed blue lines).

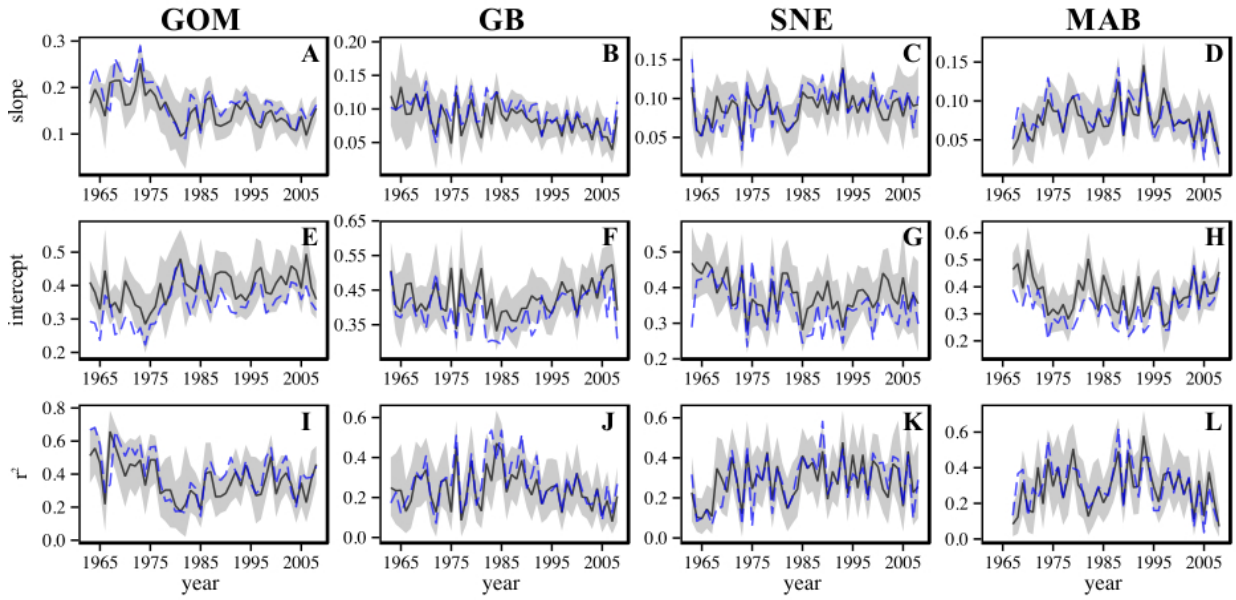

Figure 2.5. Mean A-O regression statistics for simulations with NB parameters held constant. Results are given for relationships estimated with GMA (A-C) and LMA (D-F). In each plot, 95% confidence intervals are color-coded by region.

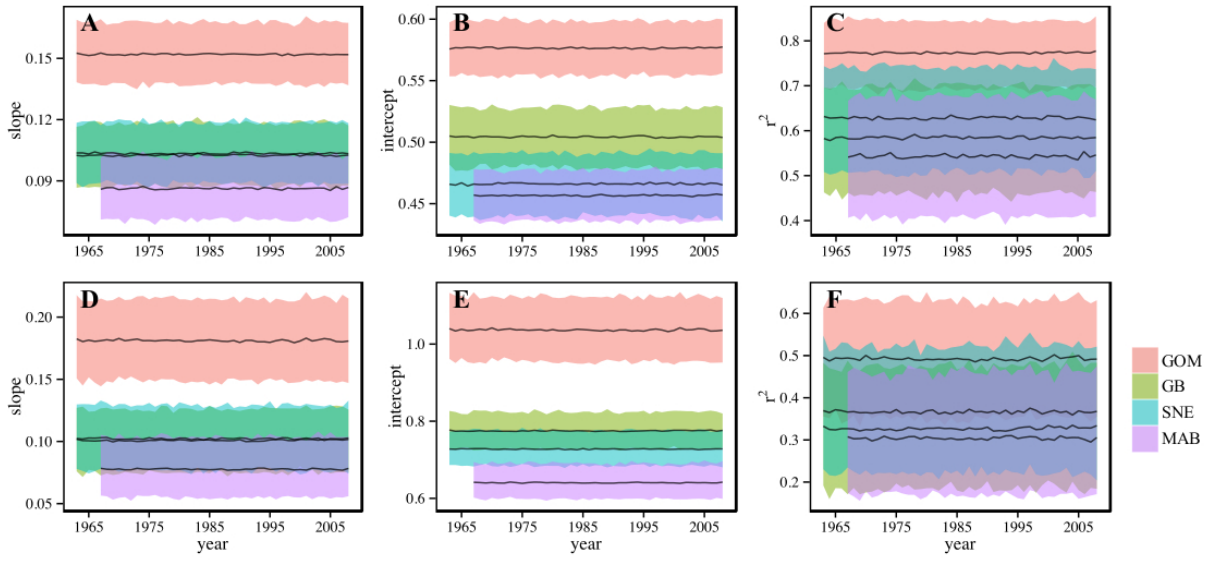

Figure 2.6. Mean A-O regression statistics for simulations in the GOM from 1973 to 1982. Results are given for relationships estimated with GMA (A-C) and LMA (D-F). Simulations including all species are shown in gray and those with schooling and colonizing species removed are in red (GMA) and blue (LMA). 95% confidence intervals are shown as shaded regions around yearly means.

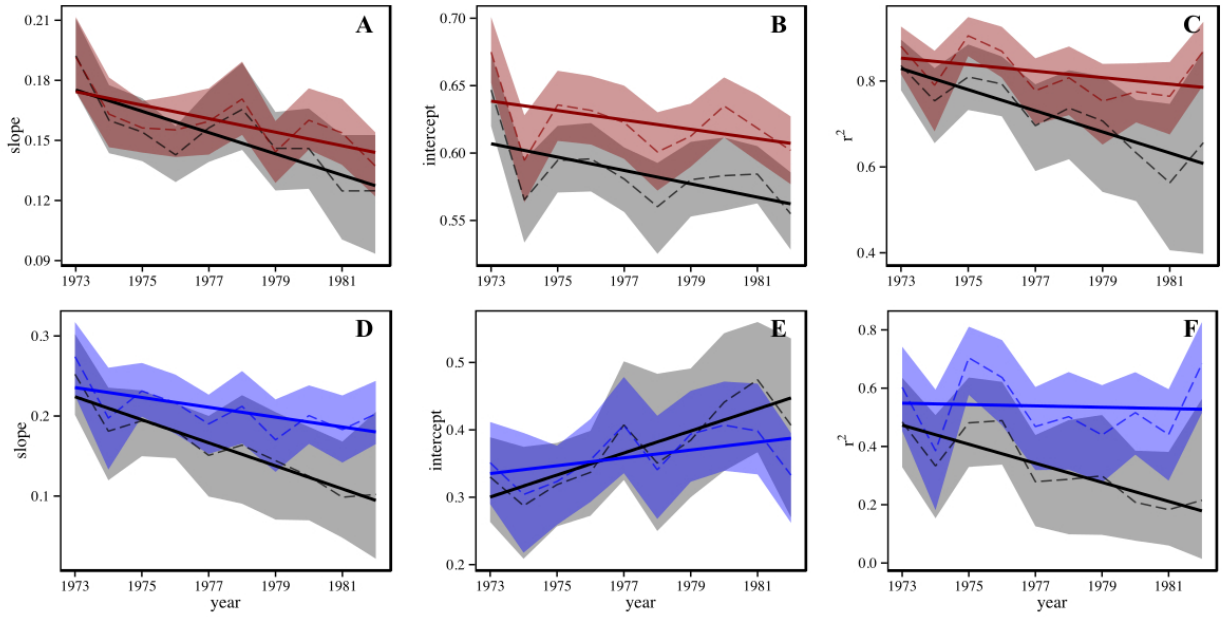

Chapter 3

Reassessment of morphological diversity of the batoid pectoral fin, with an emphasis on skates (Suborder Rajoidei)

Introduction

Batoids (Chondrichthyes: Batoidea) comprise a diverse group of cartilaginous fishes that include skates, rays, sawfishes and guitarfishes. With over 600 species (Aschliman et al. 2012), they occupy a range of environments from the deep ocean to riverine systems. Prevailing hypotheses of the interrelationships of batoids and their placement relative to other neoselachians have long been debated (Compagno 1999, Winchell *et al*. 2004 and Kriwet *et al.*, 2009). Recent work by Aschliman and colleagues (2012) has substantially improved understanding of relationships among major lineages, although questions still remain (e.g. the status of guitarfishes as a valid family). Owing to their relatively basal position in the vertebrate tree of life, batoids (and cartilaginous fishes as a whole) provide valuable context for understanding modes of diversification within a group of organisms that includes all modern fishes and tetrapods (Dahn *et al*. 2007, Pradel *et al*. 2014). This has resulted in a largely recent and dynamic research field that is continually changing the way we look at the ecology and evolution of fishes.

Batoid functional and lifestyle diversity is most prominently displayed in the rays (suborder Myliobatoidei), where some families evolved a fully pelagic life that contrasts the benthic/demersal existence typical of a majority of rays. Hydrodynamic conditions differ greatly between the sea floor and water column, selecting for disparate suites of characteristics for life in each. For pelagic rays, the ability to create lift is necessary to control position in the water column, a critical quality, as batoids lack swim bladders for buoyancy control (Rosenberger 2001). Benthic rays, on the other hand, rely more on maneuverability to navigate a structured

environment. Another major batoid group, the skates (suborder Rajoidei), have no species that have adopted a fully pelagic lifestyle. Species diversity in Rajoidei is the largest among batoids, at nearly 300 currently described species (Chiquillo *et al*. 2014). Despite this, basic knowledge on most skates is lacking, owing to the rarity of some species and because many live at abyssal depths (McEachran and Miyake 1990; Ebert and Compagno 2007). Consequently, I believe that this had led to underestimation of the extent of locomotory and lifestyle diversity in rajoids.

Variation in swimming mode is a prominent feature among batoids, relating to their diversification to new habitats and formerly unrealized lifestyles (Rosenberger 2001, Wilga and Lauder 2004). Batoid locomotion is divided between two major types, axial-based and pectoral-fin-based (Rosenberger 2001). Axial locomotion relies either partially (e.g. some guitarfishes) or fully (e.g. guitarfishes, Pristidae and Torpedinoidei) on undulations of a muscular body and tail to power propulsion (Shadwick and Gemballa 2006). In contrast, the two most diverse batoid groups (Myliobatoidei and Rajoidei) rely heavily on pectoral fins as their main source of locomotion. Among batoids with pectoral-based locomotion, species occur along a gradient from oscillation of the wings (i.e. flapping) to undulation within the wing, which is quantitatively defined by the number of waves passing along the pectoral fin margin while swimming (Rosenberger, 2001). A wave number of one has been used in the past as the threshold separating swimming styles, above which a species is described as having undulatory locomotion and below, oscillatory (Rosenberger 2001). Benthic and demersal batoids tend to have more pectoral fin waves than pelagic species.

In teleost fishes that use pectoral locomotion, fin aspect ratio has been used as a predictor of swimming ability and lifestyle (e.g. Wainwright *et al*. 2002). In many cases, the batoid body can reasonably be described as set of oversized pectoral fins with a tail. All species have pectoral

fins that are anteroposteriorly expanded, creating a disc-like body form. Daniel (1988) showed that depending on fin wave number and fluid properties, there are fin shapes (aspect ratios) that theoretically minimize the cost of transport for the individual. Within this framework he also suggested that higher aspect ratios are expected to correspond with fins that produce smaller wave numbers and have higher rigidity, patterns that have since been confirmed in empirical studies (Rosenberger 2001, Schaefer and Adams 2005, respectively). Therefore, theoretical and observational evidence suggest links between batoid pectoral form, function and lifestyle.

The primary purpose of my work was to assess the morphological diversity of a prominent feature of the batoid bauplan, their highly modified pectoral fins. In doing so, I paid special attention to the variation of rajoids relative to other batoid groups. I also investigated an issue of pectoral fin homology that arose from a recent paper (Franklin *et al*. 2014), including its consequences for our understanding of batoid shape diversity. Finally, I provide the first quantitative comparison of fin shape to both aspect ratio and swimming diversity in batoid fishes and discuss the potential implications for lifestyle diversity.

Methods

Specimen Image Collections

I collected specimen photographs for a number of batoid taxa, spanning much of the taxonomic and morphological diversity exhibited within the group. A total of 216 images were acquired and were distributed among 40 stingray species (suborder Myliobatoidei), 53 skates (suborder Rajoidei), 6 torpedo rays (suborder Torpedinoidei), 5 guitarfishes (family undefined), 1 thornback ray (suborder Platyrhinoidei) and 1 sawfish (family Pristidae, but considered a derived guitarfish). For this work, guitarfish groupings follow Aschliman *et al*. (2012), with two

clades termed “guitarfish 1” and “guitarfish 2” and a separate Pristidae group. Images came from numerous sources, including personally photographed specimens, and under a range of preservation states (table 3.1). In all cases, caution was used to include specimens where the body was in good enough condition to reasonably discern the outer margin of the batoid disc. To be used, photographs had to include a scale in the image or information regarding specimen dimensions (total length or disc width). All photographs but one (*Paratrygon aiereba*, AMNH 59865) were taken from a dorsal view, with pectoral fins spread on a flat surface. In some instances ethanol-preserved specimens exhibited curving of the distal regions of the pectoral fin. When this occurred, magnets were used to keep fins on a flat plane, again insuring natural fin orientation. Effort was made to primarily include adult specimens, but in some instances (e.g. very large species) juveniles were used. I used both male and female individuals, although sexual dimorphism does occur in some batoid species (Martinez chapter 4). However, inspection of the major axes of variation that were of primary concern here did not indicate that sex influenced interpretations.

Shape Acquisition and Major Axes of Variation

I used geometric morphometrics to describe shape variation in batoid pectoral fins. These methods employ a landmark-based registration of shape to compare specimens in multidimensional shape space (Zelditch *et al*. 2004). A total of 35 points were placed along the outer margin of the pectoral fin, with 33 sliding semilandmarks and 2 fixed landmarks on each end (fig. 3.1). Fixed or “type 1” landmarks are points that are allowed to vary in two dimensions and mark homologous and identifiable structures on all specimens (Bookstein 1991). In comparison, semilandmarks are constrained to occur along a tangent line between adjacent curve

points (whether fixed or sliding). Allowing semilandmarks to slide addresses issues relating to homology of points along a curve. The number of semilandmarks chosen were meant to reduce the total amount of shape variables produced, while still providing an appropriate fit to the fin outline. Points along outlines were captured with the program tpsDIG2 (Rohlf 2013a), creating approximately evenly spaced points along its length. Special landmark placement was needed for the lesser devil ray (*Mobula hypostoma*, AMNH 98192) because of its highly modified anterior pectoral radials (i.e. cephalic lobe) that curve into a third dimension. Here, anterior landmarks were placed along the margin of the neurocranium to the midline of the fish, in similar fashion to placement on other rays.

Shape data were extracted in the program tpsRelw (Rohlf 2013c) using generalized Procrustes analysis (GPA). This method scales, rotates and translates landmarks to reduce the sum of squared residuals of Procrustes distances between specimen shapes and an average or consensus shape (Rohlf 1999, Klingenberg 2010). It should be specified that the method for outline superimposition used here was not achieved by reducing bending energy of specimens, another commonly used approach (see Gunz and Mitteroecker, 2013). Because I had multiple specimens for some species, I used the program MorphoJ (Klingenberg 2011) to compute average shapes of species in order to avoid bias due to unequal sampling. A total of 105 specimens remained, each representing a single batoid species. As an initial examination of shape variation, I performed principal components analysis (PCA) on the GPA-aligned specimens. The PCA provided a low dimensional approximation of multivariate shape space, capturing maximum variance among a set of orthogonal axes (Zelditch *et al*. 2004). I also did separate PCAs for Rajoidei and Dasyatidae to get a better indication of shape variation within these groups.

Morphological Disparity

To compare variance in pectoral form among batoid groups, I calculated morphological disparity with the "geomorph" package (Adams and Otarola-Castillo 2013) in R (R core team 2013). Disparity was estimated as the Procrustes variance for specimens within defined groups. Pairwise comparisons were also assessed via 10,000 permutations of specimens relative to group designations. Three different sets of comparisons were done. First, I computed and tested disparity values at the family level. Sample sizes varied substantially among families, relating partially to the accessibility of rare batoid species but also to low species diversity in many families (table 3.2). A second comparison was made for Rajoidei versus Myliobatoidei, the two suborders with pectoral-based swimming styles. A final comparison again included Rajoidei and Myliobatoidei, but with the latter further divided into two subgroups, pelagic/semi-pelagic families (Gymnuridae, Mobulidae, Myliobatidae and Rhinopteridae) and benthic/demersal families (Dasyatidae, Plesiobatidae, Potamotrygonidae, Urolophidae and Urotrygonidae). The rationale for splitting the rays in the third test was that morphological variation was clearly bimodal for demersal and pelagic swimmers.

Functional Implications

I investigated the relationship between pectoral fin shapes and aspect ratio, a quantity often associated with locomotory performance. Aspect ratio was calculated as the square of the maximum chord width of the pectoral fin, divided by fin surface area (fig. 3.2). Aspect ratios were doubled for the single calculated fin to get the estimated value for both fins (Wainwright *et al*. 2002). As with landmark placement, I did not include the cephalic lobe of *Mobula hypostoma*

in aspect ratio calculations. I regressed the full pectoral fin shape on aspect ratio in MorphoJ, with a 10,000-iteration resampling procedure. I also tested for correlations between aspect ratio and shape variation described on principal components.

To account for phylogenetic non-independence, I also used comparative methods to test the relationship between shape variation (as defined by PC scores) and aspect ratio in a subset of samples. I used sequence data from Aschliman *et al*. (2012) to infer phylogenetic relationships of batoid genera based on several genes, including RAG-1, SCFD2 and a suite of mitochondrial genes representing the mtGenome (CytB, ND1, ND2, ND3, ND4, ND5, ND41, ATP6, ATP8, COI, COII, COIII). I was limited by the overlap of taxa used in this study and in Aschliman *et al*. (2012). When I had both molecular and morphological data for a given species, I used that species to represent its genus. For cases where morphological and molecular data overlapped at the genus level but species did not match, I calculated average PC scores and aspect ratios in all species that I did have for the genus in question. When this occurred, I insured that morphologies used to compute the average were not radically different from the species from which the molecular data came. Based on an appraisal of models in MEGA v.5 (Tamura *et al.* 2011), I used a General Time Reversible model of molecular evolution with gamma-distributed rate variation to estimate a maximum likelihood phylogenetic tree. I computed correlations of PC scores versus aspect ratio using phylogenetic independent contrasts in the R package ape (Paradis *et al*. 2004).

Finally, I examined relationships between PC scores, aspect ratio and mean number of pectoral waves. Fin wave data came from kinematic analyses of locomotion in nine batoid species (Rosenberger 2001), of which I had shape and aspect ratio data for seven. For an eighth, *Rhinobatos lentiginosus*, I used average PC scores and aspect ratios from two other species in the genus Rhinobatos. Franklin *et al*. (2014) also compared PC scores from their morphological

analyses to wave number using data from the same study. This provided a point of comparison between this study and theirs.

Homology of pectoral fin landmarks

I performed a second set of morphological analyses to address a question of pectoral fin homology that arose from recent work on batoid form (i.e. Franklin *et al*. 2014). Briefly, the batoid pectoral fin may be defined as the area supported by pectoral radials (e.g. fig. 3.2), which ultimately originate from the scapulocoracoid or pectoral girdle. In Myliobatoidei, which lack rostrums, pectoral radials extend to the anterior tip of the disc or body, but often fail to reach this point in most other batoids (blue line in fig. 3.1). Franklin and colleagues (2014) established the anterior extent of pectoral fins at the tip of the disc for *all* batoids (red line in fig. 3.1). To test the impacts of this definition of pectoral shape, I added a fixed landmark at anterior point of the disc to the configuration of semi-landmarks used in this study. Because I did not use the exact shape definition as in Franklin *et al*. (2014), I did not expect to recover the same results as their work. Rather, I sought to identify the affect of the anterior landmark when added to the consistently homologous pectoral fin outlines assessed in this study.

As before, I performed GPA and then did a PCA on the resulting shape data. Following Franklin *et al*. (2014), I specified the anterior-most landmark for Pristidae (i.e. *Pristis pectinata*, AMNH 55572) at a medial position along the anterior margin of the neurocranium and not the end of their derived rostral saw (fig. 3.1D). In addition, I did not include the rostral tendril on *Anacanthobatis folirostris* (MCZ 168027).

Results

Shape Acquisition and Major Axes of Variation

The first two principal components (PCs) accounted for 87.7% of total Batoid pectoral shape variation, with 71.4% attributed to PC 1. A scree plot suggested the amount of variance explained on the PCs leveled off after the third axis (fig. 3.3A). Much of the overall fin variation occurred along a gradient from rounded, oval-like to laterally expanded and triangular forms (fig. 3.4, PC 1). The largest PC 1 values included pelagic and semi-pelagic families like Myliobatidae and Gymnuridae, with a host of benthic and demersal families occupying the smallest values (Plesiobatidae, Potamotrygonidae, Urolophidae and Urotrygonidae). Dasyatidae was also oriented toward small PC 1 scores, but had a large range that went into intermediate scores on the axis. The skate families (Anacanthobatidae, Arhynchobatidae and Rajidae) were centered on intermediate PC 1 values, with Rajidae also displaying the largest range of any family. All of the axial-based swimmers (Narcinidae, Pristidae, Rhinobatidae and Torpedinidae) occurred in negative regions of PC 1.

The second PC axis was associated with changes in the location of the pectoral fin's lateral apex that effectively divides the pectoral fin into anterior and posterior regions. A majority of batoids had negative PC 2 scores, including Pristidae, Torpedinoidei, most Myliobatoidei specimens and several Rajoids. Individuals at the lower extreme of PC 2 had relatively equal-sized anterior and posterior fin regions that were relatively flat (fig. 3.4). Other rajoids and guitarfishes dominated positive PC 2 values. These specimens had posteriorly oriented fin apexes, a convex/lobe-like posterior region and a concave anterior region.

Closer examination of Rajoidei specimens revealed a fair amount of variability but an overall reiteration of diversity in the larger batoid group. Again, the largest axis of variation (PC

1) differentiated round versus triangular fins and represented over half (59.9%) of the observed variation within the group (fig. 3.5). Genera like Dipturus, Rostroraja and Zearaja had angled fins and high PC 1 scores, with Breviraja, Fenestraja and Leucoraja at lower values with rounded fins. Changes on PC 2 reflected contraction and expansion of the lateral apex and of the posterior fin base. Species with high PC 2 scores had lobed posterior pectoral fin regions and an anteriorly oriented fin apex, while those with lower scores had a flattened posterior fin and a concave anterior fin area. Variation on the third PC axis (not shown) was largely related to expansion and contraction of the posterior fin base near the point of intersection with the body. Rajoidei and Dasyatidae overlapped substantially on PC 1 in the analysis of all batoid specimens (fig. 3.4). When examined alone, 62.6% of variation in dasyatids was accounted for by PC 1 and was expressed primarily in the angularity of the outer portion of the fin margin (fig. 3.6).

Morphological Disparity

Among the five batoid families with the largest morphological disparities, three were Rajoids (table 3.2). The family Rajidae had the largest Procrustes variance (0.0069), followed by guitarfish 2 (0.0039). In contrast, Potamotrygonidae and Torpedinidae were among the families with the lowest disparities (0.0010 and 0.00033, respectively). Pairwise comparisons were only possible for the 12 families that had more than one species available (see table 3.2 for sample sizes). Among the other families tested, Rajidae had significantly larger morphological disparity than 10 other families ($p < 0.05$ for comparisons with Arhynchobatidae, Dasyatidae, Gymnuridae, Myliobatidae, Narcinidae, Potamotrygonidae, Rhinopteridae, Torpedinidae, Urolophidae, Urotrygonidae). Some caution may also be warranted as several families had only a small number of representatives and may therefore have artificially low disparity.

Between the two pectoral-swimming suborders, morphological disparity was 0.0060 for Rajoidei and 0.025 for Myliobatiodei. A permutation test indicated that Myliobatoidei had significantly higher disparity ($p < 0.0001$). However, when rays were split by habitat type, disparity was 0.0043 for pelagic rays and 0.0036 for demersal rays. In this case, rajoid disparity (i.e. 0.0060) was comparable to pelagic rays ($p=0.31$) and significantly larger than demersal rays ($p = 0.028$).

Functional Implications

Regressions of Procrustes coordinates on aspect ratio were significant ($p < 0.0001$) and explained 65.83% of total shape variance. In addition, the correlation between PC 1 and aspect ratio was very large ($r = 0.96$, n=105)(fig. 3.7), as was the phylogenetically adjusted correlation ($r = 0.93$, n=26)(see fig. 3.8 for tree used). Finally, the pectoral wave number was negatively correlated with PC 1 scores ($r = -0.97$, n=8) and aspect ratio ($r = -0.97$, n=8) (fig. 3.9).

Homology of pectoral fin landmarks

The inclusion of a landmark at the anterior-most point of the batoid disc created a substantial source of added variation. Although, the first PC described similar shape differences similar to the original configuration, the additional point decreased the amount of variation explained on the axis to 51.6% (i.e. 19.8% less than before). The anterior landmark played a substantial role in shape changes on the second PC axis, which explained 28.1% of total variation (figs. 3.10 and 3.11A). In fact, when PC 1 was plotted against PC3 (fig. 3.12), relative relationships among batoid groups resembled that of PC 1 versus 2 for the original landmark configuration (fig. 3.4). Because pectoral radials extend to the midline in Myliobatoidei, the

additional landmark was placed approximately adjacent to the most anterior pectoral fin landmark (fig. 3.1B). The consequence was that the landmark did not alter the overall shape of these specimens as much as it did for others (e.g. fig. 3.11C). In addition, the rajoid family Arhynchobatidae (i.e. softnose skates) has many species with pectoral fins that extended close to their rostral tips, shifting many of them closer to the rays than they had been previously (fig. 3.10). However, the most notable impact of the additional landmark occurred in the guitarfish groups and Pristidae (fig. 3.10), where the anterior point of the pectoral fin was well short of the added landmark (fig. 3.1D and E). Finally, the regression of full shape space on aspect ratio was still significant ($p < 0.0001$) but explained 45.03% of total variance (compared to 65.83% for the original configuration).

Discussion

Overview of batoid pectoral diversity

My research confirms that the major direction of shape variation within Batoidea occurs along an axis that contains, at one extreme rounded body forms and at the other, angular-shaped bodies. These shapes were highly correlated with aspect ratio (even for the subset of species analyzed with comparative methods). For species with pectoral-based locomotion, both shape and aspect ratio were strongly associated with swimming style, along a continuum from undulation to oscillation. This suggests that pectoral fin shape of batoids is indicative of locomotion and lifestyle diversity. As expected, pelagic and benthic/demersal rays were well differentiated relative to shape variation and aspect ratio (figs. 3.4 and 3.7). One potential exception to this general pattern was the case of gymnurid species. In my analyses, *Gymnura micrura* and *Gymnura poecilura* occurred near pelagic rays in PC 1 and PC 2 space, despite

being characterized as demersal species (Rosenberger 2001). However, there is evidence that species in this genus do aggregate in open water (Bigelow and Schroeder 1953). Moreover, Rosenberger (2001) notes that *G. micrura* shifts between more undulatory and oscillatory swimming when in benthic and pelagic environments, respectively.

Interestingly, on PCs 1 and 2 (fig. 3.4), axial-based swimmers occurred either nested within or nearby species with pectoral-based locomotion. All axial swimming species were situated at lower PC 1 values along with species that had rounded fin shapes. Most guitarfishes and the lone Platyrhinoidei representative in my analyses (*Platyrhina sp.*) were clustered near rajoids around the upper limits of PC 2. In contrast, Pristidae and Torpedinoidei were closest to demersal rays at low to intermediate PC 2 scores. Axial-based swimmers use muscular tails and bodies to aid in swimming (Rosenberger 2001). Although their pectoral fins were not radically different than pectoral-based swimmers, they were often quite reduced in size relative to the rest of the body.

Despite strong connections between pectoral shape and swimming mode, additional factors determine locomotory performance. One important element is fin rigidity. In batoids, different structural modifications impact stiffness of pectoral fins, including mode of calcification, relative spacing and staggering of radial joints, as well as cross-bracing of adjacent radials (Schaefer and Summers, 2005). Behavior is another way that batoids may control their swimming motions. For example, the guitarfish *Rhinobatos lentiginosus* often swims with its body angled upward from the horizontal (Rosenberger 2001). In addition, many batoids can alter properties of pectoral waves (e.g. frequency, wavespeed and wave number), depending on flow conditions (Rosenbeger 2001). Finally, several batoid species use pelvic fins to supplement locomotion for specific tasks like benthic walking and propelling themselves into the water

column, termed punting (Koester and Spirito, 2003). The shape of the pelvic girdle has been associated with overall swimming mode (Ekstrom & Kajiura 2014). However, given the relative importance of pectoral fins for swimming, pelvic girdles appear to be a less direct method of inferring locomotion. It may even be the case that specialization observed in pelvic fins could be due to its reduced role in primary swimming motions, allowing it to evolve in form to accomplish a range of functions.

Diversity of pectoral-based swimmers

As previously mentioned, the pectoral-based swimming mode used by Rajoidei and Myliobatoidei is by far the most common form of locomotion in batoids. Patterns of diversity between these groups are all the more noteworthy considering that they likely evolved their disc-like appearances independently of each other via convergence (Aschliman *et al*. 2014). Although they both display considerable variation in shape and aspect ratios, they achieved their observed diversity with different strategies. Further, the differences appear to be related to habitat and lifestyle diversification for each group. Myliobatoids fall into two distinct groups based on body shape and aspect ratio, which is differentiated among pelagic rays and all other rays (figs. 3.4 and 3.7). Given the change in functional demands associated with a transition from a benthic environment to a pelagic one, the observed bimodality in rays is not too surprising. At the same time, there is also shape variation within the demersal rays alone, with some highly rounded forms (e.g. family Potamotrygonidae) and others with more of a rhomboid-like shape (e.g. some Dasyatidae species). In contrast to myliobatoids, shape and aspect ratio variation in rajoids is relatively continuous. Within the batoid shape space defined by PCs 1 and 2 (fig. 3.4), rajoids occur as a single group. This seems to correspond with their uninterrupted range of habitat types

from shallow coastal waters to the deep sea (McEachran and Miyake 1990). This does not necessarily suggest that the differences in aspect ratio relate to shallow versus deep-water forms, only that there are no abrupt shifts in habitat or lifestyle that would necessitate a distinct shift in morphology.

My results indicated that shape variation was relatively large within Rajoidei, especially in the family Rajidae. Pectoral shapes of the two remaining rajoid families, Anacanthobatidae and Arhynchobatidae, are largely contained within the morphological domain of Rajidae (figs. 3.4 and 3.5). Although disparity in rajoids was significantly smaller than that of myliobatoids, the comparison might not be fair considering the large gap between demersal and pelagic rays where no species occur. When rays were divided among these major morpho-functional groups, skates displayed larger shape variance. Another interesting outcome was that while skates did overlap substantially with demersal rays on PC 1, a number of rajoid species also occupied the morphological gap between demersal and pelagic rays (fig. 3.4). Extending the relationships between shape, swimming mode and lifestyle established primarily for rays (fig. 3.9), skates would be characterized as having demersal to intermediate (or even semi-pelagic) lifestyles. Although some rajoids are quite mobile and undergo large-scale seasonal migrations (Frisk, 2010), the range of swimming/lifestyle diversity implied in my research is beyond what is currently known for these fishes. Because we know so little about skates, further work on habitat use and migration is needed in order to validate the observed morphological patterns.

Relation to previous work

In several instances, research by Franklin *et al*. (2014) came to different conclusions than I did on the nature of batoid pectoral fin diversity. I believe that most of inconsistencies can be

explained by unnecessarily arbitrary landmark choices and their treatment of shape data. Landmark placement is vital to the efficacy of geometric morphometric research (Zeldtich *et al*. 2004). Outlines present a particularly challenging case for shape analyses as they often have few distinguishable points of homology, if any (Gunz and Mitteroecker 2013). The first problem area in Franklin *et al*. (2014) was in the structure that they defined as the pectoral fin. The authors consistently defined the anterior extent of the pectoral fin at the anterior-most point of the batoid disc (fig. 3.1). However, in some batoids the pectoral fins do not extent to this location (e.g. Torpedinoidei and most Rajoidei species), and in some cases the distinction is quite large (e.g. Pristidae, and some guitarfishes). Had their paper focused on the batoid disc rather than an explicit investigation of pectoral variation and its functional and lifestyle consequences, their methods would have been more appropriate. The authors cite a difficulty in identifying the point of intersection between the propterygium and anterior disc margin (see fig. 3.2). It is indeed true that the point can be difficult to identify, but in most cases it is straightforward. One of the most concerning consequences of the landmark configuration used by Franklin *et al*. (2014) is that it reflects an incorrect homology of pectoral fins, while introducing a bias whose magnitude depends on the family considered. Although the authors did not include the highly modified rostral saw in Pristidae specimens, they did include a large section of the body anterior to the fin. To illustrate this point, it would be equivalent to a study on shark pectoral fins that included the entire head region as a functional component of locomotion. The oversight exaggerated the differences between pristid and guitarfish shapes relative to other batoids. It also caused variation in the lateral apex position of the fin to appear larger than it actually is. Moreover, their placement of the posterior extent of the fin outline and the addition of a traditional landmark at the lateral fin apex could not be identified with precision on any batoid species with rounded

body shapes (see fig. 2 in Franklin *et al*. 2014). Overall, the high correlations that I produced between shape, aspect ratio and fin wave number (fig. 3.9) increases confidence that my methods captured the true pectoral shape well. Regressions of shape on aspect ratio for my landmark configuration versus that with the additional anterior landmark (see results), suggested that the latter affected the functional equivalence of the implied fin shape by introducing unnecessary shape variation. This does not include the impacts of other landmark issues discussed above or the erroneous inclusion of the pelvic fin in the pectoral outline (see fig. 2C in Franklin *et al*. 2014).

Another major difference between my results and that of Franklin *et al*. (2014) was in the diversity of Rajoidei. Their work did not suggest the same level of rajoid shape variation as the current study. I believe this to be at least partially because the authors averaged shapes at the genus level and not by species, as done here. Their method would likely have the largest impact on rajoids because of their large species diversity relative to other batoids. Consequently, much of the rajoid shape diversity among their specimens may have been averaged away.

I also found it misleading for Franklin *et al*. (2014) to assert as a major finding of their research that "aspect ratio [sic] can predict locomotor style" without having included a formal comparison of observed shape variation to aspect ratio. Short of this analysis, the authors are really referring to *inferred* rather than *true* aspect ratio. Although it is rather clear that major variation in batoids relates to aspect ratio, they claim an association with a variable that has a well-defined quantitative definition without calculating it. This problem is of general concern, beyond the work at hand.

Overall, the patterns of morphological diversity recovered in this work reaffirm connections between form, function and lifestyle that have been suggested for batoids. However,

the large relative variation in rajoid pectoral morphology has not before been quantified. Implications for this research may impact the way we think about lifestyle variation of skates as well as mechanisms and drivers of evolution in the batoids.

Table 3.1. List of species analyzed. Wherever available, information was also provided for sex, preservation method and image contributor. For specimens that are part of an institutional collection, the catalog number was listed. Abbreviations are as follows: AMNH = American Musuem of Natural History; ANSP = Academy of Natural Sciences of Philadelphia; MCZ = Harvard Museum of Comparative Zoology; ME = Mar-Eco; MNHN = Muséum National D'Histoire Naturelle; NMNH = National Museum of Natural History (Smithsonian); SIO = Scripps Institute of Oceanography, VIMS = Virginia Institute of Marine Science; ZMUB = Museum für Naturkunde, Humboldt Universität

species name	sex	preservation	catalog #	contributor
Aetobatus narinari	M	ethanol	AMNH 3725	C. Martinez
Aetomylaeus maculatus	F	ethanol	AMNH 32500	C. Martinez
Amblyraja hyperborea	M	ethanol	MCZ 36552	F. Fish
Amblyraja jenseni	M	ethanol	MCZ 132506	F. Fish
Amblyraja jenseni	F	ethanol	MCZ 155628	F. Fish
Amblyraja jenseni	F	ethanol	MCZ 165045	A. Orlov
Amblyraja jenseni	F	fresh/frozen	ZMUB 19462	A. Orlov
Amblyraja jenseni	M	fresh/frozen	ZMUB 19463	A. Orlov
Amblyraja jenseni	F	fresh/frozen	ZMUB 19529	A. Orlov
Amblyraja radiata	F	ethanol	AMNH 71998	C. Martinez
Amblyraja radiata	F	ethanol	AMNH 71998	C. Martinez
Anacanthobatis americanus	M	ethanol	MCZ 39998	F. Fish
Anacanthobatis americanus		ethanol	MCZ 40368	F. Fish
Anacanthobatis americanus	M	ethanol	MCZ 40780	F. Fish
Anacanthobatis folirostris	F	ethanol	MCZ 168027	F. Fish
Anacanthobatis folirostris	F	ethanol	MCZ 168027	F. Fish
Arhynchobatis asperrimus	F	ethanol	MCZ 39574	F. Fish
Atlantoraja cyclophora	F	ethanol	AMNH 44001	C. Martinez
Bathyraja abyssicola	M	fresh/frozen		D. Stevenson
Bathyraja aleutica	F	ethanol	MCZ 166248	F. Fish
Bathyraja aleutica	M	fresh/frozen		D. Stevenson
Bathyraja aleutica	M	fresh/frozen		D. Stevenson
Bathyraja aleutica	F	fresh/frozen		D. Stevenson
Bathyraja interrupta	M	fresh/frozen		D. Stevenson
Bathyraja interrupta	F	fresh/frozen		D. Stevenson
Bathyraja interrupta	M	fresh/frozen		D. Stevenson
Bathyraja interrupta	F	fresh/frozen		D. Stevenson
Bathyraja interrupta	M	fresh/frozen		D. Stevenson
Bathyraja interrupta	F	fresh/frozen		D. Stevenson
Bathyraja interrupta	M	fresh/frozen		D. Stevenson
Bathyraja lindbergi	F	fresh/frozen		D. Stevenson
Bathyraja maculata	F	fresh/frozen		D. Stevenson
Bathyraja mariposa	M	fresh/frozen		D. Stevenson
Bathyraja mariposa	F	fresh/frozen		D. Stevenson

Table 3.1. *continued*

species name	sex	preservation	catalog #	contributor
Bathyraja mariposa	M	fresh/frozen		D. Stevenson
Bathyraja minispinosa	M	fresh/frozen		D. Stevenson
Bathyraja minispinosa	F	fresh/frozen		D. Stevenson
Bathyraja pallida	M	fresh/frozen	ZMUB 19465	A. Orlov
Bathyraja parmifera	M	fresh/frozen		D. Stevenson
Bathyraja parmifera	F	fresh/frozen		D. Stevenson
Bathyraja parmifera	M	fresh/frozen		D. Stevenson
Bathyraja parmifera	M	fresh/frozen		D. Stevenson
Bathyraja parmifera	M	fresh/frozen		D. Stevenson
Bathyraja richardsoni	F	fresh/frozen	ME 15303-4	A. Orlov
Bathyraja richardsoni	F	fresh/frozen	ME 16307	A. Orlov
Bathyraja spinicauda	M	fresh/frozen		C. Nozères
Bathyraja spinicauda	F	fresh/frozen		C. Nozères
Bathyraja spinicauda	M	fresh/frozen		C. Nozères
Bathyraja taranetzi	M	fresh/frozen		D. Stevenson
Bathyraja taranetzi	F	fresh/frozen		D. Stevenson
Bathyraja taranetzi	M	fresh/frozen		D. Stevenson
Bathyraja taranetzi	F	fresh/frozen		D. Stevenson
Bathyraja trachura	M	ethanol	SIO 62-203	J. D. McEachran
Bathyraja trachura	F	fresh/frozen		D. Stevenson
Benthobatis marcida	M	ethanol	AMNH 56011	C. Martinez
Breviraja claramaculata	F	ethanol	MCZ 49010	F. Fish
Breviraja colesi	M	ethanol	MCZ 41162	F. Fish
Breviraja spinosa	F	ethanol	AMNH 75991	C. Martinez
Cruriraja rugosa	M	ethanol	MCZ 49022	F. Fish
Cruriraja rugosa	M	ethanol	MCZ 49022	F. Fish
Cruriraja rugosa	F	ethanol	MCZ 49022	F. Fish
Cruriraja rugosa	M	ethanol	MCZ 49022	F. Fish
Cruriraja rugosa	F	ethanol	MCZ 51023	F. Fish
Dactylobatus clarkii	F	ethanol	MCZ 42429	F. Fish
Dasyatis americana	M	fresh/frozen		C. Martinez
Dasyatis americana	F	ethanol	MCZ 47806	F. Fish
Dasyatis americana		frozen		C. Wilga
Dasyatis americana		frozen		C. Wilga
Dasyatis centroura	M	ethanol	MCZ 40733	F. Fish
Dasyatis centroura	F	ethanol	NMNH 19481	F. Fish
Dasyatis centroura	M	ethanol	NMNH 199004	F. Fish
Dasyatis guttata	M	ethanol	AMNH 83640	C. Martinez
Dasyatis guttata	F	ethanol	MCZ 387	F. Fish
Dasyatis margaritella	F	ethanol	AMNH 41515	C. Martinez

Table 3.1. *continued*

species name	sex	preservation	catalog #	contributor
Dasyatis sabina	F	ethanol	MCZ 40736	F. Fish
Dasyatis sabina		frozen		C. Wilga
Dasyatis sayi	F	ethanol	AMNH 76453	C. Martinez
Dasyatis sayi	F	ethanol	AMNH 76453	C. Martinez
Diplobatis ommata	F	ethanol	AMNH 233744	C. Martinez
Diplobatis pictus	F	ethanol	MCZ 40373	F. Fish
Dipturus bullisi	M	ethanol	MCZ 47829	F. Fish
Dipturus flavirostris	M	ethanol	AMNH 222150	C. Martinez
Dipturus laevis	F	ethanol	AMNH 96790	C. Martinez
Dipturus olseni	M	ethanol	MCZ 40747	F. Fish
Dipturus tengu	F	ethanol	AMNH 258306	C. Martinez
Fenestraja cubensis	F	ethanol	MCZ 40394	F. Fish
Fenestraja ishiyamai	F	ethanol	MCZ 41834	F. Fish
Fenestraja ishiyamai	F	ethanol	MCZ 41834	F. Fish
Fenestraja ishiyamai	F	ethanol	MCZ 41834	F. Fish
Fenestraja plutonia	F	ethanol	AMNH 76398	C. Martinez
Fenestraja plutonia	M	ethanol	AMNH 76398	C. Martinez
Fenestraja plutonia	M	ethanol	AMNH 76398	C. Martinez
Fenestraja plutonia	F	ethanol	AMNH 76564	C. Martinez
Gurgesiella atlantica	F	ethanol	MCZ 41969	F. Fish
Gymnura micrura	F	ethanol	AMNH 73805	C. Martinez
Gymnura micrura	M	ethanol	AMNH 73890	C. Martinez
Gymnura micrura	M	ethanol	NMNH 51897	F. Fish
Gymnura micrura	M	ethanol	NMNH 51940	F. Fish
Gymnura poecilura	M	ethanol	MCZ 242	F. Fish
Heliotrygon gomesi	M	ethanol	AMNH 58402	C. Martinez
Himantura gerrardi	M	ethanol	AMNH 239347	C. Martinez
Himantura imbricata	M	ethanol	ANSP 178832	F. Fish
Himantura signifer		ethanol	ANSP 177985	F. Fish
Himantura uarnak	F	ethanol	NMNH 206132	F. Fish
Leucoraja erinacea	F	fresh/frozen		C. Martinez
Leucoraja erinacea	F	fresh/frozen		C. Martinez
Leucoraja erinacea	F	fresh/frozen		C. Martinez
Leucoraja erinacea	M	fresh/frozen		C. Martinez
Leucoraja erinacea	M	fresh/frozen		C. Martinez
Leucoraja erinacea	M	fresh/frozen		C. Martinez
Leucoraja ocellata	F	fresh/frozen		C. Martinez
Leucoraja ocellata	F	fresh/frozen		C. Martinez
Leucoraja ocellata	F	fresh/frozen		C. Martinez
Leucoraja ocellata	M	fresh/frozen		C. Martinez

Table 3.1. *continued*

species name	sex	preservation	catalog #	contributor
Leucoraja ocellata	M	fresh/frozen		C. Martinez
Leucoraja ocellata	M	fresh/frozen		C. Martinez
Malacoraja senta	M	ethanol	AMNH 72029	C. Martinez
Malacoraja senta	M	ethanol	AMNH 72029	C. Martinez
Malacoraja senta		fresh/frozen		C. Nozères
Malacoraja senta	F	ethanol	MCZ 33919	F. Fish
Mobula hypostoma	M	ethanol	AMNH 98192	C. Martinez
Myliobatis aquila	M	ethanol	AMNH 9896	C. Martinez
Myliobatis californica	M	ethanol	AMNH 56013	C. Martinez
Myliobatis freminvillei	M	ethanol	AMNH 15333	C. Martinez
Myliobatis freminvillei	M	ethanol	NMNH 204770	F. Fish
Myliobatis freminvillei	F	fresh/frozen		C. Martinez
Myliobatis freminvillei	M	fresh/frozen		C. Martinez
Myliobatis freminvillei	M	fresh/frozen		C. Martinez
Myliobatis goodei	F	ethanol	MCZ 119	F. Fish
Myliobatis goodei	M	ethanol	MCZ 167687	F. Fish
Narcine brasiliensis	F	ethanol	AMNH 1776	C. Martinez
Narcine brasiliensis	F	ethanol	AMNH 9054	C. Martinez
Neotrygon kuhlii	F	ethanol	AMNH 44080	C. Martinez
Neotrygon kuhlii	M	ethanol	ANSP 171544	F. Fish
Okamejei kenojei	F	ethanol	AMNH 44058	C. Martinez
Okamejei kenojei	F	ethanol	AMNH 34914	C. Martinez
Okamejei kenojei	F	ethanol	AMNH 34914	C. Martinez
Paratrygon aiereba	M	ethanol	AMNH 59865	C. Martinez
Pastinachus sephen	F	ethanol	NMNH 147420	F. Fish
Platyrhina sp.	F	ethanol	NMNH 130600	F. Fish
Plesiobatis daviesi	M	unknown		J. Randall (fishbase.org)
Plesiotrygon iwamae		ethanol	ANSP 178099	F. Fish
Potamotrygon motoro	M	ethanol	AMNH 59875	C. Martinez
Potamotrygon motoro	M	ethanol	MCZ 607	F. Fish
Potamotrygon orbignyi	F	ethanol	AMNH 97427	C. Martinez
Potamotrygon yepezi	M	ethanol	AMNH 243351	C. Martinez
Potamotrygon yepezi	M	ethanol	AMNH 243351	C. Martinez
Pristis pectinata	M	ethanol	AMNH 55572	C. Martinez
Pristis pectinata	F	ethanol	AMNH 55572	C. Martinez
Psammobatis lentiginosa	F	ethanol	AMNH 44019	C. Martinez
Psammobatis scobina	M	ethanol	AMNH 44004	C. Martinez
Raja asterias	M	ethanol	AMNH 1510	C. Martinez
Raja asterias	M	ethanol	AMNH 1510	C. Martinez
Raja binoculata	M	ethanol	AMNH 55759	C. Martinez

Table 3.1. *continued*

species name	sex	preservation	catalog #	contributor
Raja binoculata	F	fresh/frozen		D. Stevenson
Raja eglanteria	F	fresh/frozen		C. Martinez
Raja eglanteria	F	fresh/frozen		C. Martinez
Raja eglanteria	F	fresh/frozen		C. Martinez
Raja eglanteria	M	fresh/frozen		C. Martinez
Raja eglanteria	M	fresh/frozen		C. Martinez
Raja eglanteria	M	fresh/frozen		C. Martinez
Raja equatorialis		ethanol		J. D. McEachran
Raja miraletus	M	ethanol	AMNH 43121	C. Martinez
Raja miraletus	F	ethanol	AMNH 43121	C. Martinez
Raja rhina	F	fresh/frozen		D. Stevenson
Raja texana	F	ethanol	AMNH 85701	C. Martinez
Raja texana	F	ethanol	AMNH 85701	C. Martinez
Raja texana	M	ethanol	AMNH 85701	C. Martinez
Rajella fyllae	F	ethanol	AMNH 71966	C. Martinez
Rajella fyllae	M	ethanol	AMNH 71972	C. Martinez
Rajella fyllae	M	fresh/frozen		C. Nozères
Rajella fyllae		fresh/frozen		C. Nozères
Rhinobatos leucorhynchus	M	ethanol	AMNH 233903	C. Martinez
Rhinobatos leucorhynchus	F	ethanol	NMNH 206816	F. Fish
Rhinobatos leucospilus	F	ethanol	AMNH 232511	C. Martinez
Rhinoptera bonasus	M	ethanol	NMNH 123216	F. Fish
Rhinoptera brasiliensis	M	ethanol	MCZ 319	F. Fish
Rhynchobatus djiddensis		ethanol	ANSP 171532	F. Fish
Rioraja agassizii	F	ethanol	MCZ 549	F. Fish
Rioraja agassizii	F	ethanol	MCZ 549	F. Fish
Rostroraja alba	M	ethanol	MCZ 241	F. Fish
Rostroraja alba	M	ethanol	AMNH 40997	C. Martinez
Rostroraja alba	F	ethanol	AMNH 40997	C. Martinez
Sympterygia acuta	F	ethanol	AMNH 44005	C. Martinez
Sympterygia bonapartii	F	ethanol	AMNH 44006	C. Martinez
Taeniura lymma	F	ethanol	AMNH 44076	C. Martinez
Taeniura lymma	M	ethanol	AMNH 44076	C. Martinez
Torpedo nobiliana	F	ethanol	MCZ 44123	F. Fish
Torpedo torpedo	M	ethanol	AMNH 1509	C. Martinez
Torpedo torpedo	M	ethanol	AMNH 1509	C. Martinez
Torpedo torpedo	M	ethanol	AMNH 1509	C. Martinez
Torpedo torpedo	M	ethanol	AMNH 43124	C. Martinez
Torpedo torpedo	M	ethanol	AMNH 43124	C. Martinez
Urobatis halleri		frozen		C. Wilga

Table 3.1. *continued*

species name	sex	preservation	catalog #	contributor
Urobatis halleri		frozen		C. Wilga
Urobatis halleri		frozen		C. Wilga
Urobatis halleri		frozen		C. Wilga
Urobatis halleri		frozen		C. Wilga
Urobatis halleri		frozen		C. Wilga
Urobatis halleri		frozen		C. Wilga
Urobatis jamaicensis	F	ethanol	AMNH 44099	C. Martinez
Urobatis jamaicensis	M	ethanol	AMNH 44099	C. Martinez
Urobatis jamaicensis	M	ethanol	AMNH 254425	C. Martinez
Urogymnus asperrimus		unknown		J. Randall (fishbase.org)
Urolophus aurantiacus	F	ethanol	AMNH 26690	C. Martinez
Urolophus halleri	M	ethanol	NMNH 62381	F. Fish
Urolophus maculatus	M	ethanol	AMNH 44144	C. Martinez
Urolophus tumbesensis	F	ethanol	AMNH 44021	C. Martinez
Urotrygon aspidura	F	ethanol	AMNH 233894	C. Martinez
Urotrygon chilensis	M	ethanol	AMNH 233905	C. Martinez
Urotrygon chilensis	F	ethanol	AMNH 233905	C. Martinez
Urotrygon microphthalmum	F	ethanol	AMNH 55614	C. Martinez
Zapteryx xyster	M	ethanol	AMNH 233922	C. Martinez
Zearaja chilensis	M	ethanol	MNHN 1995-31	J. D. McEachran
Zearaja chilensis	M	ethanol		J. D. McEachran
Zearaja chilensis	M	ethanol	AMNH 44002	C. Martinez

Table 3.2. Morphological disparity for all families invesigated here. The number of observations/species included (n) is also given.

family	n	disparity
Anacanthobatidae	2	0.0030
Arhynchobatidae	20	0.0036
Dasyatidae	14	0.0031
Guitarfish 1	1	
Guitarfish 2	3	0.0039
Gymnuridae	2	0.00076
Mobulidae	1	
Myliobatidae	6	0.0017
Narcinidae	4	0.0011
Platyrhinidae	1	
Plesiobatidae	1	
Potamotrygonidae	6	0.0010
Pristidae	1	
Rajidae	31	0.0069
Rhinopteridae	2	0.00073
Torpedinidae	2	0.00033
Urolophidae	2	0.0012
Urotrygonidae	6	0.0017

Figure 3.1. Diagrams showing the definition of pectoral fin outlines used in this study (blue lines) versus that of Franklin *et al*. (2014) (red lines) for typical Rajoidei (A), Myliobatoidei (B), Torpedinoidei (C), Pristidae (D) and guitarfish (E).

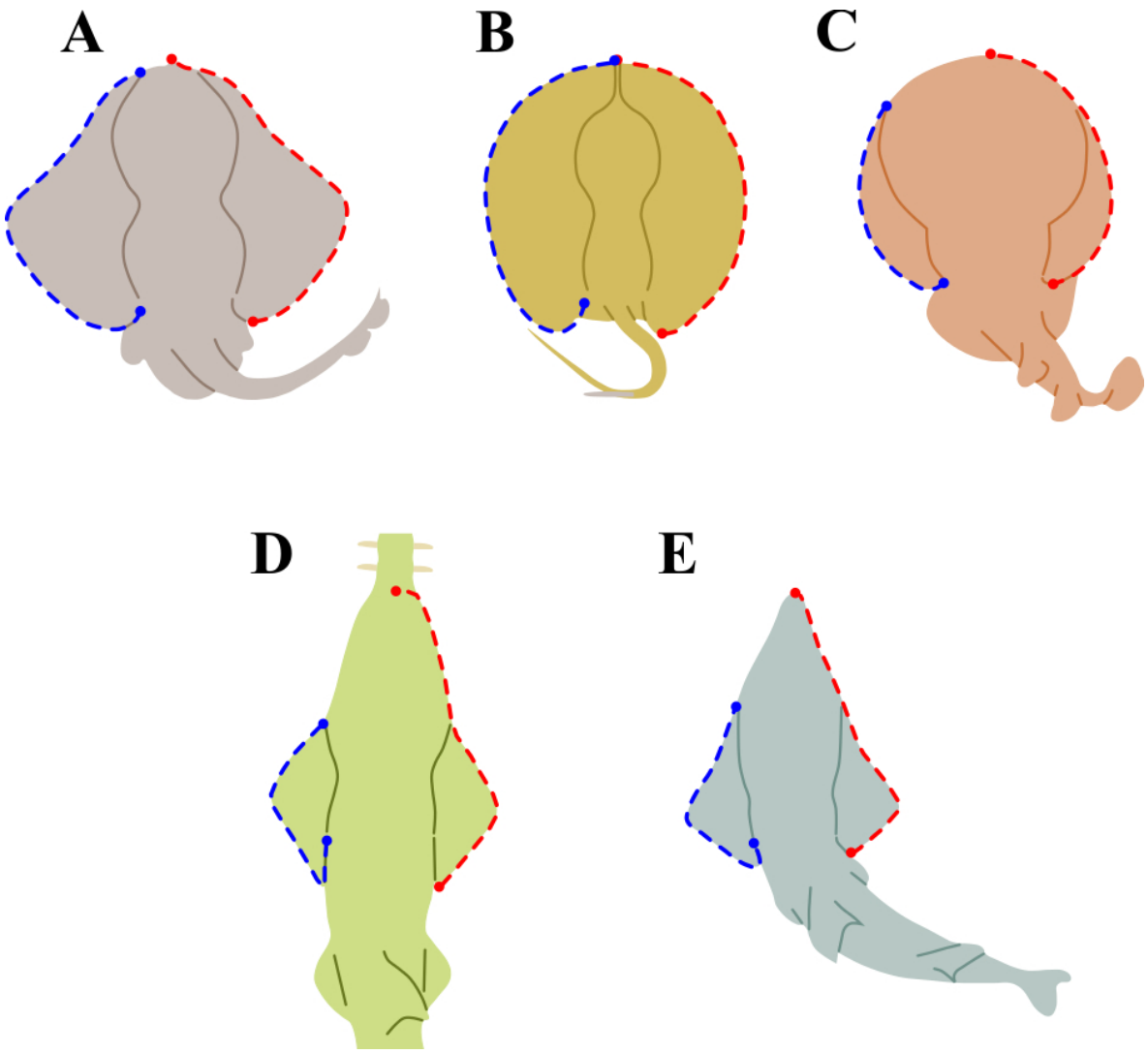

Figure 3.2. Radiograph of *Raja eglanteria*, displaying the two components used in aspect ratio calculations; maximum chord width of the pectoral fin (red bar originating at the scapulocoracoid and extending 90° relative to the axis of symmetry) and fin area (light blue shaded region). Boundaries of the pectoral fin were demarcated by the extent of pectoral radials. The anterior point of the fin area is the intersection of the propterygium and disc outline.

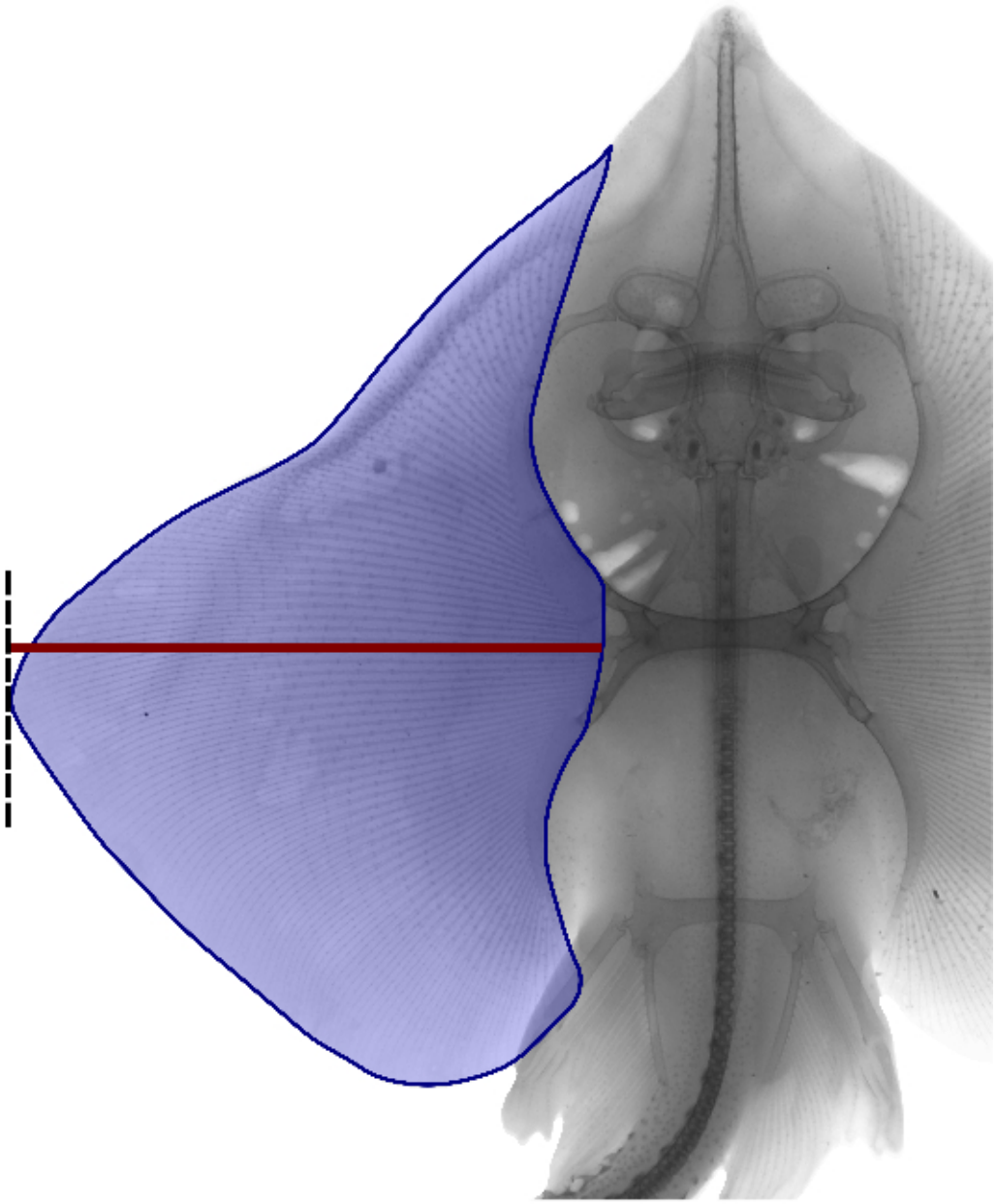

Figure 3.3. Scree plots from PCAs of shape data for all batiods (A), Rajoidei (B), and Dasyatidae (C). Results are shown for the original outline configuration (solid line) and the configuration with an additional anterior landmark (dashed line). For ease of visualization, only data for the first 10 PCs are provided.

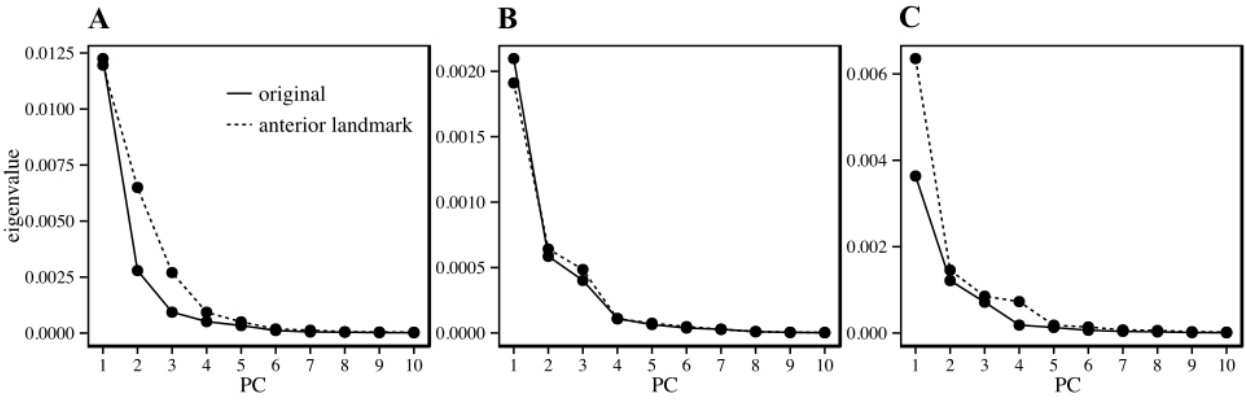

Figure 3.4. Principal components (PCs) 1 and 2 for all batoid specimens (A), with points colored by family. Shapes represent higher-level taxonomic groupings for Myliobatoidei (circles), Rajoidei (triangles) and Torpedinoidei (squares), with Platyrhinodei, Pristidae and guitarfishes all represented by diamonds. The percent of total shape variance explained by PCs is listed on respective axes. Shapes of PC endpoints (B), estimated with the thin-plate spline transformation, are also included (black outlines) and shown relative to consensus shape (gray outlines).

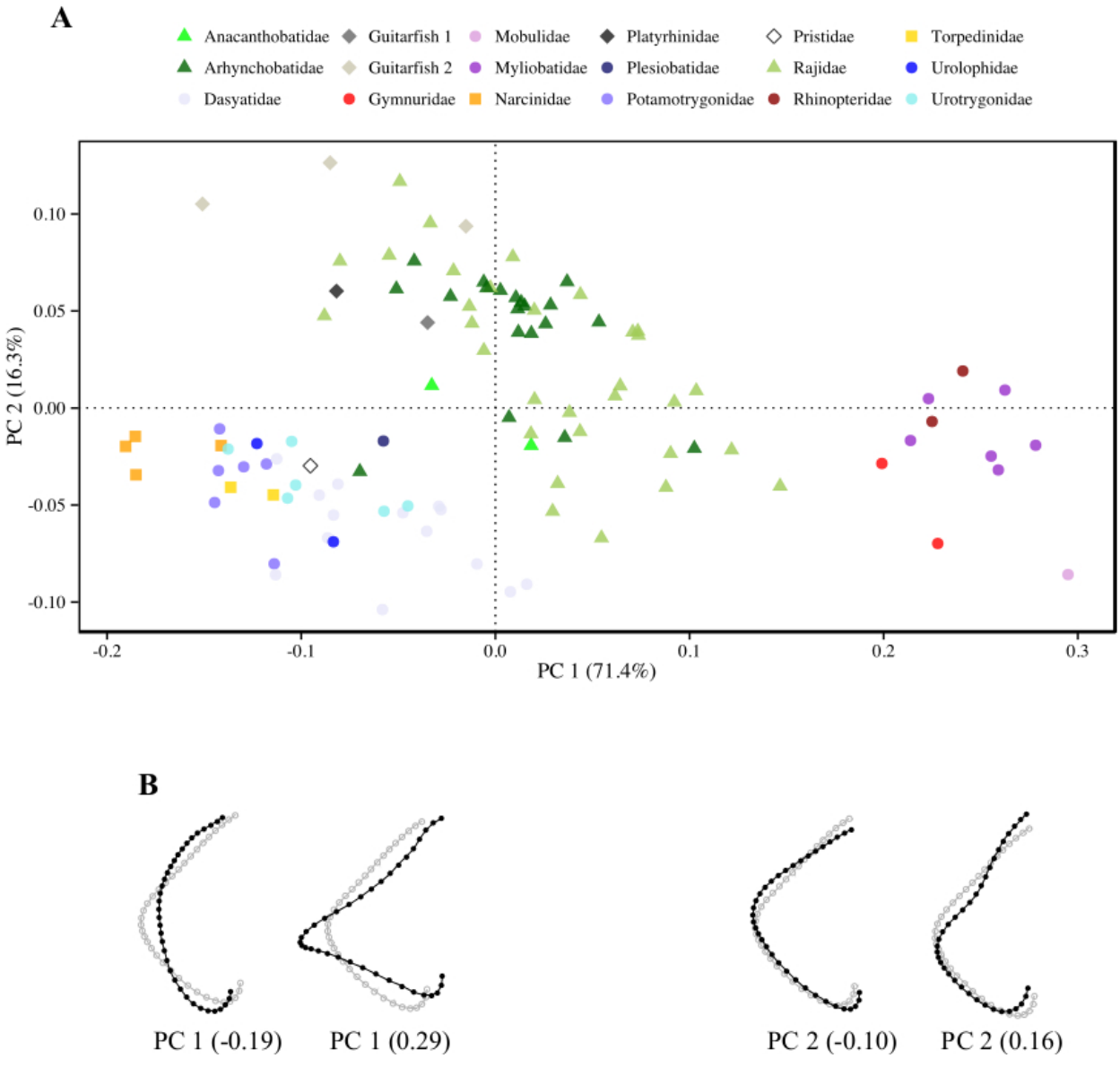

Figure 3.5. Principal components (PCs) 1 and 2 for Rajoidei specimens, with points colored and labeled by genus. The percent of total shape variance explained by PCs is listed on respective axes. Shapes of PC endpoints (B), estimated with the thin-plate spline transformation, are also included (black outlines) and shown relative to consensus shape (gray outlines).

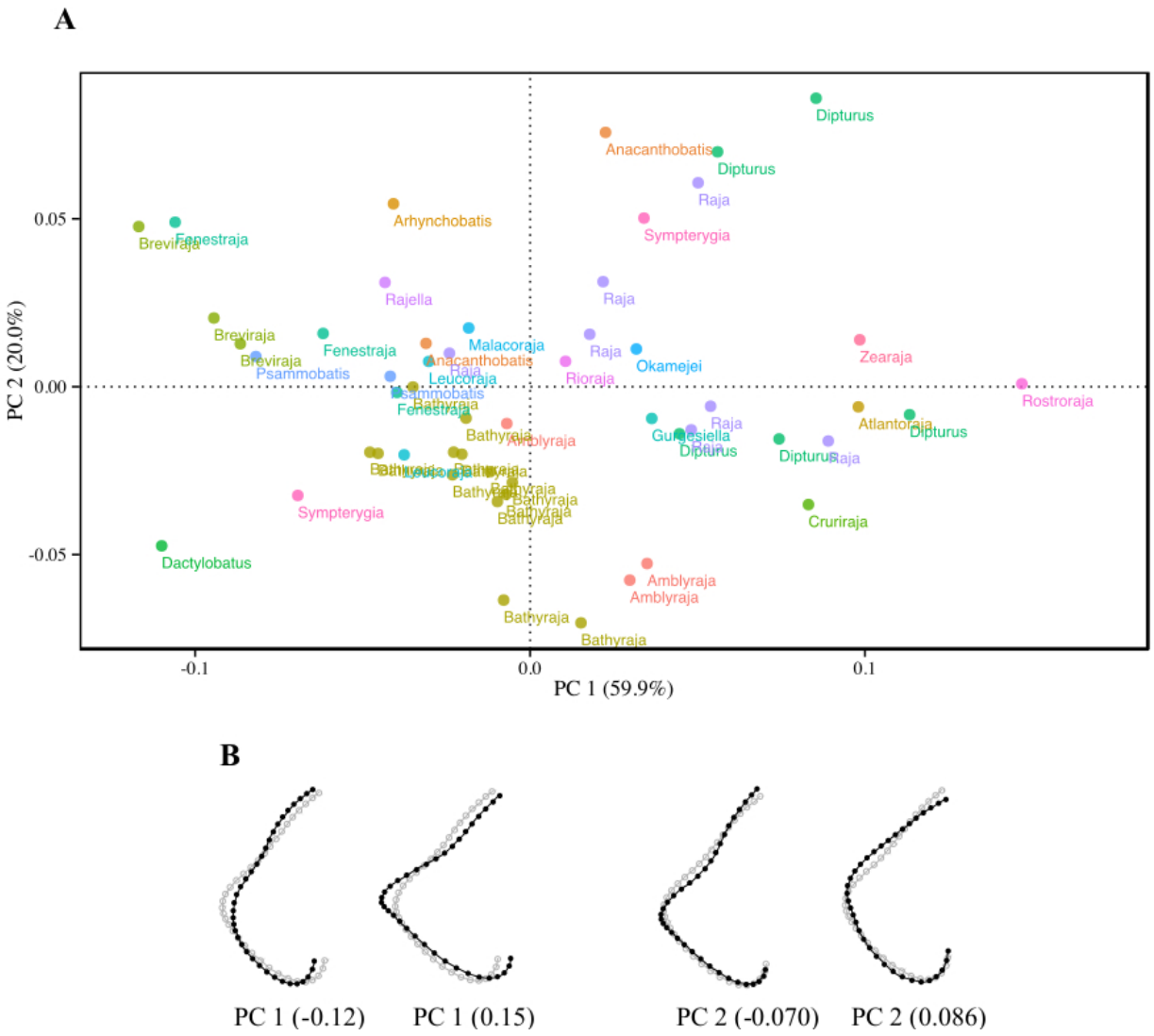

Figure 3.6. Principal components (PCs) 1 and 2 for Dasyatidae specimens, with points colored and labeled by genus. The percent of total shape variance explained by PCs is listed on respective axes. Shapes of PC endpoints (B), estimated with the thin-plate spline transformation, are also included (black outlines) and shown relative to consensus shape (gray outlines).

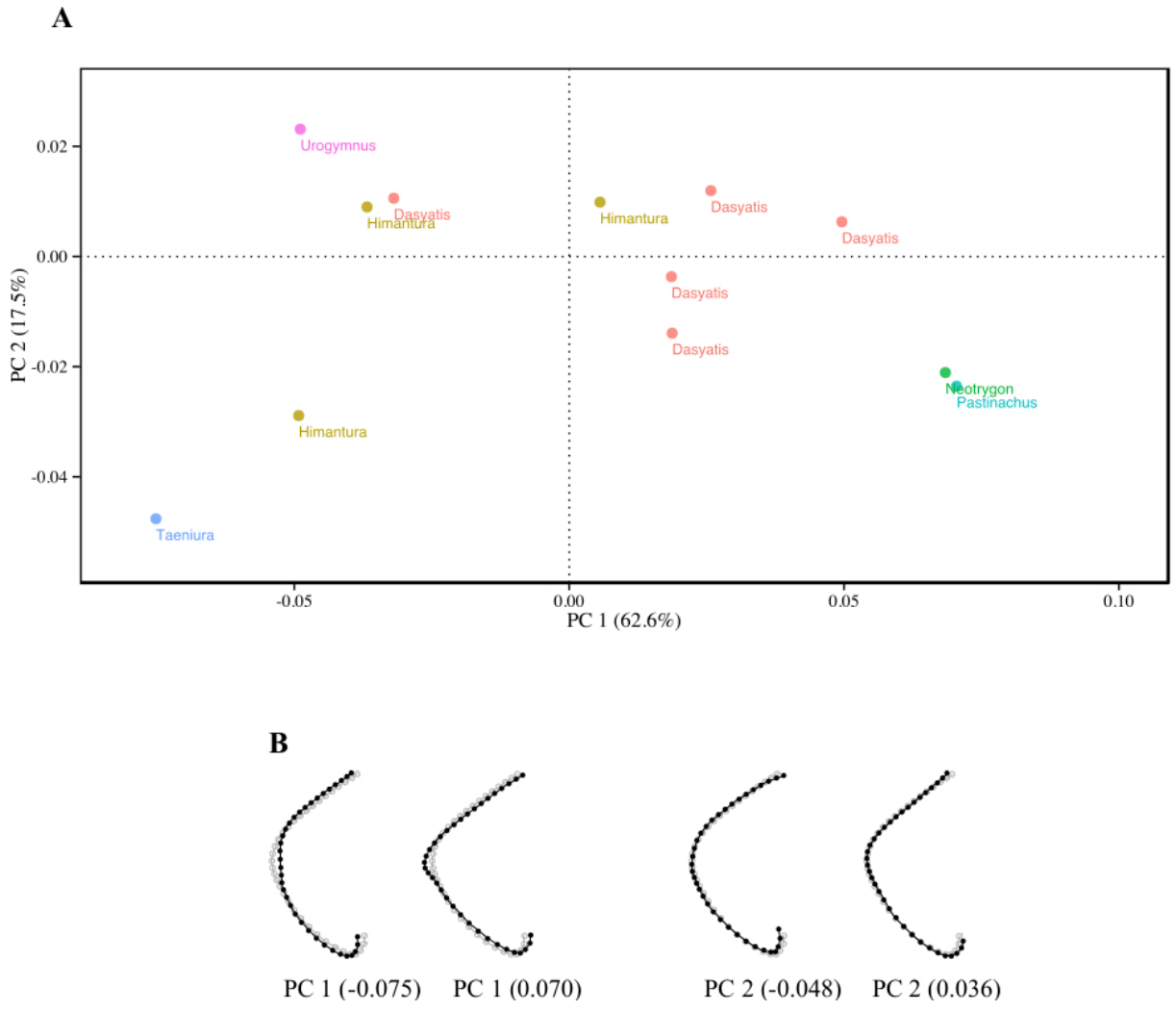

Figure 3.7. Principal component 1 versus aspect ratio. All aesthetics are as in figure 3.4.

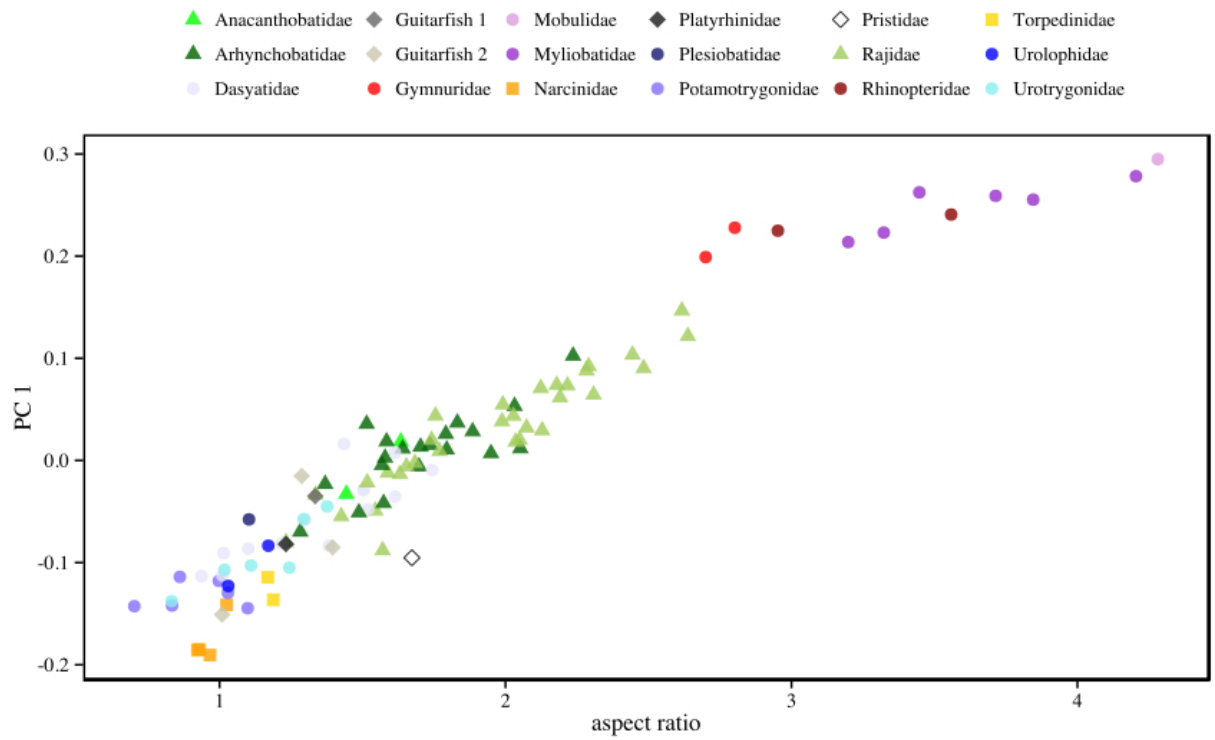

Figure 3.8. Maximum likelihood phylogenetic tree used for comparative analysis of PC 1 shape variation versus aspect ratio. For reference, aspect ratios are superimposed on the tree. Molecular sequences were collected from Aschliman *et al*. (2012).

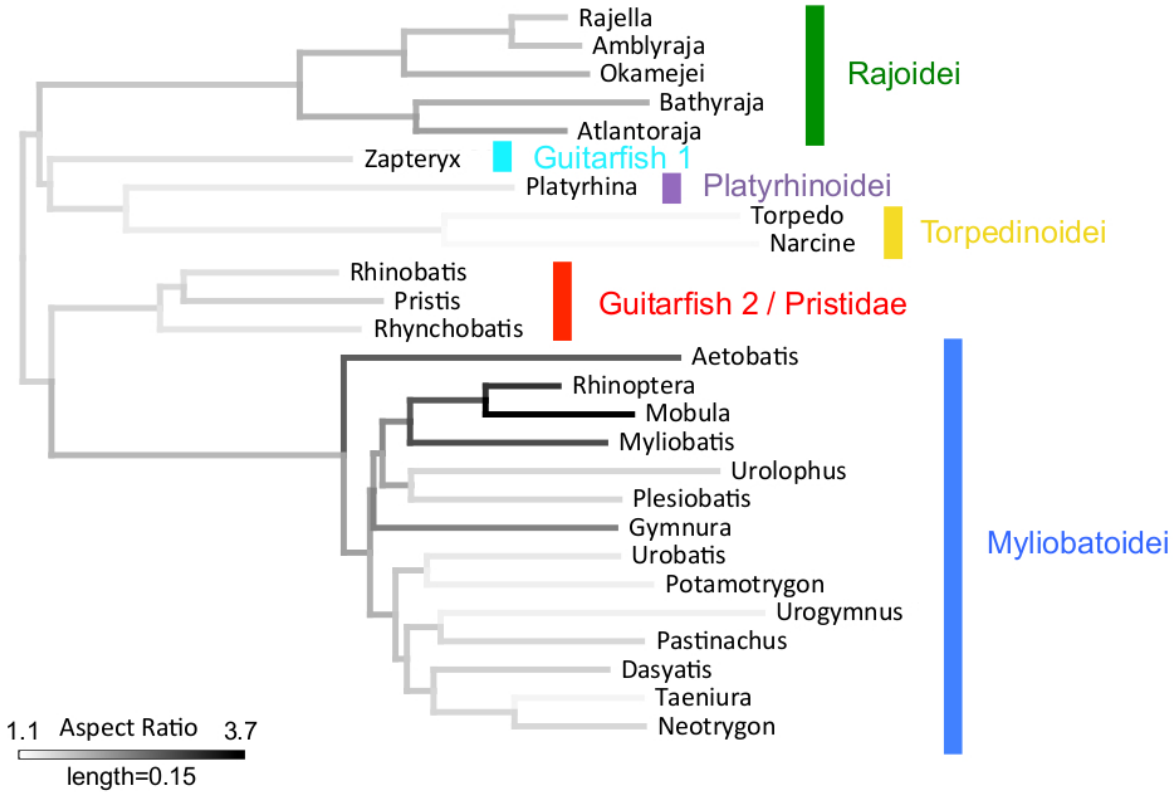

Figure 3.9. Pectoral wave numbers from Rosenberger (2001) plotted against aspect ratios (A) and PC 1 scores (B).

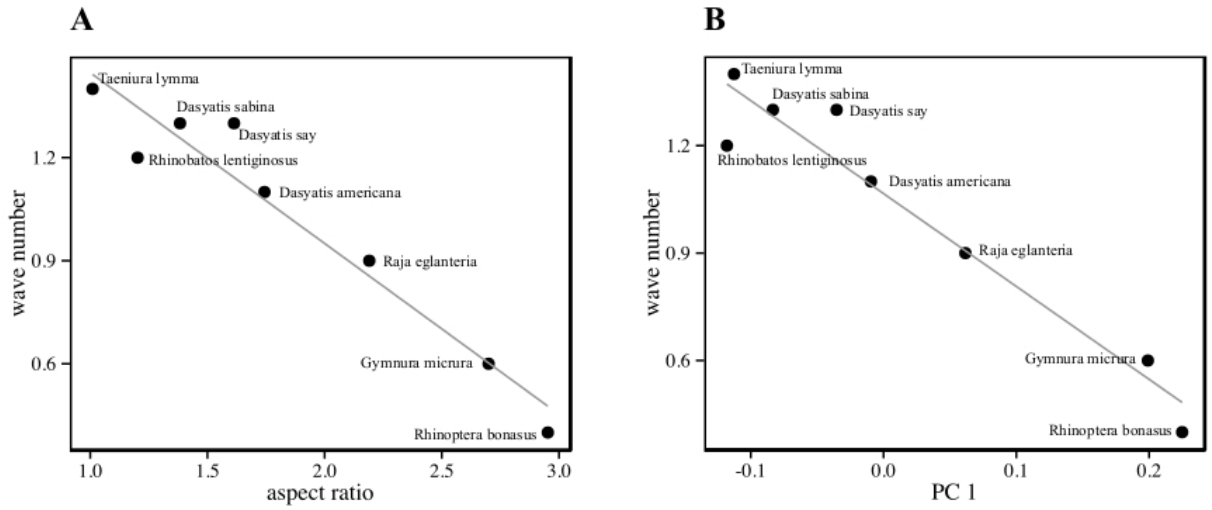

Figure 3.10. Principal components 1 and 2 for batoid specimens with an additional anterior landmark. All aesthetics are as in figure 3.4.

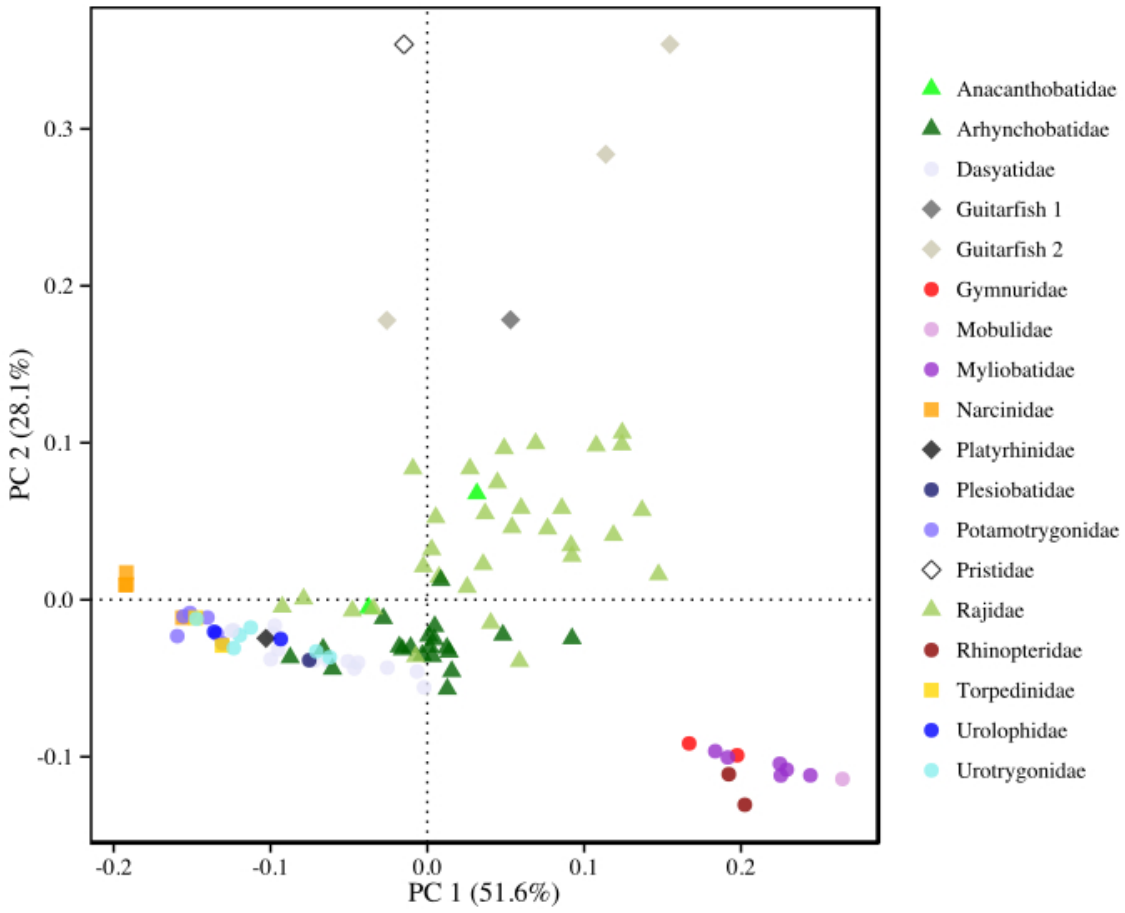

Figure 3.11. Thin-plate spline transformed outlines for all batoids (A), Rajoidei (B) and Myliobatoidei (C) with an additional anterior landmark (red dots). Shapes are shown for positive and negative PC extremes (black outlines) relative to consensus shape (gray outlines). Only the PC that best displayed the influence of the added landmark is shown.

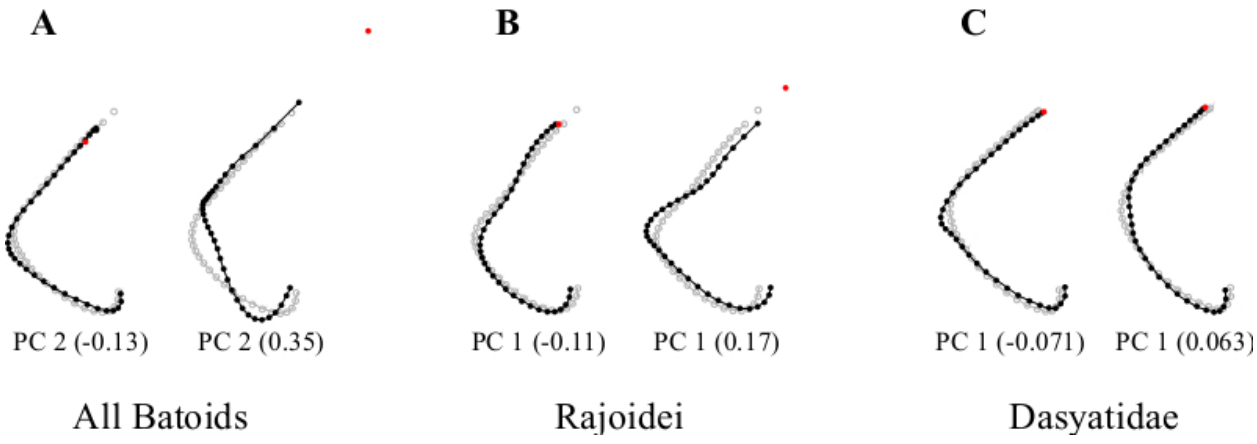

Figure 3.12. Principal components 1 and 3 for batoid specimens with an additional anterior landmark. All aesthetics are as in figure 3.4.

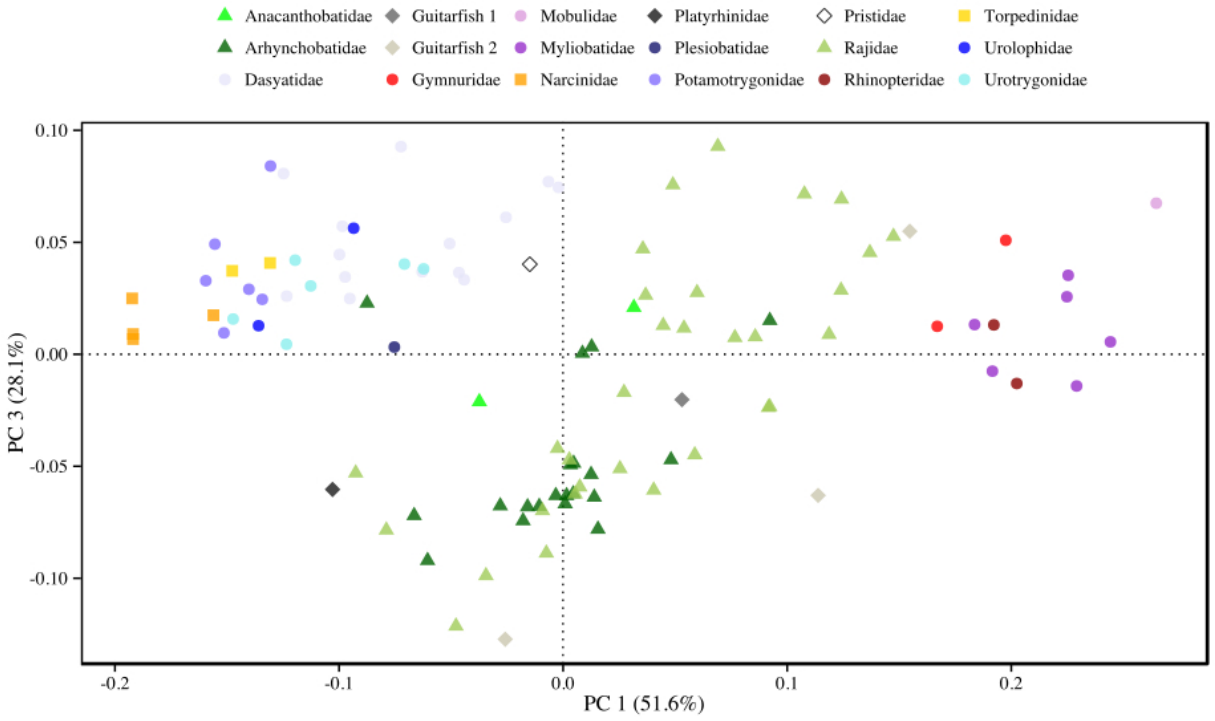

Chapter 4

Pectoral fin dimorphism in sister species of skate, *Leucoraja erinacea* and *Leucoraja ocellata*, and its potential relationship to reproductive strategies

Introduction

In skates (Batoidea: Rajoidei), the most speciose group of elasmobranch (Chiquillo *et al*. 2014), species share similar overall body plans (McEachran and Dunn 1998). However, a fair amount of variation does exist among rajoids and may be related to lifestyle diversity (Martinez, chapter 3). Within species, males and females often differ in morphological characteristics, with several instances of sexual dimorphism having been identified (e.g. Braccini and Chairamonte 2005, Orlov and Smirnov 2011, Last and Alava 2013). One of the most commonly cited examples of dimorphism is dentition, in which males generate cusped teeth at maturation to help with grasping females during copulation (e.g. McEachran 1977, Scenna *et al*. 2006, Castillo-Geniz *et al*. 2007). Other examples include variation in electric organs (Morson and Morissey 2007), alar and malar thorns (MeEachran and Konstantinou 1996; Luer and Gilbert 1985) and the presence of paired, external sex organs (i.e. claspers) in males (Pratt and Carrier 2001).

Sexual dimorphism is common in nature and may arise from a wide range of selective regimes (Lande 1980). Many of its manifestations in skates, including those listed above, have known functional implications for mating. Others, however, are not well understood and their utility is not obvious. For example, sexual dimorphism of pectoral fins was found in *Neoraja stehmanni*, *Raja straeleni* and *Raja miraletus* (Ebert *et al*. 2008) as well as *Atlantoraja cyclophora* (Oddone and Vooren 2004). In all instances, males took on a "bell-shaped" body form at maturity (Ebert *et al*. 2008). Other work has identified sex-based differences in disc width that may also be associated with these shape variations (Orlov and Cotton 2011). Despite relatively few accounts, it appears as though the bell-shaped body is a persistent characteristic of

male skates, occurring in species that span the diversity of Rajoidei (fig. 4.1). Such consistency in the direction of morphological variation across genera and families suggests a common cause. In other words, there is likely some shared characteristic among male skates that produces the distinctive pectoral shape.

Aside from brief acknowledgments of its existence, information regarding the aforementioned pectoral dimorphism and its underlying mechanisms are limited. However, one potential clue to its origin may be found in the bonnethead shark, *Sphyrna tiburo*. Upon maturity, cephalofoil shape (i.e. the modified, flattened head) of male *S. tiburo* diverges from females and becomes more sharply angled (Kajiura *et al*. 2005). Radiographs of the neurocranium indicate that the change in head shape was caused by anterior extension of the rostrum. Given the timing of change and its appearance in males only, it was suggested that dimorphism in *S. tiburo* was a side effect of endocrine signals causing elongation of skeletal elements in claspers. Because pectoral shape divergence also occurs at sexual maturity in male skates (Ebert *et al*. 2008; personal observations), I investigated the relationship between dimorphism and clasper elongation in two common species of northwest Atlantic skate, the little skate (*Leucoraja erinacea*) and winter skate (*Leucoraja ocellata*).

Like many closely related taxa, the sibling species *L. erinacea* and *L. ocellata* are similar in appearance at the juvenile stage. During this period, species discrimination is notoriously difficult (McEachran and Musick 1973). When they begin to mature, however, their adult forms are readily distinguishable. In both species, males and females display dimorphic pectoral fin shapes, although it is much more pronounced in *L. erinacea* (fig. 4.2). Relative to females, adult males have a distinct concavity in the anterior region of the pectoral fin and an exaggerated lobe-like posterior fin area that give them the distinctive bell-shaped appearance.

Despite being closely related, *L. erinacea* and *L. ocellata* have evolved disparate life histories (table 4.1). *L. erinacea* displays faster growth, approaching its asymptotic body length (L_∞) at a faster rate (k) than *L. ocellata* (Frisk and Miller 2006). In addition, female *L. erinacea* reach their peak in reproduction rapidly and decline shortly thereafter, whereas *L. ocellata* has several years at or near its reproductive maximum (Frisk *et al*. 2002). As a consequence of its overall rapid lifestyle, *L. erinacea* is much smaller and shorter-lived than *L. ocellata*, with maximum age at 12.5 and 20.5+ years, respectively (Frisk and Miller 2006). Growth and maturation of skates also determines the timing and rate of clasper elongation in males (Sosebee 2004). If, as in *S. tiburo*, clasper elongation of skates is related to growth of other skeletal structures then variation in life history (particularly related to growth and maturation rates) may influence the expression and intensity of sexual dimorphism in skates.

The overall goal of this research was to document a common form of skate sexual dimorphism in the species *L. erinacea* and *L. ocellata*. Given the apparent dependence of pectoral dimorphism on the maturation process, I investigated variation of shape with size (i.e. allometry) in these species. Divergence of allometric shape trajectories were expected to be larger for males and females of *L. erinacea* than *L. ocellata*, relative to the extent of dimorphism in each species. I also compared variation among species to investigate how differences in fin shape allometry may be related to the development of sex organs (primarily male claspers). Interspecific differences were expected to correspond with species' growth and maturation.

Methods

Specimen Collection and Imaging

Two hundred and thirty skate were collected during research trawls in the New York Bight during 2012 and 2013, including 136 *L. erinacea* (73 male, 63 female) and 94 *L. ocellata* (49 male, 45 female). While fish were caught throughout the year, most were captured during fall and summer months. Individuals ranged from 10.0-49.4 cm total length (TL) for *L. erinacea* and 18.8-95.0 cm TL for *L. ocellata*. For each species, specimens represented an ontogenetic sequence from recently hatched juvenile skate to sexually mature adults. All individuals were euthanized with Tricaine-S (MS-222) directly after being caught and were subsequently frozen until used for imaging. The treatment of specimens followed Institutional Animal Care and Use Committee (IACUC) permit number 2012-1994-NF-10.12.15-FI.

Prior to imaging, specimens were thawed such that pectoral fins were pliable and easily placed into a natural resting orientation. In addition, pelvic fins were removed to aid in visualization of the pectoral margin near the posterior point of attachment to the body. Fish were imaged with photography and radiography, although some images were not suitable for morphological analyses (e.g. low resolution radiographs or specimens with frayed fins). Dorsal photographs were taken with a 10.1 megapixel Canon Rebel xsi DSLR camera attached to a tripod. Radiographs were taken from a ventral perspective as this yielded images that best displayed the desired skeletal structures relating to pectoral fin shape (fig. 4.3). Specimens were x-rayed at one of two locations; larger skates were imaged in the marine veterinary facilities at the Riverhead Foundation (Riverhead, NY) while smaller individuals were taken to the ichthyology department at the American Museum of Natural History, AMNH (New York, NY).

Whenever possible I collected additional specimen data, including information on species identification, sex, total length, clasper length (males), cloaca depth (females) and rostrum length. As mentioned above, species determination is difficult for juvenile *L. erinacea* and *L. ocellata* at superficial levels. However, a meticulous investigation of their morphology found that they differ in their number of pectoral radials (McEachran and Musick 1973), with 63-67 in the former and 71-81 in the latter. Radial counts were made from radiographs and were confirmed for mature individuals where species identity was known. Sex was determined by the presence or absence of claspers. Clasper lengths were measured for males and averaged to generate a single value per specimen. In addition, cloaca depth was measured to the nearest millimeter using calipers (Sosebee 2004). Rostrum lengths were measured on radiographs from the base of the anterior fontanelle to the tip of the rostrum, not including the rostral appendix (fig. 4.3).

Pectoral Margin and Endoskeleton Morphology

I used geometric morphometrics to evaluate overall pectoral fin shape (i.e. the outer margin) and endoskeleton morphology. The pectoral margin was defined from the fin's posterior point of attachment with the body to anterior-most point of radial extension (blue line, fig. 4.3), using 35 landmarks (33 sliding semilandmarks, flanked by a regular landmark on each end). In contrast to traditional landmarks that are allowed to vary in all directions, semilandmarks are constrained to "slide" along a line relative to the two landmarks immediately adjacent to it. They are commonly used to analyze outlines and surfaces where designation of homologous points is difficult (Gunz and Mitteroecker 2013). Endoskeleton morphology was similarly evaluated with sliding semilandmarks. Ninety-four landmarks, distributed among five outlines, were used to

define the skeletal complex that collectively provides a structural base to the pectoral fin (red lines, fig. 4.3). This included the pectoral girdle (scapulocoracoid) and three basal radials (propterygium, mesopterygium and metapterygium). For both sets of morphological analyses, points along outlines were created in tpsDIG2 (Rohlf 2013a) and shape variables were constructed with generalized Procrustes analysis (GPA) in tpsRelw (Rohlf 2013c). GPA is an iterative procedure that scales, rotates and translates landmarks to reduce the sum of squared residuals of Procrustes distances (Klingenberg 2010). I used the thin-plate spline transformation (TPS) to visualize shapes along the major axes of variation, determined with principal components analysis (PCA).

Sexual Dimorphism and Comparisons of Interspecific Allometry

I tested for intraspecific differences in allometric shape change trajectories for pectoral fins and endoskeletons. To do this, I performed a test of common slopes in tpsRegr (Rohlf 2013b) using a multivariate analysis of covariance (MANCOVA) for partial warp scores grouped by sex and log-centroid size (CS) as the covariate. This method compares the sum of squared residuals from regressions with a common slope (sexes pooled) with that of separate slopes (males and females). CS is the square root of the sum of squared distances between landmarks and the shape centroid and is commonly used to investigate allometry in morphometric research (Frédérich and Vandewalle 2011). Following slope comparisons, I performed separate PCAs on Procrustes-aligned specimens for each species. The resulting axes were used to visualize relative shape variation relative to CS. Finally, I repeated the test of slopes to compare interspecific allometry between skates of the same sex.

Pectoral Shape and Development of Sex Organs

I regressed Procrustes coordinates on clasper length and cloaca depth (depending on sex) for all four species-sex combinations. I also regressed shape on log-CS for reference to allometric shape change in each group. The percent of total shape variation accounted for was used as an indicator of the strength of relationships. Finally, I explored allometry of rostral growth, as it was related to maturation in male bonnethead shark (Kajuira *et al*. 2005).

In order to further understand divergence of reproductive strategies, I calculated the gonadosomatic index (GSI) for male *L. erinacea* and *L. ocellata* over a range of TLs. GSI was calculated as testes mass divided by total body mass, multiplied by 100. It provided information about species' investment in testes, which is often used as an indicator of sperm production and intensity of polyandry and/or sperm competition in a wide range of taxa (Parker *et al*. 1997), including some elasmobranchs (Fitzpatrick *et al*. 2012). Due to impacts of freezing and subsequent thawing on the structural consistency of testes, additional individuals not included in morphological analyses, were collected for GSI measurements (37 *L. erinacea* and 47 *L. ocellata*). These individuals were obtained on the 5th and 6th of May 2013. Often, GSI data are collected throughout the year to account for variation in testes weight relative to peak reproductive season (e.g. Flammang *et al*. 2008). However, Sulikowski and colleagues (2004) showed that male *L. ocellata* in the Gulf of Maine display relatively stable GSI throughout the year (fig. 4.4) and that reproductive peaks are not well defined. In addition, *L. erinacea* is known to mate throughout the year (Bigelow and Schroeder 1953).

Results

Pectoral Margin and Endoskeleton Morphology

Analysis of the pectoral margin indicated that the largest axis of variation (PC 1) was primarily associated with species differences (fig. 4.5). Most change on this axis was concentrated in the posterior region of the pectoral fin, where *L. erinacea* was much more rounded and lobe-like in shape. In contrast, *L. ocellata* had a fairly flat posterior fin area that came to a point, creating a clearly defined lateral apex. Females also appeared to be shifted slightly toward lower PC 1 values relative to conspecific males. Unlike PC 1, shape changes on PC 2 were mostly in the anterior pectoral fin region. Male *L. erinacea* set positive and negative endpoints of this axis, with bell-shaped fins at large PC 2 values and a more uniformly round shape that is indicative of juvenile skates on the opposite end (fig. 4.1A).

Endoskeleton shape change on PC 1 (fig. 4.6) was associated mainly with variation in the length of the metapterygium (i.e. the posterior basal radial). Male and female *L. ocellata* were concentrated primarily in the upper regions of PC1, with shorter metapterygia. Some juvenule *L. erinacea* also occurred in this area and achieved increasingly negative values as they grew. PC 2 variation was again set by male *L. erinacea*, where decreasing PC scores relate to increasing deflection of the metapterygiun outward and also a subtle increase in concavity of the propterygium. It also appears that some male *L. ocellata* are oriented at lower PC 2 values than females. An additional change that occurs with deceasing PC 2 is the expansion of the scapulocoracoid near its connection to the metapterygium. This may potentially be a leading contributor to the overall change in angle observed in the metapterygium. At first glance, the single male *L. erinacea* at the lower extreme of figure 4.6 seems to be a potential error.

However, inspection of this specimen indicates that it is not a mistake and represents an individual with especially pronounced adult male morphology.

Sexual Dimorphism and Comparisons of Interspecific Allometry

Males and Females of *L. erinacea* displayed significantly different regression slopes in the relationship between non-affine shape variation (i.e. partial warps) and log-CS for both pectoral margin ($p = 0.0013$) and endoskeleton shape ($p < 0.0001$). In this species, signs of divergence are strong at large log-CS values (fig. 4.7A & B). In *L. ocellata*, allometric patterns of pectoral margin shape change were best described with a single slope that included both males and females (table 4.2). Although slopes were similar, it did appear that females might have a longer shape trajectory than males (fig. 4.7C). In contrast to pectoral margins, endoskeletons in *L. ocellata* displayed different rates of allometric change between sexes ($p = 0.0008$).

In all interspecific comparisons of allometry, males and females of contrasting species had significantly different slopes (table 4.2). In addition, the variance of shape-size relationships appeared smaller for endoskeletons than pectoral fin margins (fig. 4.8), at least in the shape space defined by PC 1 and PC 2.

Pectoral Shape and Development of Sex Organs

Clasper length and cloaca depth increased rapidly when individuals reached sexual maturity, making their relationship with TL highly non-linear (fig. 4.9). In male *L. erinacea*, clasper length was associated with 41.7% and 42.5% of variation in pectoral margin and endoskeleton shape, respectively (table 4.3). In comparison, log-CS only accounted for 3.7% and 13.1% of respective variance (table 4.4). As expected, relationships between cloaca depth and

shape were much weaker for female *L. erinacea*, with the endoskeleton showing the strongest association at 19.7% of variance accounted for. Regressions of shape on log-CS in female *L. erinacea* accounted for even less of shape variation than did cloaca depth, although it was still comparable. In *L. ocellata*, regressions for different sexes were much more similar than they were in *L. erinacea* (tables 4.3 and 4.4). Clasper and cloaca depths were similarly related to shape variation in *L. ocellata*, which accounted for 10-14% of shape variation in both sexes (table 4.3). In addition, allometry was more-strongly associated with pectoral margin shape in *L. ocellata*, accounting for roughly twice the amount of observed variation of relationships with sex organs (tables 4.3 and 4.4). Finally, rostrum lengths scaled similarly with log-CS for species and sexes (fig. 4.10).

The GSI increased at sexual maturity in both species, but did so much more rapidly and to a larger degree in *L. erinacea* (fig. 4.11). Although GSI comparisons have TL on the abscissa and not CS, the relationship between TL and CS is very strong and scales linearly for all groups (fig. 4.12).

Discussion

Allometric changes in pectoral shape, and its corresponding internal structure, pointed to markedly different intraspecific growth patterns in *L. erinacea*. However, in *L. ocellata* this was only true for the endoskeleton, as allometry of the fin margin shape was not significantly differentiated between sexes. Overall, the endoskeleton appeared to provide better discrimination between allometric trends than the pectoral outline (table 4.2). It may be that the endoskeleton is the more appropriate morphological comparison here because of its direct relation to the suggested mechanism (i.e. the elongation of skeletal elements at maturity). In other words, the

relationship between pectoral margin shape and clasper size is likely mediated by the shape of basal radials and the scapulocoracoid, much like head shape in *S. tiburo* was shown to be the indirect effect of clasper elongation on rostrum length (Kajiura *et al*. 2005).

One interesting outcome of this work was that the only group that did not display a significant trend between pectoral margin shape and log-CS was the one that actually changed the most over ontogeny, male *L. erinacea*. This may be quite easily explained, considering that the overall pectoral shapes of juveniles are quite similar and are followed by extremely rapid shape change at maturity. Figure 4.7A displays this process, with much of the shape variation in males (dark blue points) oriented roughly perpendicular to the log-CS axis. It was also surprising that allometry accounted for so little of shape variance, ranging from a low of 3.68% for fin margins in male *L. erinacea* to a high of 27.26% for fin margins in female *L. ocellata* (table 4.4). Although allometry can be a large determinant of shape, my results are by no means unprecedented. Drake and Klingenberg found that size only accounted for 3.4% of shape variation in St. Bernard skulls. In skates, this may result from large variance in shape itself. In the PCAs that included all specimens (figs. 4.5 and 4.6), the first three axes explained only 73.7% and 79.1% of shape variation for the endoskeleton and overall fin shapes, respectively.

In addition to sexual dimorphism, interspecific shape allometry also varied significantly between *L. erinacea* and *L. ocellata*. Female *L. erinacea* displayed larger variation than *L. ocellata* in the length of the metapterygium (fig. 4.6, PC2), which became longer with increasing CS. Relatively shorter metapterygia in *L. ocellata* may explain the flattened shape of the posterior region of their pectoral fins at maturity (fig. 2). Larger interspecific differences were observed in male skates. *L. erinacea* displayed rapid shape variation at sexual maturity that closely tracked clasper elongation. Clasper length also increased substantially in *L. ocellata*, but

its pectoral changes were not as pronounced. This discrepancy may potentially be explained by the rate at which maturation (and clasper elongation) occurs in both species. Clasper growth profiles show that the transition period to the adult stage covers a relatively small TL range in *L. erinacea* versus *L. ocellata* (fig. 4.9, gray bars). It is difficult to determine with precision the TL at which the juvenile-to-adult transition occurs in male *L. ocellata* (Sosebee 2004), which is why only relative ranges are discussed here. In terms of time, interspecific differences in the transition to maturity are even larger than in TL, since somatic growth rates are slower in *L. ocellata* (table 4.1). Similarly, disparities in maturation have been found for females (Frisk and Miller 2009), where the size range (in cm TL) from the onset of maturity to functional maturity (based on oocyte state) occurred over 1cm in *L. erinacea* and 10 cm in *L. ocellata*. Therefore, a subtle bell-shape body in male *L. ocellata* may result from their tendency to grow slower, spreading skeletal growth over a much longer growth period. In contrast, the more extreme morphology in male *L. erinacea* may signify that skeletal changes happen so quickly that the body can hardly keep pace. Evidence for this can be found in the endoskeleton, where it was common to observe pectoral radials in *L. erinacea* displaying what I have termed "cramming" between the outer fin margin and the increasingly concave propterygium (fig. 4.13). Additional warping of skeletal elements can be seen in the lateral region of the scapulocoracoid, near the origin of the basal radials. Comparisons of other species are needed to substantiate these patterns, but if true, they suggest that the rate of somatic growth may set the upper limit on rates of clasper and skeletal growth for maturing males.

Evidence of the premium placed on reproductive competitiveness by *L. erinacea* can be found in its GSI relative to *L. ocellata*. Disproportionate allocation of resources to testes and rapid skeletal growth in *L. erinacea* must come at a cost and are unlikely to be present if not for

some benefit to individual fitness. As previously noted, the period of peak reproductive value is brief in *L. erinacea* (Frisk *et al*. 2002). As a consequence, individuals must act quickly and compete for mating opportunities while it is most profitable to do so. Rapid rates of GSI increase, clasper elongation and associated shape change in *L. erinacea* suggest a race to maturation with an intensity that is not realized in *L. ocellata*. Therefore, the magnitude of sexual dimorphism in *L. erinacea* and *L. ocellata*, which is primarily related to changes in male pectoral fins at maturation, appears to be regulated by interspecific differences in life history and reproductive strategies.

The implications of this work for the larger Rajoidei group are quite intriguing. If the patterns observed here hold for other skates, the relative degree of dimorphism may then be indicative of reproductive biology and maturation. Further research is certainly needed to confirm relationships between clasper elongation, pectoral shape and life history in other species.

Table 4.1. von Bertalanffy growth parameters from Frisk and Miller (2006). Estimates are shown for asymptotic length (L∞), growth rate (k) and the theoretical age at size zero (t0).

	L_∞ (cm)	k (year^{-1})	t_0 (years)
L. erinacea (male)	60.13	0.17	–1.16
L. erinacea (female)	53.94	0.2	–1.22
L. ocellata (male)	115.92	0.08	–1.88
L. ocellata (female)	114.1	0.07	–2.10

Table 4.2. Interspecific and intraspecific tests of allometric slopes (MANCOVA).

	pect. margin			endoskeleton		
comparison	λ_{WILKS}	F_S	**p**	λ_{WILKS}	F_S	**p**
L. erinacea (male v female)	0.32	2.11	0.0013	0.20	3.98	< 0.0001
L. ocellata (male v female)	0.20	1.49	0.14	0.10	3.30	0.0008
Males (L. erinacea v L. ocellata)	0.17	3.89	< 0.0001	0.055	14.32	< 0.0001
Females (L. erinacea v L. ocellata)	0.25	1.80	0.025	0.03	17.39	< 0.0001

Table 4.3. Regressions of Procrustes-aligned shapes on clasper lengths and cloaca depths

	pect. margin			endoskeleton		
group	**% variance explained**	**n**	**p**	**% variance explained**	**n**	**p**
L. erinacea (male)	41.66	62	< 0.0001	42.52	61	< 0.0001
L. erinacea (female)	8.55	53	0.0029	19.65	53	< 0.0001
L. ocellata (male)	11.1	45	< 0.0001	12.99	46	< 0.0001
L. ocellata (female)	14.1	43	0.0001	10.06	43	0.0002

Table 4.4. Regressions of Procrustes-aligned shapes on log-centroid size (CS).

	pect. margin			endoskeleton		
group	% variance explained	n	p	% variance explained	n	p
L. erinacea (male)	3.68	73	0.057	13.09	72	0.0001
L. erinacea (female)	7.51	63	0.0021	10.79	63	0.0005
L. ocellata (male)	22.82	48	< 0.0001	11.82	49	< 0.0001
L. ocellata (female)	27.26	45	< 0.0001	8.43	45	0.0005

Figure 4.1. Comparison of sexual dimorphism in pectoral fin shapes for a selection of skate species; male (A) and female (B) *Raja eglanteria*; male (C) and female (D) *Rajella Fyllae*; male (E) and female (F) *Bathyraja minispinosa*; and male (G) and female (H) *Bathyraja pallida*. Images A and B came from personal collection, C from Claude Nozeres (DFO, Canada), D from Roberta Miller (DFO, Canada), E & F from Duane Stevenson (NMFS AFSC), and G & H from Alexei Orlov (VNIRO, Russia).

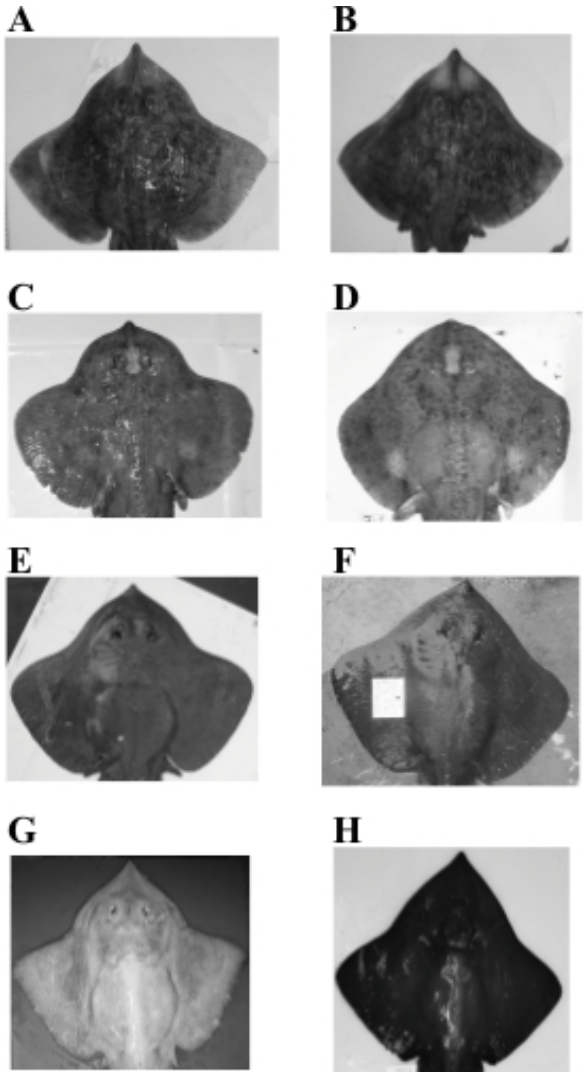

Figure 4.2. Pectoral shape variation in male *L. erinacea* (A), female *L. erinacea* (B), male *L. ocellata* (C) and female *L. ocellata* (D). On the left half of images are juveniles (with 1cm bar below) and the right side of images are adults (with 5cm bar below).

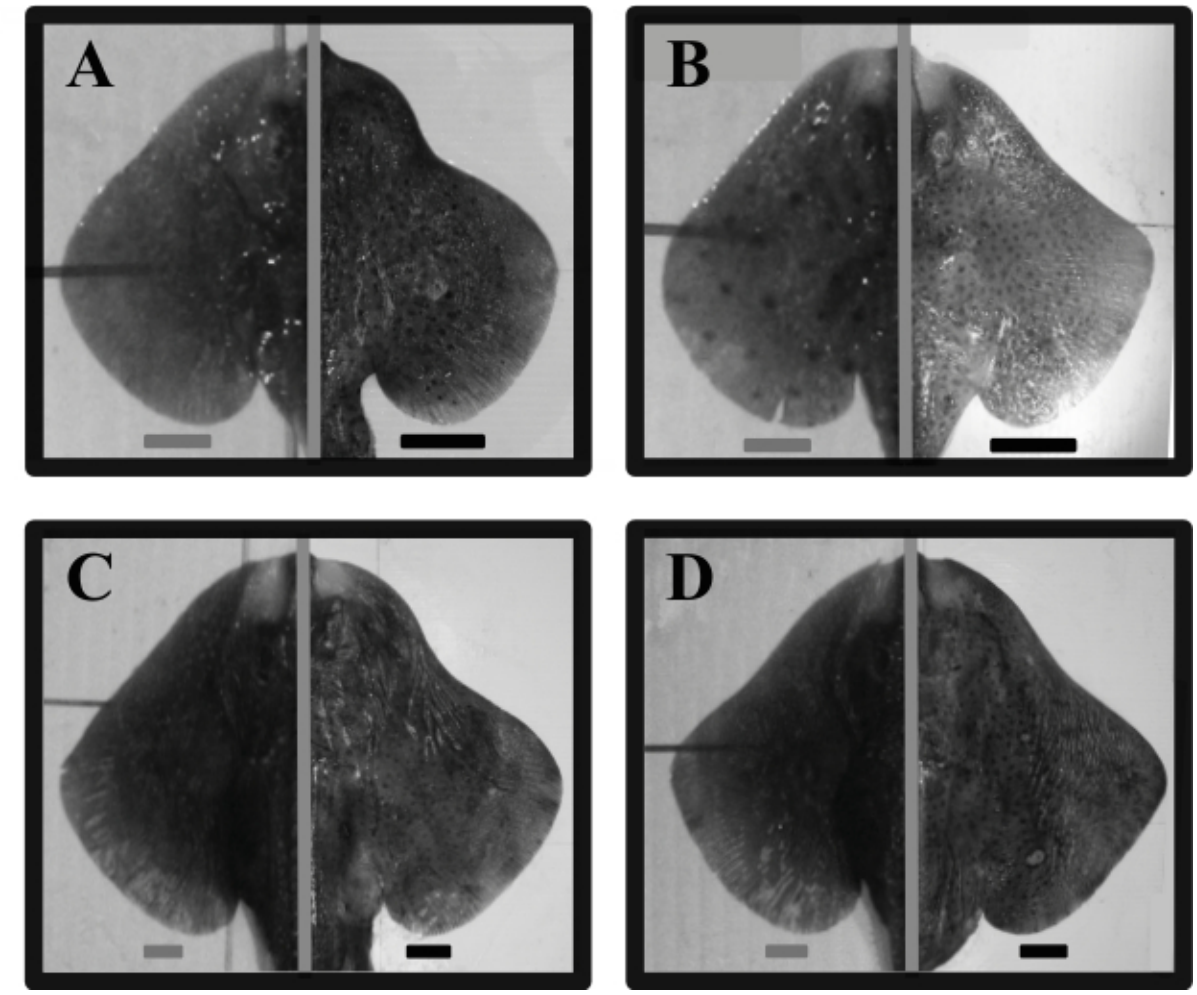

Figure 4.3. Skate endoskeleton diagram (right) with features of interest labeled; rostrum length used in this study (*ros*), rostral appendix (*rap*), propterygium (*pt*), mesopterygium (*msp*), metapterygium (*mtp*) and scapulocoracoid (*sc*). In addition, the outlines used for morphological analyses are shown (right), with the number of landmarks on each provided in parentheses. The pectoral fin margin was evaluated as a single outline (blue dashed line) and the endoskeleton configuration included five (red dashed lines). Sliding landmarks were evenly spaced along the outlines shown, with a true landmark on each end (colored circles). Note that for the endoskeleton, the anteriormost landmark is shared among two outlines (making 94 total endoskeleton landmarks).

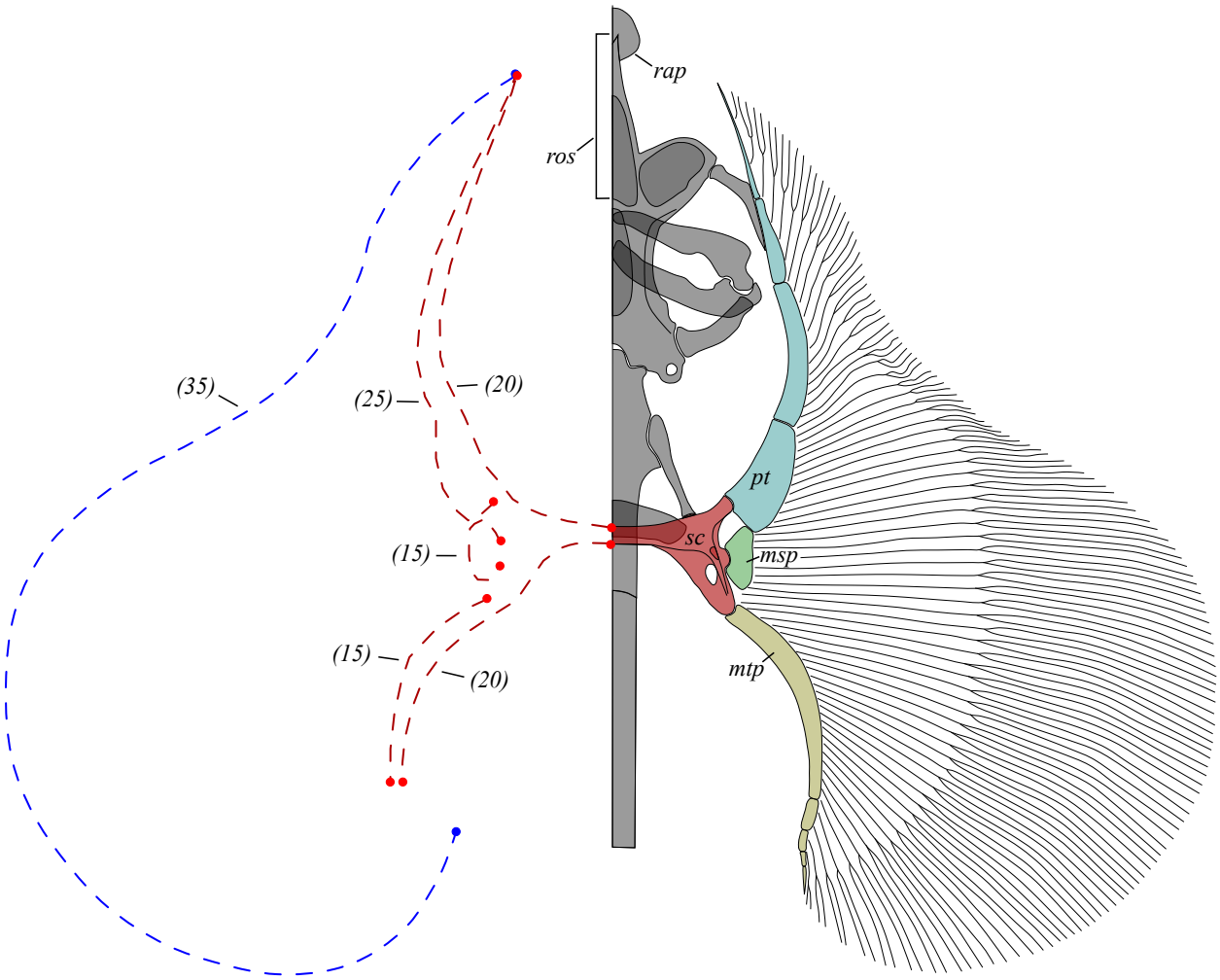

Figure 4.4. From Sulikowski *et al*. (2004); monthly means of gonadosomatic indices for male (dark blue) and female (light blue) *L. ocellata* in the Gulf of Maine. Vertical bars are standard errors.

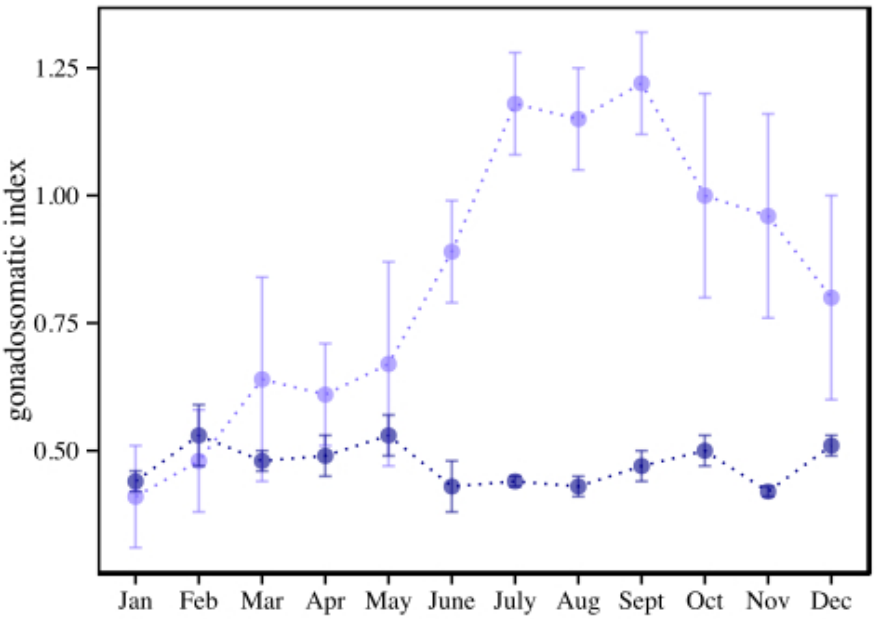

Figure 4.5. PC 1 and PC 2 for shape analyses of pectoral margins. Also included are shapes representing PC extremes (black outlines), relative to consensus shape (gray outlines). Shape visualizations were made with the thin-plate spline transformation.

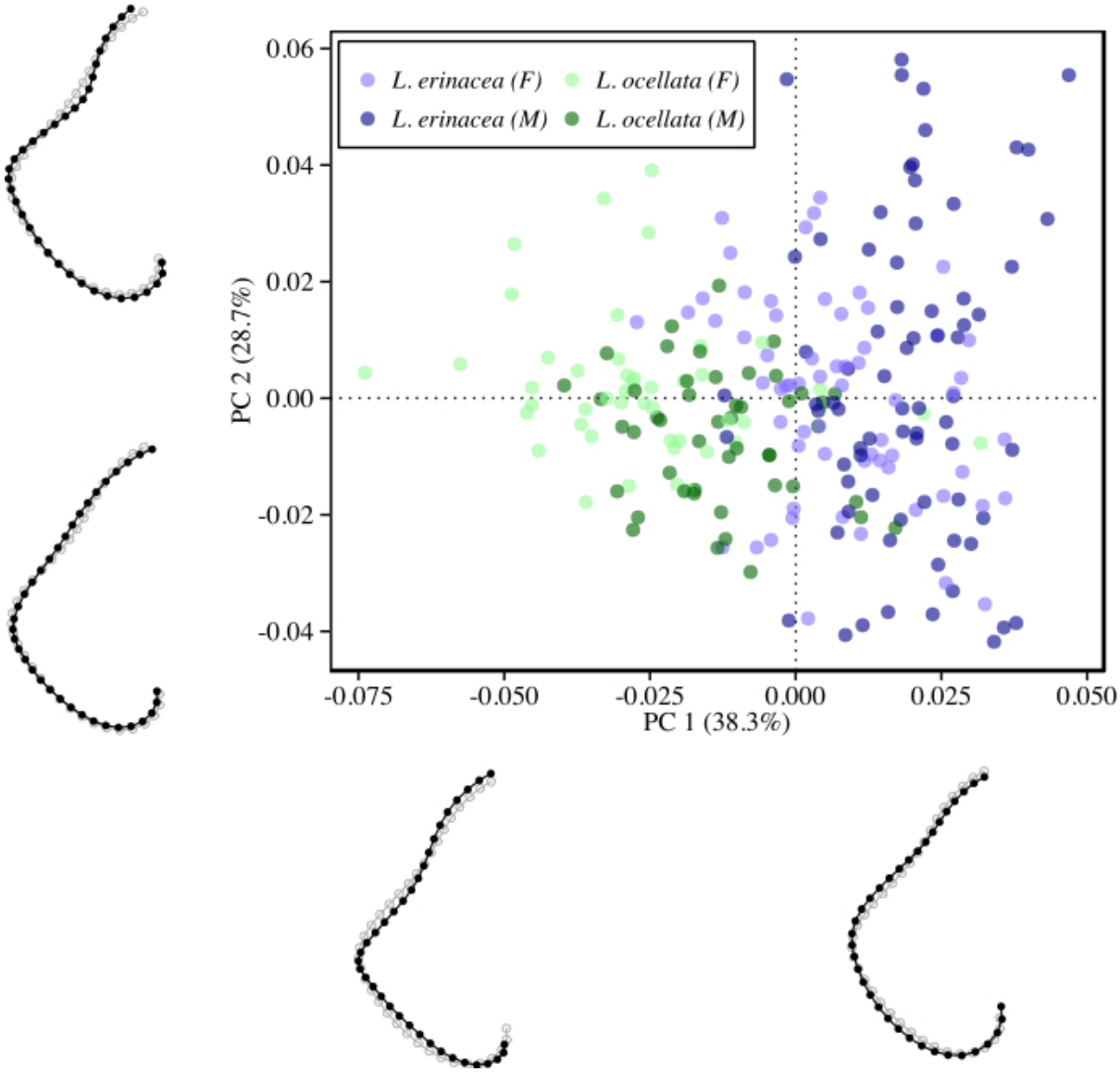

Figure 4.6. PC 1 and PC 2 for endoskeleton shape analyses. Also included are shapes representing PC extremes (black outlines), relative to consensus shape (gray outlines). Shape visualizations were made with the thin-plate spline transformation.

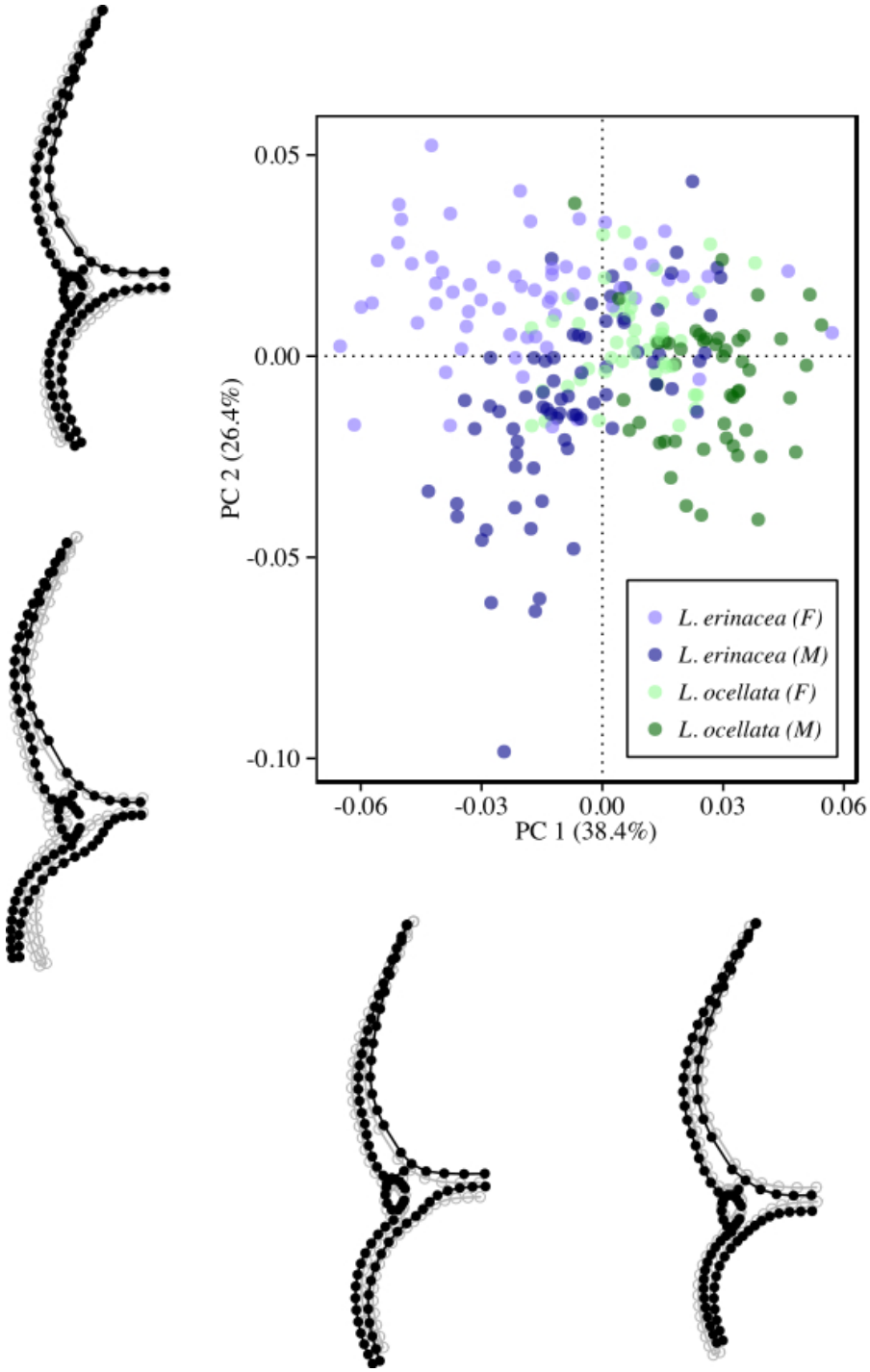

Figure 4.7. 3D plots of log-centroid size versus PC1 and PC2 in separate PCAs for *L. erinacea* fin margins (A), *L. erinacea* endoskeletons (B), *L. ocellata* fin margins (C) and *L. ocellata* endoskeletons (D). Shaded regions are 95% equal frequency ellipses. Color schemes are as in figures 4.5 and 4.6.

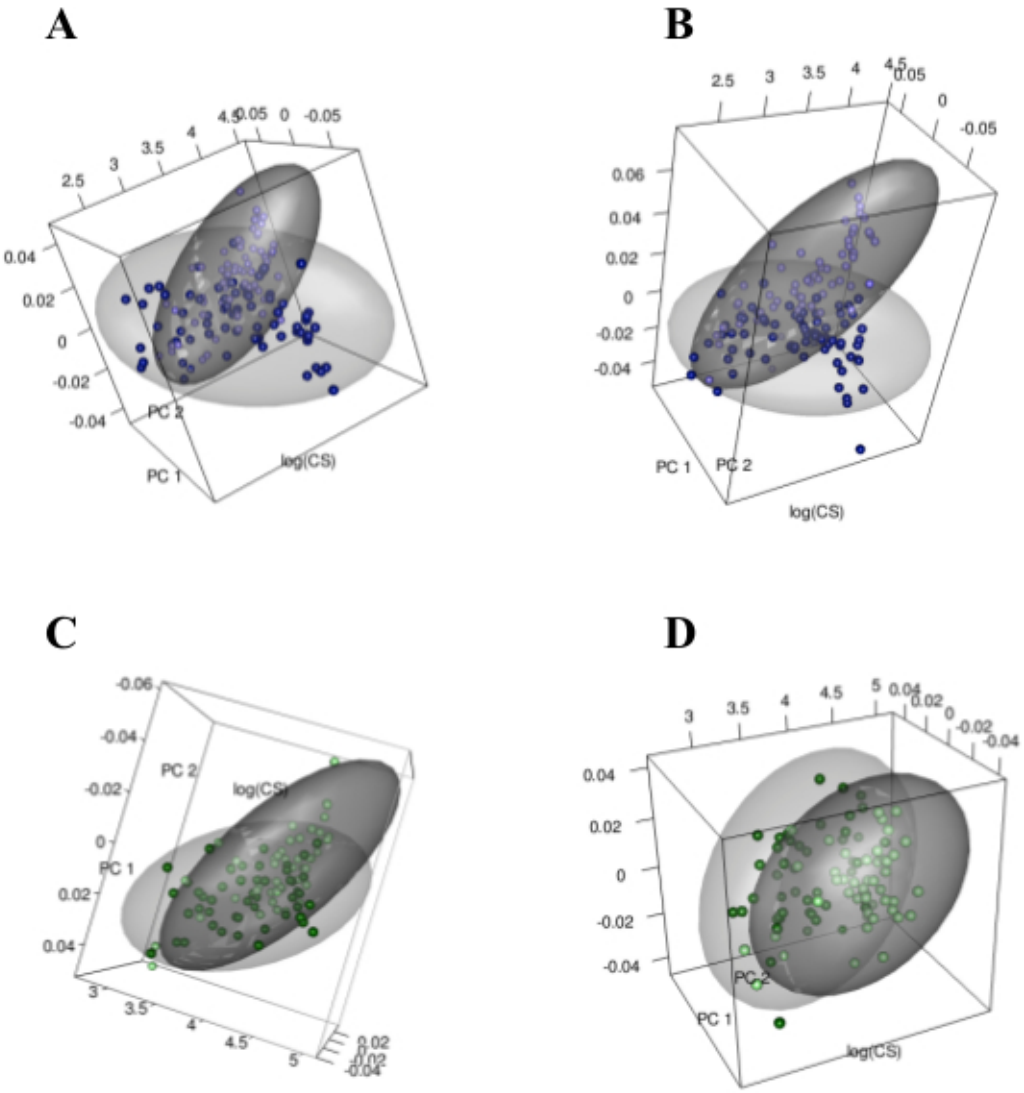

Figure 4.8. 3D plots of log-centroid size versus PC1 and PC2 in separate PCAs for interspecific male fin margins (A), male endoskeletons (B), female fin margins (C) and female endoskeletons (D). Shaded regions are 95% equal frequency ellipses. Color schemes are as in figures 4.5 and 4.6.

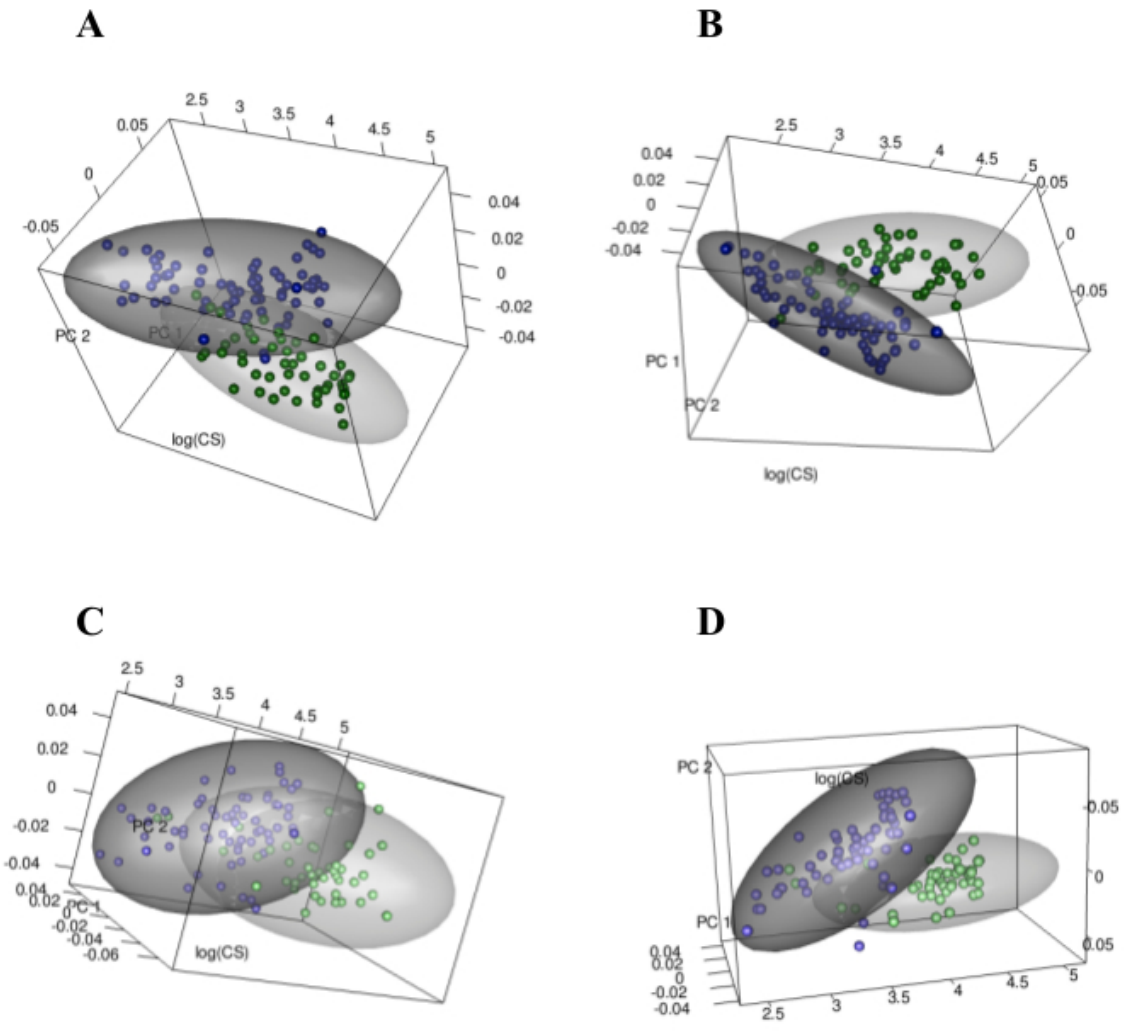

Figure 4.9. Clasper length (A) and cloaca depth (B) versus log-centroid size. Color schemes are as in figures 4.5 and 4.6. For reference, data are included on additional specimens collected by the National Marine Fisheries Service, Northeast Fishery Science Center (light points in background). Gray bars mark represent approximate ranges for male transition to maturity.

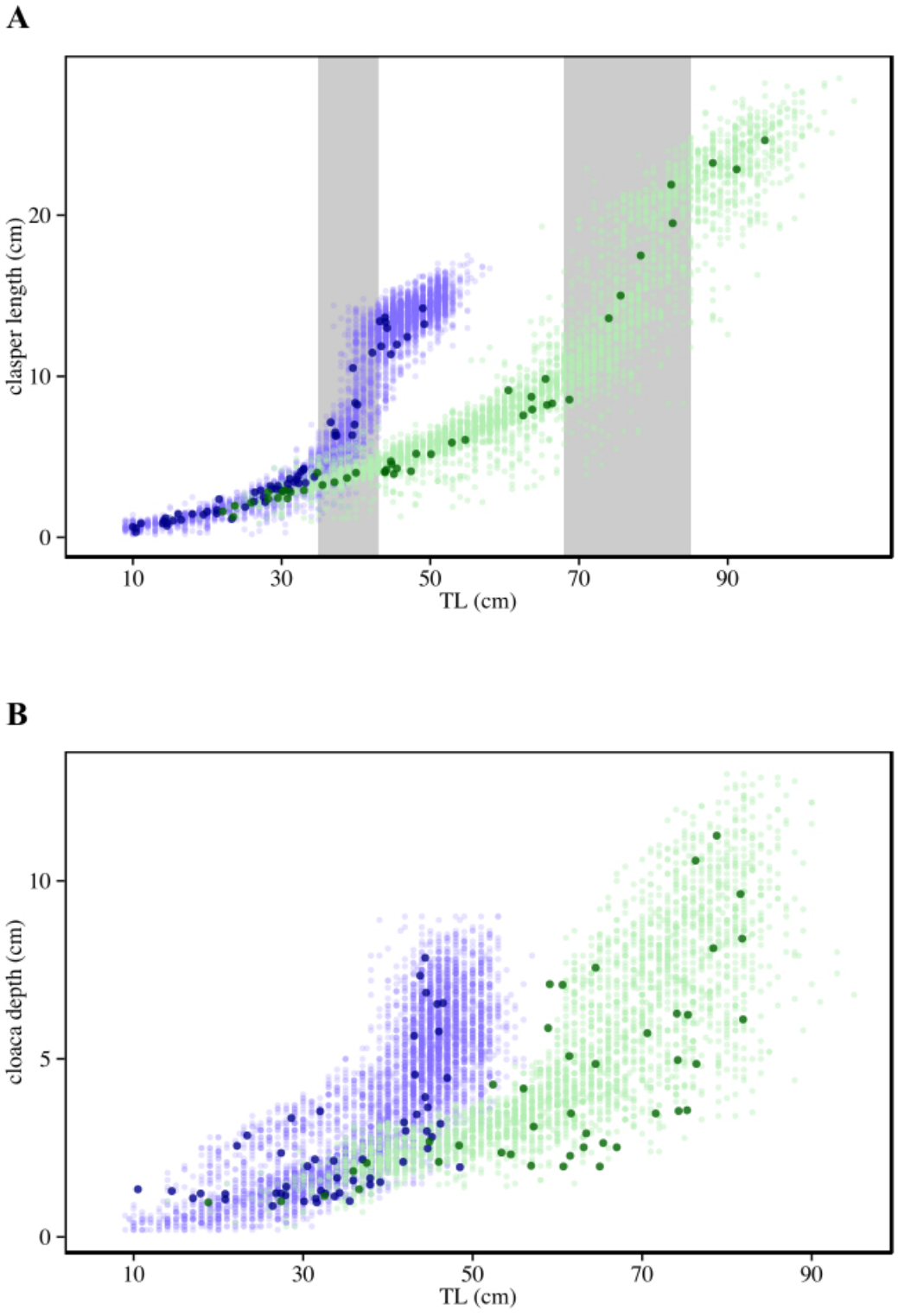

Figure 4.10. Rostrum length versus total length. Color schemes are as in figures 4.5 and 4.6.

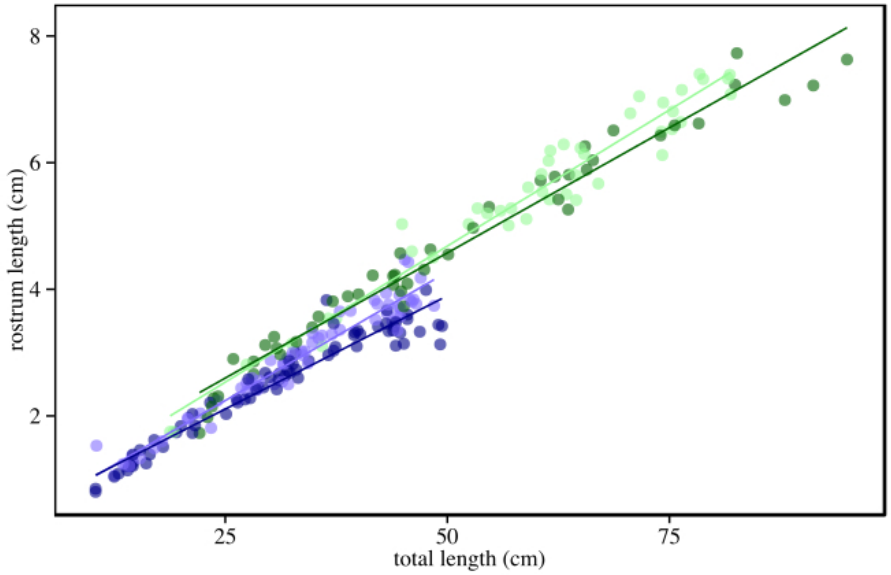

Figure 4.11. Gonadosomatic index (GSI) versus log-total length. Color schemes are as in figures 4.5 and 4.6. Linear regression lines are included to display overall directions of variation.

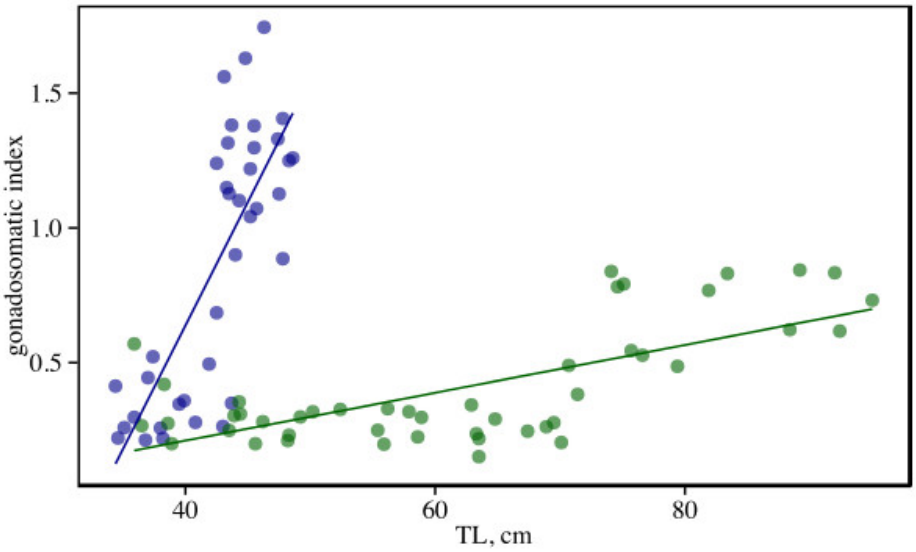

Figure 4.12. Total length versus centroid size. Color schemes are as in figures 4.5 and 4.6.

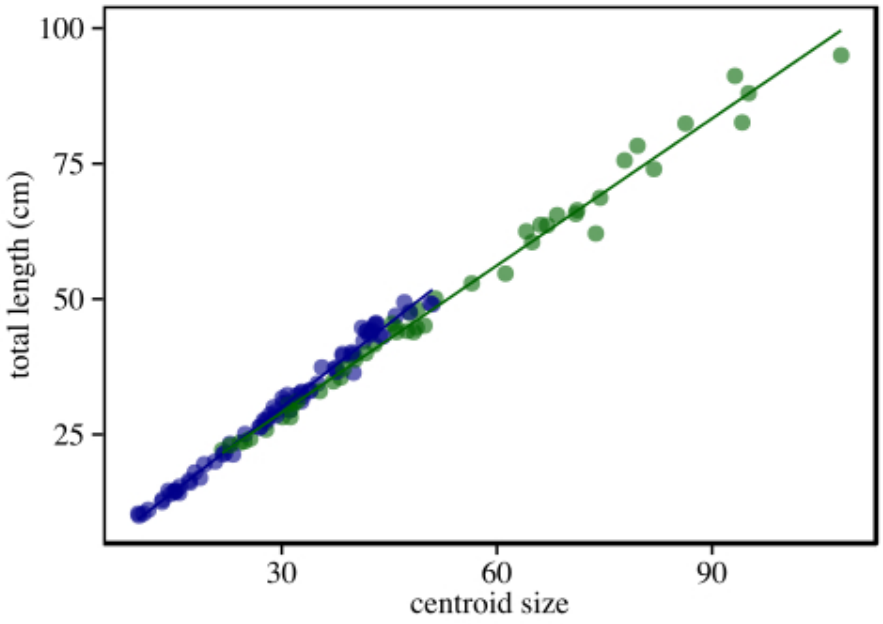

Figure 4.13. Radiographs of male (A) and female (B) *L. erinacea*, displaying pectoral "cramming" in the former. Red circles indicate areas where the effect is most noticeable. For reference, black bars are 2cm in length.

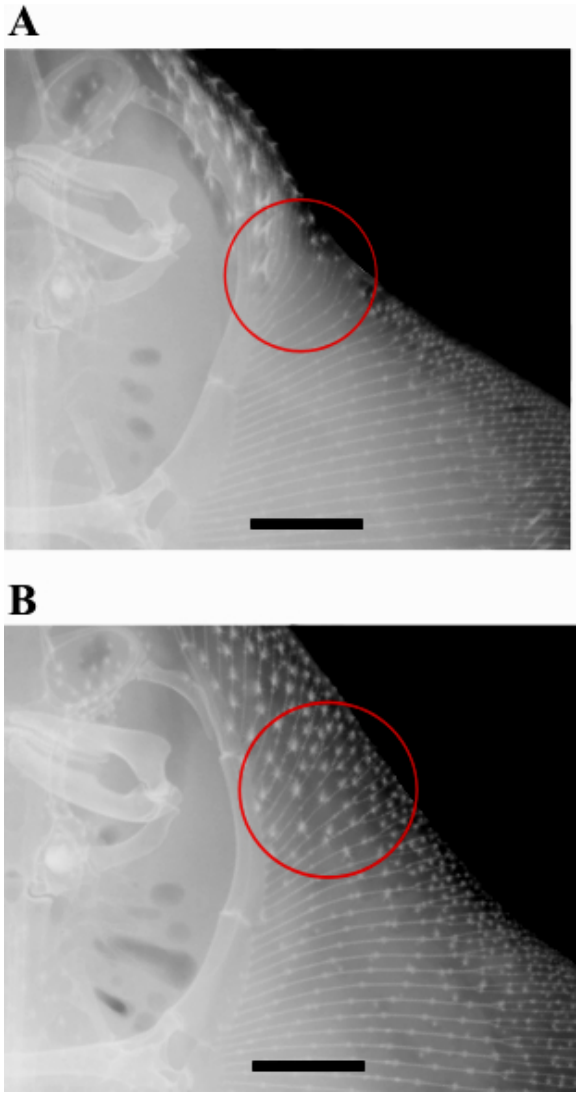

Summary

The work presented in this dissertation provides a number of new insights in two different research areas. In addition, the work undertaken in each chapter led to deeper understanding of patterns, processes and underlying diversity of the respective systems examined. In chapter one, I found evidence of community trends with time that were most marked in northern regions (GOM and GB) and moderate (SNE) or almost non-existent (MAB) in southern areas. Further, there were regionally significant associations with local water temperatures and large-scale oceanic and atmospheric processes (AMO and Gulf Stream), although the exact mechanism has not yet been established. In the GOM and GB, it appeared that at least some portion of observed change was associated with rise of species with rapid colonization potential. These types of changes have indeed been documented and projected for north Atlantic ecosystems (Christensen *et al*. 2003). This is important because it shows that temporal variation in the interspecific A-O relationship did indeed reflect real and important features of communities.

Research in the second chapter largely complemented the work in chapter one. The ability to recreate trends observed in natural communities from a collection of spatial strategies does speak to the characteristics of communities captured by the interspecific A-O relationship. However, the most potentially important utility of this approach is something that I was only able to scratch the surface of (i.e. manipulations of parameters for hypothesis testing). In one of my tests, I was able to substantially impact the occurrence of trends by removing species that I designated as rapid colonizers. Simple exercises like this can allow investigators to test hypothetical scenarios in their own research and may even help to better understand the A-O relationship itself.

In the third chapter, my results pointed to potentially large variation in lifestyle diversity of skates. This has implications for the way researchers think about skates relative to other batoids. The relationship between shape variation and aspect ratio suggested a fairly consistent pattern among batoid groups that is also tied to functionality. It also raises questions as to adaptive constraints that result in skates occurring over a contiguous morpho-functional space, relative to the bimodal diversity observed in rays.

Finally, in chapter four, I provided evidence that the sexual dimorphism observed in many skate species could be linked to clasper elongation. The intensity of the dimorphism in *L. erinacea* coincides with a fish that also has a number of traits suggestive of strong sexual competition (e.g. early/rapid maturation and high GSI). Neither the prevalence of the pectoral fin dimorphism nor its link to clasper growth has been suggested before this research.

References Cited

Adams DC, Otarola-Castillo E. 2013. Geomorph: an R package for the collection and analysis of geometric morphometric shape data. *Methods in Ecology and Evolution*. **4**, pp. 393-399.

Berkeley SA, Hixon MA, Larson RJ, Love MS. 2004. Fisheries sustainability via protection of age structure and spatial distribution of fish populations. *Fisheries*. **29**, pp. 23-32.

Bianchi G, Gislason H, Graham K, Hill L, Jin X, Koranteng K, Manickchand-Heileman S, Payá I, Sainsbury K, Sanchez F, Zwanenburg K. 2000. Impact of fishing on size composition and diversity of demersal fish communities. *ICES Journal of Marine Science*. **57**, pp. 558-571.

Bigelow HB, Schroeder WC. 1953. *Fishes of the western North Atlantic: Part 2: sawfishes, guitarfishes, skates and rays. Chimaeriods*. Sears Foundation for Marine Research, Mem. 1, Part 2, New Haven, CT. 588 pp.

Blackburn TM, Cassey P, Gaston KJ. 2006. Variations on a theme: sources of heterogeneity in the form of the interspecific relationship between abundance and distribution. *Journal of Animal Ecology*. **75**, pp. 1426-1439.

Bookstein FL. 1991. *Morphometric tools for landmark data: geometry and biology*. Cambridge University Press, New York, NY. 435 pp.

Borregaard MK, Rahbek C. 2010. Causality of the relationship between geographic distribution and species abundance. *Quarterly Review of Biology*. **85**, pp. 3-25.

Bourne DW. 1987. The fisheries. In: *Georges Bank* (ed. R Backus). MIT Press, Cambridge, MA, pp. 409-424.

Braccini JM, Chiaramonte GE. 2005. Intraspecific variation in the external morphology of the sand skate. *Journal of Fish Biology*. **61**, pp. 959-972.

Bremer JRA, Frisk MG, Miller TJ, Turner J, Viñas J, Kwil K. 2005. Genetic identification of cryptic juveniles of little skate and winter skate. *Journal of Fish Biology*. **66**, pp. 1177-1182.

Brown JH. 1984. On the relationship between abundance and distribution of species. *American Naturalist*. **124**, pp. 255-279.

Buckley HL, Freckleton RP. 2010. Understanding the role of species dynamics in abundance-occupancy relationships. *Journal of Ecology*. **98**, pp. 645-658.

Carpenter SR, Kitchell JF, Hodgson JR. 1985. Cascading trophic interactions and lake productivity: fish predation and herbivory can regulate lake ecosystems. *Bioscience*. **35**, pp. 634-639.

Castillo-Geniz JL, Nishizaki OS, Perez-Jiménez JC. 2007. Morphological variation and sexual dimorphism in the California skate, *Raja inornata*, Jordan and Gilbert 1881 from the Gulf of California, Mexico. *Zootaxa*. **1545**, pp. 1-16.

Chih-hao H, Reiss CS, Hunter JR, Beddington JR, May RM, Sugihara G. 2006. Fishing elevates variability in the abundance of exploited species. *Nature*. **443**, pp. 859-862.

Chiquillo KL, Ebert DA, Slager CJ, Crow KD. 2014. The secret of the mermaid's purse: Phylogenetic affinities within the Rajidae and the evolution of a novel reproductive strategy in skates. *Molecular Phylogenetics and Evolution*. **75**, pp. 245-251.

Christensen V, Guénette S, Heymans JJ, Walters CJ, Watson R, Zeller D, Pauly D. 2003. Hundred-year decline of North Atlantic predatory fishes. *Fish and Fisheries*. **4**, pp. 1-24.

Collie JS, Richardson K, Steele JH. 2004. Regime shifts: can ecological theory illuminate the mechanisms? *Progress in Oceanography*. **60**, pp. 281-302.

Compagno LJV. 1999. Systematics and Body Form. In *Sharks, Skates and Rays: The Biology of Elasmobranch Fishes* (ed. Hamlett WC). The Johns Hopkins University Press, London. Pp. 1-42.

Connell JH, Slatyer RO. 1977. Mechanisms of succession in natural communities and their role in community stability and organization. *American Naturalist*. **111**, pp. 1119-1144.

Cowley MJR, Thomas CD, Wilson RJ, León-Cortés JL, Gutiérrez D, Bulman CR. 2001. Density-distribution relationships in British butterflies. II. An assessment of mechanisms. *Journal of Animal Ecology*. **70**, pp. 426-441.

Dahn RD, Davis MC, Pappano WN, Shubin NH. 2007. Sonic hedgehog function in chondrichthyan fins and the evoloution of appendage patterning. *Nature*. **445**, pp. 311-314.

Daskalov GM, Grishin AN, Rodionov S, Mihneva V. 2007. Trophic cascades triggered by overfishing reveal possible mechanisms of ecosystem regime shifts. *Proceedings of the National Academy of Sciences, USA*. **104**, pp. 10518-10523.

Drake AG, Klingenberg CP. 2008. The pace of morphological change: historical transformation of skull shape in St Bernard dogs. *Proceedings of the Royal Society B: Biological Sciences*. **275**, pp. 71-76.

Drinkwater KF. 2006. The regime shift of the 1920s and 1930s in the North Atlantic. *Progress in Oceanography*. **68**, pp. 134-151.

Dulvy NK, Freckleton RP, Polunin NVC. 2004. Coral reef cascades and the indirect effects of predator removal by exploitation. *Ecology Letters*. **7**, pp. 410-416.

Dulvy NK, Rogers SI, Jennings S, Stelzenmüller V, Dye SR, Skjoldal HR. 2008. Climate change and deepening of the North Sea fish assemblage: a biotic indicator of warming seas. *Journal of Applied Ecology*. **45**, pp. 1029-1039.

Duplisea D, Frisk M, Trenkel V. 2009. Does range size contraction of Georges Bank fishes signal an extinction debt caused by habitat destruction? ICES Conference and Meeting Documents. ICES CM 2009/H:07.

Ebert DA, Compagno LJV. 2007. Biodiversity and systematics of skates (Chondrichthyes: Rajiformes: Rajoidei). *Environmental Biology of Fishes*. **80**, pp. 111-124.

Ebert DA, Compagno LJV, Cowley PD. 2007. Aspects of the reproductive biology of skates (Chondrichthyes: Rajiformes: Rajoidei) from southern Africa. *ICES Journal of Marine Science*. **65**, pp. 81-102.

Ekstrom LJ, Kajiura SM. 2014. Pelvic girdle shape predicts locomotion and phylogeny in batoids. *Journal of Morphology*. **275**, pp. 100-110.

Elmqvist T, Folke C, Nyström M, Peterson G, Bengtsson J, Walker B, Norberg J. 2003. Response diversity, ecosystem change, and resilience. *Frontiers in Ecology and the Environment*. **1**, pp. 488-494.

Estes JA, Duggins DO. 1995. Sea otters and kelp forests in Alaska: generality and variation in a community ecological paradigm. *Ecological Monographs*. **61**, pp. 75-100.

Fisher JAD, Frank KT. 2004. Abundance-distribution relationships and conservation of exploited marine fishes. *Marine Ecology-Progress Series*. **279**, pp. 201-213.

Fitzpatrick JL, Kempster RM, Daly-Engal TS, Collin SP, Evans JP. 2012. Assessing the potential for post-copulatory sexual selection in elasmobranchs. *Journal of Fish Biology*. **80**, pp. 1141-1158.

Flammang BE, Ebert DA, Cailliet GM. 2008. Reproductive biology of deep-sea catsharks (Chondrichthyes: Scyliorhinidae) in the eastern North Pacific. Environmental Biology of Fishes. **81**, pp. 35-49.

Fogarty MJ, Murawski SA. 1998. Large-scale disturbance and the structure of marine systems: fishery impacts of Georges Bank. *Ecological Applications*. **8**, pp. S6-S22.

Frank KT, Petrie B, Choi JS, Leggett WC. 2005. Trophic cascades in a formerly cod-dominated ecosystem. *Science*. **308**, pp. 1621-1623.

Freckleton RP, Noble D, Webb TJ. 2006. Distributions of habitat suitability and the abundance-occupancy relationship. *The American Naturalist*. **167**, pp. 260-275.

Frédérich B, Vandewalle P. 2011. Bipartite life cycle of coral reef fishes promotes increasing shape disparity of the head skeleton during ontogeny: an example from damselfishes (Pomacentridae). BMC Evolutionary Biology. **11**:82.

Frisk MG. 2010. Life History Strategies of Batoids. In *Sharks and Their Relatives II: Biodiversity, Adaptive Physiology and Conservation* (Carrier JC, Musick JA and Heithaus MR eds.). CRC Press, New York, NY. Pp. 283-316.

Frisk MG, Duplisea DE, Trenkel VM. 2011. Exploring the abundance-occupancy relationships for the Georges Bank finfish and shellfish community from 1963-2006. *Ecological Applications*. **21**, pp. 227-240.

Frisk MG, Miller TJ. 2006. Age, growth, and latitudinal patterns of two Rajidae species in the northwestern Atlantic: little skate (*Leucoraja erinacea*) and winter skate (*Leucoraja ocellata*). Canadian Journal of Fisheries and Aquatic Sciences. **63**, pp. 1078-1091.

Frisk MG, Miller TJ. 2009. Maturation of little skate and winter skate in the western Atlantic from Cape Hatteras to Georges Bank. *Marine and Coastal Fisheries: Dynamics, Management, and Ecosystem Science.* **1**, pp. 1-10.

Frisk MG, Miller TJ, Fogarty MJ. 2002. The population dynamics of little skate *Leucoraja erinacea*, winter skate *Leucoraja ocellata*, and barndoor skate *Dipturus laevis*: predicting exploitation limits using matrix analyses. ICES Journal of Marine Science. **59**, pp. 576-586.

Gaston FJ, Blackburn TM. 2003. Dispersal and the interspecific abundance-occupancy relationship in British birds. *Global Ecology & Biogeography*. **12l**, pp. 373-379.

Gaston KJ, Blackburn TM, Lawton JH. 1997. Interspecific abundance-range size relationships: an appraisal of mechanisms. *Journal of Animal Ecology*. **66**, pp. 579-601.

Gaston KJ, Blackburn TM, Lawton JH. 1998. Aggregation and interspecific abundance-occupancy relationships. *Journal of Animal Ecology*. **67**, pp. 995-999.

Gaston FJ, Warren PH. 1997. Interspecific abundance-occupancy relationships and the effects of disturbance: a test using microscosms. *Oecologia*. **112**, pp. 112-117.

Gunz P, Mitteroecker P. 2013. Semilandmarks: a method for quantifying curves and surfaces. *Histrix, the Italian Journal of Mammology*. **24**, pp.103-109.

Hardin G. 1960. The competitive exclusion principle. *Science*. **131**, pp. 1292-1297.

Hartley S. 1998. A positive relationship between local abundance and regional occupancy is almost inevitable (but not all positive relationships are the same). *Journal of Animal Ecology*. **67**, pp. 992-994.

Heino J. 2005. Positive relationship between regional distribution and local abundance in stream insects: a consequence of niche breadth or niche position? *Ecography*. **28**, pp. 345-354.

Holt AR, Gaston KJ, Fangliang H. 2002. Occupancy-abundance relationships and spatial distribution: a review. *Basic and Applied Ecology*. **3**, pp. 1-13.

Holt AR, Warren PH, Gaston KJ. 2004. The importance of habitat heterogeneity, biotic interactions and dispersal in abundance-occupancy relationships. *Journal of Animal Ecology*. **73**, pp. 841-851.

Hughes RM, Kaufmann PR, Herlihy AT, Kincaid TM, Reynolds L, Larsen DP. 1998. A process for developing and evaluating indices of fish assemblage integrity. *Canadian Journal of Fisheries and Aquatic Sciences*. **55**, pp. 1618-1631.

Jacobson LD. 2005. Essential fish habitat source document: longfin inshore squid, *Loligo pealeii*, life history and habitat characteristics. NOAA technical memorandum, NMFS-NE-193. U.S. Department of Commerce, Northeast Fisheries Science Center, Woods Hole, MA.

Joyce TM, Deser C, Spall MA. 2000. The relation between decadal variability of subtropical mode water and the North Atlantic oscillation. *Journal of Climate*. **13**, pp. 2550-2569.

Kajiura SM, Tyminski JP, Forni JB, Summers AP. 2005. The sexually dimorphic cephalofoil of bonnethead sharks, *Sphyrna tiburo*. The Biological Bulletin. **209**, pp. 1-5.

Klingenberg CP. 2010. Evolution and development of shape: integrating quantitative approaches. *Nature Reviews, Genetics*. **11**, pp. 623-635.

Klingenberg CP. 2011. MorphoJ: an integrated software package for geometric morphometrics. *Molecular Ecology Resources*. **11**, pp. 353-357.

Knight JR, Folland CK, Scaife AA. 2006. Climate impacts of the Atlantic Multidecadal Oscillation. *Geophysical Research Letters*. **33**, L17706.

Koester DM, Spirito CP. 2003. Punting: an unusual mode of locomotion in the little skate, *Leucoraja erinacea* (Chondrichthyes: Rajidae). Copeia. **3**, pp. 552-561.

Konishi M, Nakano S, Iwata T. 2001. Trophic cascading effects of predatory fish on leaf litter processing in a Japanese stream. *Ecological Research*. **16**, pp. 415-422.

Kriwet J, Kiessling W, Klug S. 2009. Diversification Trajectories and Evolutionary Life-History Traits in Early Sharks and Batoids. *Proceedings of the Royal Society of London, Biological Sciences*. **276**, pp. 945-951.

Lande R. 1980. Sexual dimorphism, sexual selection, and adaptation in polygenic characters. *Evolution*. **34**, pp. 292-305.

Last PR, Alava M. 2013. *Dipturus amphispinus* sp. nov., a new longsnout skate (Rajoidei: Rajidae) from the Phillipines. *Zootaxa*. **3752**, pp. 214-227.

Lear WH. 1998. History of fisheries in the Northwest Atlantic: the 500-year perspective. *Journal of Northwest Atlantic Fishery Science*. **23**, pp. 41-73.

Link JS, Brodziak JKT, Edwards SF, Overholtz WJ, Mountain D, Jossi JW, Smith TD, Fogarty MJ. 2002. Marine ecosystem assessment in a fisheries management context. *Canadian Journal of Fisheries and Aquatic Sciences*. **59**, pp. 1429-1440.

Lucey SM, Nye JA. 2010. Shifting species assemblages in the northeast US continental shelf large marine ecosystem. *Marine Ecology Progress Ser*ies. **415** pp. 23-33.

Luer CA, Gilbert PW. 1985. Mating behavior, egg deposition, incubation period, and hatching in the clearnose skate, Raja eglanteria. *Environmental Biology of Fishes*. **13**, pp. 161-171.

Martinez CM. 2014. Dissertation Chapter 1. Patterns and trends of community habitat occupation in the northwest Atlantic coastal shelf ecosystem.

Martinez CM. 2014. Dissertation Chapter 3. Reassessment of morphological diversity of the batoid pectoral fin, with an emphasis on skates (Suborder Rajoidei).

Martínez-Meyer E, Díaz-Porras D, Peterson AT, Yáñez-Arenas C. 2013. Ecological niche structure and rangewide abundance patterns of species. *Biology Letters*. **9**, 20120637.

McEachran JD. 1977. Reply to 'Sexual dimorphism in skates (Rajidae)'. *Evolution*. **31**, pp. 218-220.

McEachran JD, Dunn KA. 1998. Phylogenetic analysis of skates, a morphologically conservative clade of elasmobranchs (Chondrichthyes: Rajidae). *Copeia*. **1998**, pp. 271-290.

McEachran JD, Konstantinou. 1996. Survey of the variation in alar and malar thorns in skates: phylogenetic implications (Chondrichthyes: Rajoidei). *Journal of Morphology*. **228**, pp. 165-178.

McEachran JD, Miyake T. 1990. Zoogeography and bathymetry of skates (Chondrichthyes, Rajoidei). In *Elasmobranchs as living resources: advances in the biology, ecology, systematics, and the status of the fisheries*. NOAA Technical Report, NMFS 90. Pp. 305-326.

McEachran JD, Musick JA. 1973. Characters for distinguishing between immature specimens of the sibling species, Raja erinacea and Raja ocellata (Pisces: Rajidae). *Copeia*. **1973**, pp. 238-250.

McLeod AI. 2011. Kendall: Kendall rank correlation and Mann-Kendall trend test. R Package version 2.2, http://cran.r-project.org/web/packages/Kendall/index.html.

Miller TJ, Das C, Politis PJ, Miller AS, Lucey SM, Legault CM, Brown RW, Rago PJ. 2010. Estimation of Albatross IV to Henry B. Bigelow calibration factors. NEFSC reference document 10-05. U.S. Department of Commerce, Northeast Fisheries Science Center, Woods Hole, MA.

Morson JM, Morrissey JF. 2007. Morphological variation in the electric organ of the little skate (*Leucoraja erinacea*) and its possible role in communication during courtship. *Environmental Biology of Fishes*. DOI 10.1007/s10641-007-9221-x.

Norse EA, Watling L. 1999. Impacts of mobile fishing gear: the biodiversity perspective. *American Fisheries Society Symposium*. **22**, pp. 31-40.

Nye JA, Link JS, Hare JA, Overholtz WJ. 2009. Changing spatial distribution of fish stocks in relation to climate and population size in the Northeast United States continental shelf. *Marine Ecology Progress Series*. **393**, pp. 111-129.

Oddone MC, Vooren CM. 2004. Distribution, abundance and morphometry of *Atlantoraja cyclophora* (Regan, 1903) (Elasmobranchii: Rajidae) in southern Brazil, southwestern Atlantic. **2**, pp. 137-144.

Odum EP. 1969. The strategy of ecosystem development. *Science*. **164**, pp. 262-270.

Orlov AM, Cotton CF. 2011. Sexually dimorphic morphological characters in five north Atlantic deepwater skates (Chondrichthyes: Rajiformes). Journal of Marine Biology. 2011. DOI 10.115/2011/842821.

Orlov AM, Smirnov AA. 2011. New data on sexual dimorphism and reproductive biology of Alaska skate *Bathyraja parmifera* from the northwestern Pacific Ocean. *Journal of Ichthyology*. **51**, pp. 590-603.

Paradis E, Claude J, Strimmer 2004. APE: analysis of phylogenetics and evolution in R language. Bioinformatics. **20**, pp. 289-290.

Parker GA, Ball MA, Stockley P, Gage MJG. 1997. Sperm competition games: a prospective analysis of risk assessment. *Proceedings of the Royal Society of London B: Biological Sciences*. **264**, pp. 1793-1802.

Parmesan C, Yohe G. 2003. A globally coherent fingerprint of climate change impacts across natural systems. *Nature*. **421**, pp. 37-42.

Pauly D, Christensen V, Dalsgaard, Froese R, Torres, F Jr. 1998. Fishing down marine food webs. *Science*. **279**, pp. 860-863.

Pauly D, Palomares M-L. 2005. Fishing down marine food web: it is far more pervasive than we thought. *Bulletin of Marine Science*. **76**, pp. 197-211.

Peña-Molino B, Joyce TM. 2008. Variability in the slope water and its relation to the Gulf Stream path. *Geophysical Research Letters*. **35**, LO3606.

Perry AL, Low PJ, Ellis JR, Reynolds JD. 2005. Climate change and distribution shifts in marine fishes. *Science*. **308**, pp. 1912-1915.

Petchey OL, Gaston KJ. 2002. Functional diversity (FD), species richness and community composition. *Ecology Letters*. **5**, pp. 402-411.

Pradel A, Maisey JG, Tafforeau P Mapes RH, Mallat J. 2014. A Paleozoic shark with osteichthyan-like branchial arches. Nature. **509**, pp. 608-611.

Pratt Jr. HL, Carrier JC. 2001. A review of elasmobranch reproductive behavior with a case study on the nurse shark, *Ginglymostoma cirratum*. *Environmental Biology of Fishes*. **60**, pp. 157-188.

R Core Team. 2013. R: A language and environment for statistical computing. R Foundation for Statistical Computing, Vienna, Austria. URL http://www.R-project.org/.

Reid RN, Cargnelli LM, Griesbach SJ, Packer DB, Johnson DL, Zetlin CA, Morse WW, Berrien PL. 1999. Essential fish habitat source document: Atlantic herring, *Clupea harengus*, life history and habitat characteristics. NOAA technical memorandum, NMFS-NE-126. U.S. Department of Commerce, Northeast Fisheries Science Center, Woods Hole, MA.

Rindorf A, Lewy P. 2012. Estimating the relationship between abundance and distribution. *Canadian Journal of Fisheries and Aquatic Sciences*. **69**, pp. 382-397.

Rochet M, Trenkel VM. 2003. Which community indicators can measure the impact of fishing? A review and proposals. *Canadian Journal of Fisheries and Aquatic Sciences*. **60**, pp. 86-99.

Rohlf FJ. 1999. Shape Statistics: Procrustes Superimpositions and Tangent Spaces. *Journal of Classification*. **16**, pp. 197-223.

Rohlf FJ. 2013a. tpsDIG2, v2.17. Freeware available at: life.bio.sunysb.edu/morph/. Last updated 30 April 2013.

Rohlf FJ. 2013b. tpsRegr, v1.40. Freeware available at: life.bio.sunysb.edu/morph/. Last updated 6 October 2013.

Rohlf FJ. 2013c. tpsRelw, v1.53. Freeware available at: life.bio.sunysb.edu/morph/. Last updated 2 October 2013.

Sagarese SR, Cerrato RM, Frisk MG. 2011. Diet composition and feeding habits of common fishes in Long Island bays, New York. *Northeastern Naturalist*. **18**, 291-314.

Scenna LB, García de la Rosa SB, Díaz de Astarloa JM. 2006. Trophic ecology of the Patagonian skate, *Bathyraja macloviana*, on the Argentine continental shelf. *ICES Journal of Marine Science*. **63**, pp. 867-874.

Schaefer JT, Summers AP. 2005. Batoid wing skeletal structure: novel morphologies, mechanical implications, and phylogenetic patterns. *Journal of Morphology*. **264**, pp. 298-313.

Shadwick RE, Genballa S. 2006. Structure, kinematics, and muscle dynamics in undulatory swimming. In *Fish Biomechanics: Volume 23, Fish Physiology* (eds. Shawick RE, Lauder GV). Elsevier Academic Press, San Diego, CA. pp. 241-280.

Solow AR. 1993. A simple test for change in community structure. *Journal of Animal Ecology*. **62**, pp. 191-193.

Sosebee KA. 2004. Maturity of Skates in Northeast United States Waters. *Journal of Northwest Atlantic Fishery Science*. **35**, pp. 141-153.

Sosebee KA, Cadrin SX. 2006. A Historical Perspective on the Abundance and Biomass of Northeast Demersal Complex Stocks from NMFS and Massachusetts Inshore Bottom Trawl Surveys, 1963-2002. NEFSC reference document 06-05. U.S. Department of Commerce, Northeast Fisheries Science Center, Woods Hole, MA.

Stone PA, Snell HL, Snell HM. 1994. Behavioral diversity as biological diversity: introduced cats and lava lizard wariness. Conservation Biology. **8**, pp. 569-573.

Storch D, Gaston KJ. 2004. Untangling ecological complexity on different scales of space and time. *Basic and Applied Ecology*. **5**, 389-400.

Sulikowski JA, Tsang PCW, Huntting Howell W. 2004. An annual cycle of steroid hormone concentrations in the winter skate, *Leucoraja ocellata*, from the western Gulf of Maine. *Marine Biology*. **144**, pp. 845-853.

Tamura K, Peterson D, Peterson N, Stecher G, Nei M, Kumar S. 2011. MEGA5: molecular evolutionary genetics analysis using maximum likelihood, evolutionary distance, and maximum parsimony methods. Molecular Biology and Evolution. **28**, pp. 2731-2739.

Venables WN and Ripley BD. 2002. Modern applied statistics with S. Fourth Edition. Springer, New York, NY. ISBN 0-387-95457-0.

Wainwright PC, Bellwood DR, Westneat MW. 2002. Ecomorphology of locomotion in labrid fishes. *Environmental Biology of Fishes*. **65**, pp. 47-62.

Walther G, Post E, Convey P, Menzel A, Parmesan C, Beebee TJC, Fromentin J, Hoegh-Guldberg O, Bairlein F. 2002. Ecological responses to recent climate change. *Nature*. **416**, 389-395.

Webb TJ, Freckleton RP, Gaston KJ. 2012. Characterizing abundance-occupancy relationships: there is no artefact. *Global Ecology and Biogeography*. **21**, pp. 952-957.

Webb TJ, Noble D, Freckleton RP. 2007. Abundance-occupancy dynamics in a human dominated environment: linking interspecific and intraspecific trends in British farmland and woodland birds. *Journal of Animal Ecology*. **76**, 123-134.

Wilga CAD, Lauder GV. 2004. Biomechanics of Locomotion in Sharks, Rays and Chimeras. In *Biology of sharks and their relatives* (eds. Carrier CJ, Musick JA, Heithaus MR). CRC Press, New York, NY. Pp. 139-164.

Wilson PD. 2008. The pervasive influence of sampling and methodological artefacts on a macroecological pattern: the abundance-occupancy relationship. *Global Ecology and Biogeography*. **17**, pp. 457-464.

Wilson PD. 2011. The consequences of using different measures of mean abundance to characterize the abundance-occupancy relationship. *Global Ecology and Biogeography*. **20**, pp. 193-202.

Winchell CJ, Martin AP, Mallatt J. 2004. Phylogeny of Elasmobranchs Based on LSU and SSU Ribosomal RNA Genes. *Molecular Phylogenetics and Evolution*. **31**, pp. 214-224.

Wright DH. 1991. Correlations between incidence and abundance are expected by chance. *Journal of Biogeography*. **18**, pp. 463-466.

Zeileis A, Leisch F, Hornik K, Kleiber C, Hansen B. 2013. Strucchange: Testing, monitoring, and dating structural changes. R Package version 1.5-0, http://cran.r-project.org/web/packages/strucchange/index.html.

Zelditch ML, Swiderski DL, Sheets HD, Fink WL. 2004. *Geometric Morphometrics for Biologists: A Primer*. Elsevier Academic Press, San Deigo, CA. 443 pp.

Zuckerberg B, Porter WF, Corwin K. 2009. The consistency and stability of abundance-occupancy relationships in large-scale population dynamics. *Journal of Animal Ecology*. **78**, pp. 172-181.